REGENERATION OF SENSORY HAIR CELLS AND PROGENITOR SELF-RENEWAL REQUIRE LOCALIZED INTERACTIONS BETWEEN THE NOTCH AND WNT SIGNALING PATHWAYS

by

Marco Andres Romero-Carvajal

A dissertation submitted to the faculty of
The University of Utah
in partial fulfillment of the requirements for the degree of

Doctor of Philosophy

Department of Neurobiology and Anatomy

The University of Utah

August 2015

The University of Utah Graduate School

STATEMENT OF DISSERTATION APPROVAL

The dissertation of **Marco Andres Romero-Carvajal**

has been approved by the following supervisory committee members:

Tatjana Piotrowski	, Chair	**6/1/2015** Date Approved
Richard Dorsky	, Member	**6/1/2015** Date Approved
Edward Levine	, Member	**6/1/2015** Date Approved
Rodney Stewart	, Member	**6/1/2015** Date Approved
Monica Vetter	, Member	**6/1/2015** Date Approved

and by **Monica Vetter** , Chair/Dean of

the Department/College/School of **Neurobiology and Anatomy**

and by David B. Kieda, Dean of The Graduate School.

ABSTRACT

Mechanosensory hair cell damage leads to permanent hearing loss. The zebrafish mechanosensory organs (neuromasts) are an excellent model for the study of hair cell regeneration. Neuromasts have a central group of sensory hair cells surrounded by support cells and the outermost mantle cells. While adult mammalian hair cells cannot regenerate, neuromast hair cells have the ability to do so via support cell proliferation. In this study, we used proliferation assays and lineage analyses that demonstrated the existence of proliferative compartments in the posterior lateral line neuromasts where support cells either self-renew or differentiate. These spatially restricted lineage decisions within the progenitor pool resemble the spatial heterogeneities within the intestinal crypt or the hair follicle niche that guide stem cell transit amplification or differentiation. In addition, we identified the mantle cells as a quiescent support cell pool that do not proliferate in response to selective hair cell ablation, but that re-enter the cell cycle when hair cell and support cells numbers are drastically reduced. By combining our lineage analysis with gene expression analyses, genetic manipulations, and the use of chemical inhibitors, we were able to dissect the roles of Notch and Wnt signaling during homeostasis and regeneration. We demonstrate that Notch signaling restricts hair cell differentiation and maintains the spatial pattern of support cell proliferation through Wnt signaling inhibition.

Thus, Notch–Wnt signaling interactions are required to maintain pools of amplifying support cells in the poles and maintain tissue homeostasis by balancing self-renewal and differentiation.

A mi familia…

TABLE OF CONTENTS

ABSTRACT iii

ACKNOWLEDGEMENTS ix

PREFACE xiii

CHAPTERS

1. INTRODUCTION: MECHANOSENSORY SYSTEMS AND HAIR CELL DEVELOPMENT 1

- Hair cells 2
- Vertebrate mechanosensory systems 2
  - The inner ear 3
  - The lateral line 4
- Molecular mechanisms of hair cell development in the 6
- inner ear and the lateral line 6
  - The ectodermal placodes 6
  - The Notch signaling pathway 8
  - Wnt signaling pathway 9
  - FGF signaling pathway 10
  - Hair cell development in the inner ear 11
- Concluding remarks 15
- References 16

2. SUPPORT CELL EARLY RESPONSES TO HAIR CELL DEATH AND THE ROLE OF *SPALT-LIKE 1B* IN HAIR CELL REGENERATION 27

- Abstract 27
- Introduction 28
  - Hair cell death 28
  - Regeneration in the inner ear and lateral line 30
- Preliminary results and future directions 35
  - Identification of early-response genes involved in hair cell regeneration. 35
  - Notch signaling is downregulated 1 hour after hair cell death 38
  - The list of upregulated transcripts might be enriched for 39
  - Wnt-target genes 39

The role of the primordium central cells in hair cell differentiation 41
The role of sall1b in lateral line development 41
Experimental procedures 44
Fish lines and regeneration experiments 44
Cell dissociation and FACS 45
Microarray analysis of gene expression 46
In situ hybridization 46
Immunohistochemistry 46
Morpholino injections 47
Pharmacological inhibitors 47
Author contributions 47
Acknowledgements 48
References 48

3. REGENERATION OF SENSORY HAIR CELLS REQUIRES LOCALIZED INTERACTIONS BETWEEN THE NOTCH AND WNT PATHWAYS 72

Introduction 73
Results 76
Time-lapse and fate analyses define dynamics of cell division and differentiation in homeostatic and regenerating NMs 76
Support cell lineages are restricted to different compartments
Notch and Wnt pathway members are expressed in complementary compartments during homeostasis 80
Inhibition of Notch signaling mimics expression changes observed during regeneration 82
Notch inhibits proliferation and differentiation through different mechanisms 84
Notch signaling inhibits proliferation via inhibition of Wnt and by a Wnt-independent mechanism 85
Wnt and Notch signaling control proliferation in overlapping and distinct compartments 87
Wnt does not affect hair cell differentiation during hair cell regeneration 88
Mantle cells can re-enter the cell cycle 89
Discussion 90
Self-renewal and differentiation occur in distinct compartments and are regulated by Notch/Wnt interactions 91
Expression of Notch pathway genes 92
Different dosages of Notch affect differentiation and proliferation 93
Why is the Notch-regulated restriction of amplifying divisions to the poles important? 94
Support cells throughout the NM are multipotent 95

Mantle cells are quiescent but proliferate in response to severe injury 96
Conclusion 97
Experimental procedures 97
Fish lines and regeneration experiments 97
Time-lapse imaging and image acquisition 98
Pharmacological inhibitors and BrdU incorporation 98
Heat-shock experiments 99
Immunohistochemistry 99
In situ hybridization 100
Author contributions 100
Acknowledgments 101
References 101
Supplemental experimental procedures 107
Spatial analysis 107
Cell movement analysis 108
In situ hybridization 109
Supplemental references 110

4. DISCUSSION AND FUTURE DIRECTIONS 138

Different pools of support cells maintain tissue homeostasis in the zebrafish lateral line neuromasts 139
Mantle cells as an independent cell population 139
The support cells are multipotent progenitors that self-renew and differentiate into hair cells 141
Heterogeneities within the neuromasts mantle and support cells guide cell fate decision 142
A compartment for hair cell differentiation? 143
Notch signaling 144
Wnt signaling 145
A Wnt-Notch negative feedback loop control tissue homeostasis in the neuromast 146
Notch signaling has dose-dependent effect over proliferation and Wnt signaling activation 148
Hair cell death changes the proliferative state of the neuromast in a Notch-independent manner 149
Other differentiation signals 149
Other regulators of proliferation 150
Polar compartments 151
Mantle cells 153
Conclusion 154
References 155

ACKNOWLEDGEMENTS

I am very grateful and honored to have worked with Tatjana Piotrowski and all the people she has mentored during these five years. I think the lab has the optimal environment for scientific work and creativity, and Tatjana has been keen in driving the group to success. Tatjana is a great mentor and colleague who has always supported our academic progress and the advancement of our projects. I am deeply thankful for her mentorship and I will do my best to demonstrate the quality of the training I received. Joaquín Navajas Acedo, Linjia Jiang, and Agnė Kozlovskaja-Gumbrienė have been directly involved in one part of my thesis research and produced important contributions. Their friendship, hard work, scientific input, and high tolerance for my messiness are some of the main reasons this project has been successfully published. Marina Venero-Galanternik and Mark Lush have been true friends and my family since they picked me up from the Salt Lake City airport six years ago. As if it wasn't enough for them to put up with me every day, they also read and corrected my manuscripts, abstracts, and posters like their own. Muchas gracias! Rob Duncan was my first mentor when I joined the lab and taught me the tools and the skills of working with zebrafish. Similarly, Masataka Nikaido and Andy Aman are great friends from whom I learned a lot during their time at the Piotrowksi lab. I am thankful to Julia Snyder, Megan Senecal, Minh Tu Nguyen, Ana Gabriel, and

Suzy Fan for their hard work as technicians and their friendship. Lauren Cockrell, Britany Fitzwater, Karen Evans, Robin Erhardt, and Nicole Caldwell are amazing administrative personnel at the Stowers Institute and at the University of Utah, to whom I am very grateful for taking care of me and all the paperwork and timelines I am always missing. During my stay in the lab, I also had the chance to share some of the things I have learned with a few amazing students like Eric Young, Joaquín Navajas Acedo, and Raquel Barajas. Their curiosity and hard work were my motivation to improve my experiments, to write better, to learn more, and to share everything I learn.

The Neurobiology and Anatomy department and the Molecular Biology program at the University of Utah kindly received me as an applicant and as a PhD student and have never stopped supporting my academic endeavor. I am deeply thankful to Richard Dorsky, Ed Levine, Rodney Stewart, and Monica Vetter, members of my thesis committee, and Sheryl Scott, director of graduate studies, for their mentorship and feedback. Their inspiring lectures, guidance through the career, and important feedback were crucial for my advancement and the success of my dissertation. I would also like to thank the Chien, Dorsky, Vetter, and Sanchez labs for being always generous with their time and reagents during my short stay at the U.

The Stowers Institute is one of the main founding sources of my research and the place where I have worked for the last four years. I am grateful to everyone there for their kindness and invaluable support. Thanks to Alejandro Sanchez-Alvarado, Rob Krumlauf, Linheng Li, and Ting Xie for their interest in

our research, constant input, and suggestions for this project. In addition, thanks to Kim Tu for her friendship and for proofreading my dissertation. All the facilities maintained by the Stowers Institute have also contributed directly to this project through their dedication and hard work. In particular, the Stowers fish facility has maximized the productivity of the lab and truly excelled in zebrafish husbandry. I am thankful to all the aquatics staff for their help. Richard Alexander, Sean McKinney, Cindy Madera, and Jeffrey Lange and the microscopy center have been very supportive with my exaggerated use of the confocal, always helpful with suggestions in image acquisition, and great teachers. I learned a lot from them. I am also grateful to Hua Li, Jay Unruh, Ariel Paulson, and Chris Seidel for their help in statistical analysis, experimental design, bioinformatics, and genomics.

I would like to thank all the friends I have met in Utah and in Kansas city. The only reason I didn't go back to Ecuador every time the weather reached -32C or 35C is because they made me feel at home. I cannot name them all in a single page, 5 maybe? Although it is sad not to see you guys more often, I am glad I met you all and I am honored to have shared with you so many experiences, learned with you, laughed, and cried. You will always be in my heart and now your home is in Ecuador, any time you want to come. Thank you very much! Gracias! Muito agradeçido! Спасибі شكرا Շնորհակալություն धन्यवाद

ありがとうございます。谢谢

Esta tesis esta dedicada a mi familia. Papá, Mamá, Juano y Felipe. Ustedes han sido mi fortaleza y mi ejemplo, mis ganas de volver al país. Gracias

a ustedes soy lo que soy y he logrado todo lo que me he propuesto. Siempre pienso en ustedes cuando las cosas son dificiles, pienso en mi lugar de origen y al que siempre puedo volver.

Cuando supe que me separaría de Sofía, lo único que supe es que la volvería a encontrar. Todos estos sueños que estoy intentando cumplir, en todos estas tú y hacia allá vamos. No me ha estorbado la distancia porque contigo me duermo todos los días, contigo me levanto y sé que lo nuestro vale la pena…. Some things last.

PREFACE

Regeneration is the ability to regrow or replace missing body parts after injury or disease. This ability is widespread across animals, from complete body regeneration and “immortality” in cnidarians and flatworms, to complete limb and organ regeneration in salamanders or fish. On the contrary, most mammals have a very limited ability to regenerate except for skin wound repair, fingertips, and the liver. Aside from their varying regenerative capacity after injury, every animal has the ability, also in variable levels, to renew most of tissues during their lifespan, for example the skin or blood. Both physiological tissue self-renewal and organ regeneration depend on the existence of tissue-specific stem cells that can proliferate to compensate tissue loss, and also differentiate into the cell types that give a tissue its proper form and function. Stem cells must also have the ability to self-renew to preserve the regenerative potential.

In the field of regeneration, it has been a longstanding question whether tissues that cannot regenerate either lack proliferative stem cells or lack the signals that promote regeneration. However, even in species that we know readily regenerate, the mechanisms that allow cells to both differentiate and self-renew throughout their lifespan are still unknown. This question becomes crucial when the answer might have medical implications, for example, in spinal cord or brain injuries and the treatment of deafness. Precisely, the impaired regeneration

capacity in humans has led the field to address the mechanisms of regeneration used by other species and possibly to propose new therapies and treatments.

The following manuscript is part of an effort in the lab to understand the cellular and molecular mechanisms of regeneration of sensory cells using the zebrafish as a model system. Sensory cells are differentiated cells that transduce environmental information such as sound waves, mechanical force, or light into signals interpreted by the central nervous system. These cells are often surrounded by other cells that support the sensory function of the epithelium and regenerate the cells lost due to the constant exposure to the external environment. The inner ear, in particular, has specialized mechanosensory cells called hair cells that transduce the indirect movement caused by sound waves. Although not directly exposed to the environment, vertebrate hair cells are particularly sensitive to very high noise, infections, pollutants, antibiotic drugs, or chemotherapeutic agents, which can cause immediate disability. Accordingly, most nonmammalian vertebrates, like fish, amphibians, reptiles, and birds, can replace these cells during lifespan through cellular and molecular mechanisms that are yet to be fully understood. In contrast, the mature mammalian inner ear cannot replace lost hair cells, and sensorineural deafness and balance disorders are the main consequences. From research in multiple species, it is clear that the inner ear sensory epithelia, even in mammals, have the potential to replace hair cells, which bring the possibility of treatment and possibly cure of sensorineural deafness.

The zebrafish is an extremely amenable system to analyze mechanosensory hair cell regeneration at a cellular level due to its accessibility for imaging, and for chemical and genetic manipulations. In this manuscript, I took advantage of these attributes to generate a detailed lineage analysis of the support cell response to hair cell death and the signals involved in the regenerative process. I divided the manuscript in four main chapters: Chapter 1 is an introductory chapter that reviews the current knowledge about hair cells, mechanosensory system development, and the molecular mechanisms of hair cell formation. In Chapter 2, I reviewed the mechanisms of hair cell regeneration in the avian inner ear and the zebrafish lateral line. In this chapter, I also present unpublished results of a gene expression analysis one hour after hair cell death. This analysis led first to the discovery of an early downregulation in the Notch signaling pathway and also of multiple genes that are expressed specifically in the self-renewing stem cells. Chapter 3 has recently been accepted for publication and presents a detailed cell lineage analysis through which I uncovered spatially restricted pools of support cells with different proliferative capacities and differentiation potential. Finally, through manipulations in the Wnt signaling, Notch signaling, and combinations, I describe a possible molecular mechanism that maintains tissue homeostasis through the molecular interactions between the Notch and Wnt signaling pathways. The results presented in this manuscript are discussed in Chapter 4.

CHAPTER 1

INTRODUCTION: MECHANOSENSORY SYSTEMS AND HAIR CELL DEVELOPMENT

The importance of hair cell regeneration and the cues to understand this process lie within the vital roles hair cells play, their morphology, and their developmental origin. Indeed, multiple vertebrate behaviors rely heavily on the function of hair cells located within specialized sensory systems like the inner ear or the fish lateral line (Jorgensen, 1989; Müller and Littlewood-Evans, 2001). In spite of the diversity in organ adaptations, the hair cell ultra-structure is surprisingly homologous among vertebrates, and the mechanosensory organs follow a similar developmental pattern, from cranial placodes (Fritzsch and Straka, 2014; Jorgensen, 1989). These placodes can generate both hair cells and the support cells from which hair cells regenerate through multiple processes of cell fate specification linked to the morphogenesis of the sensory organ (Baker et al., 2008; Fritzsch et al., 2007; Schlosser, 2010). Particularities of the mechanosensory organs, their morphogenesis and the molecular regulation of hair cell differentiation will be addressed in the following introductory chapter with a special focus on the inner ear and the fish lateral line.

Hair cells

In vertebrates, hair cells are not sensory neurons but specialized epithelial cells that harbor multiple cytoplasmic projections on their apical end that project towards a liquid filled lumen to sense fluid movement. These projections are called stereocilia and kinocilia. There are multiple stereocilia in the apical surface and each one has actin filaments of constant length. Hair cells only have one single axonemal cilium (9+2 arrangement of microtubules) called kinocilium (Schwander et al., 2010). In the apical surface, the planar localization of the kinocilium with respect to the stereocilia is eccentric and polarized (Eaton, 1997). Due to the fact that each stereocilium is linked to others and to the kinocilium through extracellular filaments, the polarization of the kinocilium and stereocilia forces these structures to act as a bundle that deflects directionally in response to mechanical stimuli (Figure 1.1A). This deflection then opens mechanically gated ion channels that induce cell membrane depolarization and subsequent transduction of the stimuli information to the innervating afferent neurons that synapse to the hair cell. Most mechanosensory hair cells are also innervated by efferent fibers that modulate the excitatory potential of the hair cell (Ghysen and Dambly-Chaudière, 2004; Sienknecht et al., 2014).

Vertebrate mechanosensory systems

In vertebrates, hair cells arise from mechanosensory organs which also have one or more types of support cells (Figure 1.1B). These organs are necessary to perceive body motion, changes in position, gravity, and the

changes in movement and pressure of the surrounding fluids (Fritzsch and Straka, 2014).

The inner ear

The vertebrate inner ear is a complex hollow structure filled with endolymph that harbors five or more different types of mechanosensory organs important for hearing and balance (Figure 1.1C-1.1D). The ampullae or cristae sense the position of the head and angular acceleration, since hair cells in these organs detect the fluid motion funneled by the semicircular canals. There are three canals, each one positioned 90 degrees from the other, and each one harbors one crista on its base. Cristae hair cells have unidirectional hair cell polarization (Ekdale, 2015; Sienknecht et al., 2014). Separated from the semicircular, the vestibular organs have hair cells projecting to an extracellular gelatinous matrix with embedded calcium carbonate crystals called otoconia. The changes in velocity during body motion are first transduced to the otoconia through inertia and then to the macular hair cells. These hair cells have paired opposite polarities in a linear direction (Figure 1.1B). Due to the position of the maculae and the hair cell polarity, they can only sense positive and negative acceleration in a single direction (Lundberg et al., 2015). There are two main macular organs, the saccule and the utricle. In fish, the otoconia coalesce and form spheres called otoliths which transduce linear movements, gravity, and vibration in the aquatic environment (Nicolson, 2005). The fish saccule is specialized in detecting underwater sound and, in some fish, is associated to

bone structures and the swim bladder to increase sound detection. Other hearing maculae like the lagenar macula and the neglected macula develop into separate compartments (Fritzsch et al., 2013). Terrestrial vertebrates, facing different challenges, evolved another macular organ specialized in hearing called basilar papilla or cochlea (Baker et al., 2008). The cochlear duct is a linear canal that houses a sensory epithelium attached to a basement membrane called basilar membrane. On the apical side, hair cell kinocilia and stereocilia are physically linked to a second acellular membrane called the tectorial membrane (Ekdale, 2015; Schwander et al., 2010). The sensory epithelium is also complex showing morphologically distinct types of support cells and hair cells (organ of Corti). The acellular membranes as well as the pressure of the endolymph contained in the cochlear duct transduce vibrations caused by sound to the hair cells, which detect different sound frequencies depending on the distance to the entrance of the cochlear duct (Schwander et al., 2010).

The lateral line

The lateral line system consists of multiple mechanosensory organs called neuromasts. These sensory organs are distributed along the body surface of all aquatic vertebrates, which allows stimuli perception relative to any part of the body (Figure 1.1C). The spatial arrangement of neuromasts across the body varies dramatically from species to species and even within individuals. According to the neuromast developmental origin and position, the lateral line can be broadly classified in anterior and posterior (Jorgensen, 1989; Lush and

Piotrowski, 2014). Also, neuromasts appear either as single neuromast or in rows or stiches. In fish, some neuromasts are internalized in canals formed by the dermal bones or scales, and become full of fluid. Each neuromast is formed of a single cell epithelium with a central group of hair cells and two surrounding populations of support cells, the inner support cells and mantle cells (Figure 1.1E-1.1F). The hair cells are covered in a gelatinous cupula that covers the cilia and protrudes to the surrounding water through the skin. Hair cell polarity in neuromasts is similar to the one found in the vestibular organs, with paired opposite polarities; therefore, a single neuromast can sense only bi-directional linear water movement and oscillations (Sienknecht et al., 2014). However, neuromasts of different developmental origins seem to have different hair cell orientation, ensuring appropriate sampling of changes in water motion in every direction (López-Schier and Hudspeth, 2006; López-Schier et al., 2004). Aside from the most simple role of the lateral line in sensing water columns and current direction, the neuromast hair cells can perceive low frequency oscillations, discriminate the source, and provide information about distance, movement, and even identification; hence playing an important behavioral role in prey-predator interactions, feeding, navigation, schooling, and mating.

Molecular mechanisms of hair cell development in the inner ear and the lateral line

The ectodermal placodes

Hair cells originate from thickenings of the inner ectodermal layer called placodes, which are only present in the head region of the early vertebrate embryo. The placodes that form mechanosensory hair cells are the otic placode, the lateral line placodes (multiple cranial placodes present in most acuatic vertebrates), the paratympanic organ placode (in most bird species, alligators, and the tuatara), and the spiracular organ placode (only in cartilaginous fish, non-teleost ray-finned fish, and lobe-finned fish)(O'Neill et al., 2012; Piotrowski and Baker, 2014). The electroreceptive or ampullary organs of aquatic vertebrates also develop from the lateral line placode (Modrell et al., 2011). The other sensory placodes like the olfactory placode, the trigeminal placode, and the epibranchial placodes form mostly sensory neurons and ganglia (O'Neill et al., 2012; Sai and Ladher, 2015; Schlosser, 2010). Together with the neural crest cells, the cranial placodes are responsible to form the main vertebrate sensory organs and their anatomical structures that enhance stimuli sensation.

The diversity of hair-cell-forming placodes and sensory systems is an evidence of the importance of mechanosensation and its role in the adaptation of vertebrates to different environments. Although these hair cell forming placodes develop spatially separated one from the other, they share a common mechanism to form hair cells that requires multiple steps of tissue patterning and

binary cell fate decisions. These events first specify a nonsensory domain that will form the structural epithelia that surrounds the mechanosensory organs, and a neurosensory domain. The neurosensory domain will later differentiate into pro-neural cells, that form neurons, and the pro-sensory cells, which differentiate into hair cells and support cells (Chatterjee et al., 2010; Groves and Fekete, 2012). The otic and lateral line placodes share striking molecular similarities like the expression of *Pax2* and *Sox2* transcription factors (Baker and Bronner-Fraser, 2001).

The steps of placode specification, patterning, and cell fate decisions are highly controlled by multiple signaling pathways that ultimately activate the expression of transcription factors important for the inner ear or lateral line developmental programs and specifically, the formation of hair cells. The inner ear hair cells and the neuromast hair cells are homologous and multiple genes associated with human deafness are required for neuromast hair cell function and development (Nicolson, 2005; Whitfield, 2002). This homology is the same for hair cells in every vertebrate because the molecular mechanisms that control hair cell differentiation and function are highly conserved, even among metazoans. Indeed, the genes encoding the bHLH (basic helix-loop-helix) transcription factor *atonal* in *Drosophila* flies and its vertebrate homologue *Atoh1* are both required for mechanosensory hair cell development. Atoh1 is required for the activation of the expression of hair cell specific genes in vertebrates (Cai et al., 2015). Amazingly, *atonal* can rescue hair cell development in *Atoh1* mutant mice (Fritzsch and Straka, 2014; Wang et al., 2002). Other conserved

hair cell specific transcription factor genes are *Pou4f3* or *Gfi1.* Hair cells also have similar structural components like the unconventional myosin Myo7a or Prestin which are important for hair cell sensory function (Fritzsch and Straka, 2014). During hair cell development, *Atoh1* expression is directly activated by the pro-sensory transcription factor Sox2 which then represses it (Neves et al., 2013); however, its expression is actively modulated by multiple signaling pathways like Notch and Wnt. In fact, Notch, Wnt, FGF, and other molecules, are important signaling pathways in the induction and specification of the otic and lateral line placodes.

The Notch signaling pathway

The Notch receptors are transmembrane heterodimeric proteins with a large intracellular domain (NICD) that signals to the nucleus, and a large extracellular domain (NECD) that acts as a receptor for transmembrane proteins of the DSL family (Delta-Serrate-Jagged and Lag2 ligands) expressed in adjacent cells. Ligand-receptor interactions facilitate the cleavage of NECD by a metalloproteinase and the endocytosis of both the ligand and NECD by the ligand-expressing cell. Simultaneously, an intracellular cleavage, mediated by a γ -secretase, releases NICD which is translocated to the nucleus where it acts as a co-activator of a transcription factor known as CSL or RBP-jκ (Perdigoto and Bardin, 2013; Sancho et al., 2015). Since the ligands are not secreted proteins, signaling interactions require direct cell to cell contact. The Delta ligands are known to inhibit the Notch receptor function when both are co-expressed (*cis*

interaction), but they activate the Notch receptor in neighboring cells (*trans*), promoting a binary effect where the cell that expresses the ligand cannot activate Notch signaling (Sprinzak et al., 2010). This mutually exclusive signaling state is used to create fine patterns and funnel binary cell fate decisions. The bHLH transcriptional repressors from the Hes/Hey/Her family are among the best characterized Notch transcriptional targets and act mostly as inhibitors of differentiation. One of the known targets of Hes1 is *Atoh1*; hence, cells with active Notch signaling do not express *Atoh1* (Millimaki et al., 2007).

Wnt signaling pathway

The Wnt signaling pathway uses proteins from the Wingless/Wnt family as ligands to activate β-catenin-mediated transcription. Wnt ligands are small hydrophobic proteins that are secreted into the extracellular space and bind to G-protein-coupled receptors of the Frizzled family. The Frizzled receptors require a co-receptor from the LRP family to bind the Wnt ligand and to inhibit the β-catenin destruction complex. This destruction complex is formed by the kinases GSK3 and CK1, the scaffold protein APC and Axin which target and phosphorylate β-catenin for proteasome-mediated degradation. The Wnt-Frizzled-Lrp increases their affinity to GSK3, which is directly inhibited by Lrp. The inhibition of the destruction complex increases the amount of cytoplasmic β-catenin which can enter the nucleus and activate transcription as a co-factor of the Tcf/Lef transcription factors (Clevers et al., 2014; Munnamalai and Fekete, 2013; Niehrs, 2012). The Wnt signaling roles during development are context-

dependent and cannot be classified under a single category due to the high plasticity of the pathway and its interaction with other pathways. There are multiple secreted proteins like Dkk, Wif, or Sfrp that compete with the Wnt ligands, or inhibit the Frizzled-Lrp receptors to modulate the activation of the pathway. Similarly, the R-spondin secreted proteins act like Wnt co-activators by binding to the Lgr receptors and inhibiting a membrane complex that blocks Lrp (Cruciat and Niehrs, 2013; Niehrs, 2006). In addition, different Wnt ligands and Frizzled receptors can activate a pathway that do not stabilize β-catenin but rather affects planar cell polarization, cell shape, and polarized migration (Tissir and Goffinet, 2013). In neural differentiation, it is known that β-catenin can activate *Atoh1* expression in a Wnt-dependent manner by directly binding to its 3'enhancer (Jansson et al., 2015; Shi et al., 2014).

FGF signaling pathway

Fibroblast growth factors (FGF) are secreted glycoproteins that activate tyrosine kinase receptors of the FGFR family. The FGF ligands are attached to the extracellular matrix upon secretion. At the receiving cells, membrane-associated glycoproteins called HSPGs (Heparan Sulfate Proteoglycans) sequester and present the ligands to homodimers of the FGFR receptor. The FGF-FGFR-HSPG complex activates the intracellular kinase domain of the receptor and the phosphorylation of adaptor proteins such as Frs2, GTPases like RAS, kinases like phosphoinositide 3-kinase (PI3K), or the phospholipase Cγ (PLCγ). RAS induces the activation of intracellular mitogen-activated protein

kinases (MAPK) like ERK and ERK which ultimately phosphorylate and activate transcription factors like Myc, c-Fos, or c-Myc. FGF signaling has been associated with multiple cellular functions related to cell survival, cell cycle progression, differentiation, and morphogenesis (Brooks et al., 2012; Turner and Grose, 2010). During hair cell formation, FGF ligands are actively expressed in the pro-sensory domain and its roles are just beginning to be uncovered.

Hair cell development in the inner ear

During inner ear development, the otic placode undergoes morphogenesis to form a cup and then an internalized vesicle that will be remodeled into the cochlea (most ventral), vestibule (medial), and semicircular canals (most dorsal). To gain such organization, multiple molecular events pattern the early placode and the later vesicle into its main axis: dorso-ventral, anterior-posterior, and medial-lateral axis (Wu and Kelley, 2012). The placodal anterior-posterior axis is specified first due to a retinoic acid gradient produced in the somites and degraded in the ectoderm anterior to the placode. This signaling event specifies the neurosensory domain in the anterior-medial part of the otic vesicle. From experiments in mice and chicken, it is known that the cells within this domain can be identified by the expression of multiple transcription factors like *Lnfng, Six1, Sox2,* and *Ngn1.* The most anterior *Ngn1* expressing cells also express neuronal markers like *NeuroD* and the *Delta1,* and through Delta-Notch interactions, later diverge to form the pro-neural domain (Bok et al., 2007; Whitfield and Hammond, 2007). These cells actively delaminate during the early stages of morphogenesis

and migrate out of the otic domain to form the vestibulo-acoustic ganglion in mammals or the stato-acoustic ganglion in fish. The neurons from this ganglion project axons towards the sensory organ from which they delaminated, and innervate the mechanosensory hair cells. The inner ear mechanosensory organs derive from the remaining pro-sensory domain and appear sequentially during the morphogenesis of each associated structure from dorsal to ventral: first the semicircular canal cristae, then the vestibular maculae, and finally the ventral lagenar macula and basal papilla (Neves et al., 2013). Notch and FGF signaling are required for the specification of the pro-sensory domains (Hartman et al., 2010). Within the developing pro-sensory domain, multiple signaling pathways promote the differentiation of hair cells and support cells. *Atoh1a* is also expressed in the pro-sensory domain and then it is restricted to the hair cells and some support cells that will act as precursors during later development and regeneration. Notch and FGF signaling promote the maintenance of *Sox2* in support cells and modulate *Atoh1* expression (Jacques et al., 2012a; Millimaki et al., 2007; Ono et al., 2014). In addition, some of the pro-sensory cells also express the Wnt target and Wnt signaling activator *Lgr5* (Chai et al., 2011). The formation of support cells and hair cells is marked by the progressive restriction of *Atoh1* to the newly formed hair cells mediated by Notch signaling. Simultaneously, Sox2 inhibits *Atoh1* expression in support cells which progressively exit the cell cycle as evidenced by the increased expression of the cell cycle inhibitor $p27^{kip}$ also called *cdkn1b* (Chai et al., 2011; Jansson et al., 2015). Wnt signaling plays multiple roles during inner ear development. Aside of

otic vesicle patterning, Wnt seems to be important also for the patterning of the developing mechanosensory organs by inducing *Atoh1a* expression in the prosensory domain. Wnt also plays a role in the expansion of the progenitor pool by enhancing proliferation of a subset of *Sox2* expressing cells that also express *Lgr5* (Jacques et al., 2012b; Munnamalai and Fekete, 2013; Shi et al., 2012, 2014). However, the mechanisms that regulate Wnt signaling activation, its interactions with the other signaling pathways to induce proliferation, and finally to restrict proliferation in the mature epithelium are still being investigated (Figure 1.2).

Hair cell development in the lateral line

Although drastically different, neuromast development parallels the development of the inner ear sensory organs. Current research in lateral line development and regeneration may provide great insight into the molecular mechanisms that control hair cell formation at a cellular level, given the advantages of studying development in superficial organs. The lateral line system develops from several cranial placodes which undergo dramatic morphogenetic processes to distribute neuromasts across the body surface (Piotrowski and Baker, 2014). Broadly, there are two developmental mechanisms by which neuromasts are formed: the anterior lateral line neuromasts originate from a placode that grows in a single direction, elongating itself and forming a sensory ridge from which neuromasts split through unknown mechanisms (Ghysen and Dambly-Chaudière, 2004; Nuñez et al., 2009). The posterior lateral line neuromasts, in contrast, arise from multiple migrating primordia that originate

in the placode and periodically deposits sensory organs while migrating across the midline of the trunk and tail of the developing larvae (Figure 1.3A-1.3C). The pre-migratory placode is also patterned by Retinoic Acid signaling (Sarrazin et al., 2010) and its most anterior region is specified as pro-neural through Delta-Notch mechanisms. This region is not migratory and expresses *neurod*; therefore it differentiates into the neurons of the lateral line ganglion (Mizoguchi et al., 2011). During neuronal differentiation, the anterior placode undergoes a first round of morphogenesis, forming the first neuromasts and a posterior mesenchymal population that is actively expressing Wnt signaling called leading region. The leading region expresses FGF ligands like *fgf3* and *fgf10* under the control of Wnt/β-catenin signaling to activate FGF signaling in the immediate newly formed neuromasts attached to the leading region. The Wnt region and the FGF region express different chemokine receptors that promote placode migration towards the tail. FGF signaling restricts Wnt signaling to the leading region by inducing the expression of the Wnt inhibitor *dkk1b* to maintain the two expression domains and promote migration (Aman and Piotrowski, 2008). During this process, new neuromasts are formed by the leading region through mechanisms not well understood. Notch signaling seems to play a similar role as in the inner ear during neuromast formation, since it can modulate FGF signaling in the forming neuromast and restrict the expression of *Atoh1* (Figure 1.3.D) (Matsuda and Chitnis, 2010). While Wnt signaling plays mostly a patterning role by controlling FGF signaling and migration, its role on pro-sensory expansion becomes evident once neromasts split from the migrating primordium. It has

been recently proposed that neuromast growth during development and regeneration is controlled by an autoregulatory mechanism by which Wnt signaling promotes neuromast proliferation and hair cell differentiation. Hair cells then express *dkk2* which would suppress Wnt signaling and growth once the appropriate number of hair cells is reached (Figure 1.3E-1.3F)(Head et al., 2013; Jacques et al., 2014; Wada et al., 2013).

In all, hair cell formation requires of multiple proliferative signals that ensure the multiplication of the hair cell progenitors, combined with differentiation signals. The development of the proper number of hair cells seems to require a negative feedback mechanism that controls the sensory organ size and Notch and Wnt are important through vertebrates in regulating this process. In addition, hair cell development is always coupled to multiple other signaling events that drive mechanosensory organ morphogenesis. It is possible that the program for hair cell development is reused in vertebrate species to regenerate sensory hair cells. In Chapter 2, I will review the current knowledge about hair cell regeneration in vertebrates and provide some preliminary results of a gene expression analysis of hair cell regeneration.

Concluding remarks

- Vertebrate mechanosensory organs are formed of support cells and hair cells
- Inner ear hair cells in vertebrates and neuromast hair cells are homologous structures that share similar mechanisms of development.

- Atoh1 transcriptional program activates hair cell differentiation.
- The inner ear and lateral line developmental programs use multiple signaling pathways to modulate the temporal and spatial pattern of *Atoh1* gene expression and ultimately induce hair cell formation.
- Notch signaling is important for the binary steps of differentiation between the pro-neural and pro-sensory placodal domains, and between the support and hair cell fates.

References

Aman, A., and Piotrowski, T. (2008). Wnt/beta-catenin and Fgf signaling control collective cell migration by restricting chemokine receptor expression. Dev. Cell *15*, 749–761.

Baker, C. V, and Bronner-Fraser, M. (2001). Vertebrate cranial placodes I. Embryonic induction. Dev. Biol. *232*, 1–61.

Baker, C.V.H., O'Neill, P., and McCole, R.B. (2008). Lateral line, otic and epibranchial placodes: developmental and evolutionary links? J. Exp. Zool. B. Mol. Dev. Evol. *310*, 370–383.

Bok, J., Chang, W., and Wu, D.K. (2007). Patterning and morphogenesis of the vertebrate inner ear. Int. J. Dev. Biol. *51*, 521–533.

Brooks, A.N., Kilgour, E., and Smith, P.D. (2012). Molecular pathways: fibroblast growth factor signaling: a new therapeutic opportunity in cancer. Clin. Cancer Res. *18*, 1855–1862.

Cai, T., Jen, H.-I., Kang, H., Klisch, T.J., Zoghbi, H.Y., and Groves, A.K. (2015). Characterization of the transcriptome of nascent hair cells and identification of direct targets of the atoh1 transcription factor. J. Neurosci. *35*, 5870–5883.

Chai, R., Xia, A., Wang, T., Jan, T.A., Hayashi, T., Bermingham-McDonogh, O., and Cheng, A.G.-L. (2011). Dynamic expression of Lgr5, a Wnt target gene, in the developing and mature mouse cochlea. J. Assoc. Res. Otolaryngol. *12*, 455–469.

Chatterjee, S., Kraus, P., and Lufkin, T. (2010). A symphony of inner ear

developmental control genes. BMC Genet. *11*, 68.

Clevers, H., Loh, K.M., and Nusse, R. (2014). An integral program for tissue renewal and regeneration: Wnt signaling and stem cell control. Science (80-.). *346*, 1248012–1248012.

Cruciat, C.-M., and Niehrs, C. (2013). Secreted and transmembrane wnt inhibitors and activators. Cold Spring Harb. Perspect. Biol. *5*, a015081.

Eaton, S. (1997). Planar polarization of Drosophila and vertebrate epithelia. Curr. Opin. Cell Biol. *9*, 860–866.

Ekdale, E.G. (2015). Form and function of the mammalian inner ear. J. Anat. n/a – n/a.

Fritzsch, B., and Straka, H. (2014). Evolution of vertebrate mechanosensory hair cells and inner ears: toward identifying stimuli that select mutation driven altered morphologies. J. Comp. Physiol. A. Neuroethol. Sens. Neural. Behav. Physiol. *200*, 5–18.

Fritzsch, B., Beisel, K.W., Pauley, S., and Soukup, G. (2007). Molecular evolution of the vertebrate mechanosensory cell and ear. Int. J. Dev. Biol. *51*, 663–678.

Fritzsch, B., Pan, N., Jahan, I., Duncan, J.S., Kopecky, B.J., Elliott, K.L., Kersigo, J., and Yang, T. (2013). Evolution and development of the tetrapod auditory system: an organ of Corti-centric perspective. Evol. Dev. *15*, 63–79.

Ghysen, A., and Dambly-Chaudière, C. (2004). Development of the zebrafish lateral line. Curr. Opin. Neurobiol. *14*, 67–73.

Groves, A.K., and Fekete, D.M. (2012). Shaping sound in space: the regulation of inner ear patterning. Development *139*, 245–257.

Hartman, B.H., Reh, T.A., and Bermingham-McDonogh, O. (2010). Notch signaling specifies prosensory domains via lateral induction in the developing mammalian inner ear. Proc. Natl. Acad. Sci. *107*, 15792–15797.

Head, J.R., Gacioch, L., Pennisi, M., and Meyers, J.R. (2013). Activation of canonical Wnt/β-catenin signaling stimulates proliferation in neuromasts in the zebrafish posterior lateral line. Dev. Dyn. *242*, 832–846.

Jacques, B.E., Puligilla, C., Weichert, R.M., Ferrer-Vaquer, A., Hadjantonakis, A.-K., Kelley, M.W., and Dabdoub, A. (2012a). A dual function for canonical Wnt/β-catenin signaling in the developing mammalian cochlea. Development *139*, 4395–4404.

Jacques, B.E., Puligilla, C., Weichert, R.M., Ferrer-Vaquer, A., Hadjantonakis, A.-K., Kelley, M.W., and Dabdoub, A. (2012b). A dual function for canonical Wnt/β-catenin signaling in the developing mammalian cochlea. Development *139*, 4395–4404.

Jacques, B.E., Montgomery, W.H., Uribe, P.M., Yatteau, A., Asuncion, J.D., Resendiz, G., Matsui, J.I., and Dabdoub, A. (2014). The role of Wnt/β-catenin signaling in proliferation and regeneration of the developing basilar papilla and lateral line. Dev. Neurobiol. *74*, 438–456.

Jansson, L., Kim, G.S., and Cheng, A.G. (2015). Making sense of Wnt signaling—linking hair cell regeneration to development. Front. Cell. Neurosci. *9*, 66.

Jorgensen, J.M. (1989). The Mechanosensory Lateral Line (New York, NY: Springer New York).

López-Schier, H., and Hudspeth, A.J. (2006). A two-step mechanism underlies the planar polarization of regenerating sensory hair cells. Proc. Natl. Acad. Sci. U. S. A. *103*, 18615–18620.

López-Schier, H., Starr, C.J., Kappler, J.A., Kollmar, R., and Hudspeth, A.J. (2004). Directional cell migration establishes the axes of planar polarity in the posterior lateral-line organ of the zebrafish. Dev. Cell *7*, 401–412.

Lundberg, Y.W., Xu, Y., Thiessen, K.D., and Kramer, K.L. (2015). Mechanisms of otoconia and otolith development. Dev. Dyn. *244*, 239–253.

Lush, M.E., and Piotrowski, T. (2014). Sensory hair cell regeneration in the zebrafish lateral line. Dev. Dyn. *243*, 1187–1202.

Matsuda, M., and Chitnis, A.B. (2010). Atoh1a expression must be restricted by Notch signaling for effective morphogenesis of the posterior lateral line primordium in zebrafish. Development *137*, 3477–3487.

Millimaki, B.B., Sweet, E.M., Dhason, M.S., and Riley, B.B. (2007). Zebrafish atoh1 genes: classic proneural activity in the inner ear and regulation by Fgf and Notch. Development *134*, 295–305.

Mizoguchi, T., Togawa, S., Kawakami, K., and Itoh, M. (2011). Neuron and Sensory Epithelial Cell Fate Is Sequentially Determined by Notch Signaling in Zebrafish Lateral Line Development. J. Neurosci. *31*, 15522–15530.

Modrell, M.S., Bemis, W.E., Northcutt, R.G., Davis, M.C., and Baker, C.V.H. (2011). Electrosensory ampullary organs are derived from lateral line placodes in bony fishes. Nat. Commun. *2*, 496.

Müller, U., and Littlewood-Evans, A. (2001). Mechanisms that regulate mechanosensory hair cell differentiation. Trends Cell Biol. *11*, 334–342.

Munnamalai, V., and Fekete, D.M. (2013). Wnt signaling during cochlear development. Semin. Cell Dev. Biol. *24*, 480–489.

Neves, J., Abelló, G., Petrovic, J., and Giraldez, F. (2013). Patterning and cell fate in the inner ear: a case for Notch in the chicken embryo. Dev. Growth Differ. *55*, 96–112.

Nicolson, T. (2005). The Genetics of Hearing and Balance in Zebrafish Teresa. Annu. Rev. Genet. *39*, 9–22.

Niehrs, C. (2006). Function and biological roles of the Dickkopf family of Wnt modulators. Oncogene *25*, 7469–7481.

Niehrs, C. (2012). The complex world of WNT receptor signalling. Nat. Rev. Mol. Cell Biol. *13*, 767–779.

Nuñez, V. a, Sarrazin, A.F., Cubedo, N., Allende, M.L., Dambly-Chaudière, C., and Ghysen, A. (2009). Postembryonic development of the posterior lateral line in the zebrafish. Evol. Dev. *11*, 391–404.

O'Neill, P., Mak, S.-S., Fritzsch, B., Ladher, R.K., and Baker, C.V.H. (2012). The amniote paratympanic organ develops from a previously undiscovered sensory placode. Nat. Commun. *3*, 1041.

Ono, K., Kita, T., Sato, S., O'Neill, P., Mak, S.-S., Paschaki, M., Ito, M., Gotoh, N., Kawakami, K., Sasai, Y., et al. (2014). FGFR1-Frs2/3 signalling maintains sensory progenitors during inner ear hair cell formation. PLoS Genet. *10*, e1004118.

Perdigoto, C.N., and Bardin, A.J. (2013). Sending the right signal: Notch and stem cells. Biochim. Biophys. Acta *1830*, 2307–2322.

Piotrowski, T., and Baker, C.V.H. (2014). The development of lateral line placodes: taking a broader view. Dev. Biol. *389*, 68–81.

Sai, X., and Ladher, R.K. (2015). Early steps in inner ear development: induction and morphogenesis of the otic placode. Front. Pharmacol. *6*, 19.

Sancho, R., Cremona, C.A., and Behrens, A. (2015). Stem cell and progenitor fate in the mammalian intestine: Notch and lateral inhibition in homeostasis and disease. EMBO Rep. *16*, 571–581.

Sarrazin, A.F., Nunez, V.A., Sapede, D., Tassin, V., Dambly-Chaudiere, C., and

Ghysen, A. (2010). Origin and Early Development of the Posterior Lateral Line System of Zebrafish. J. Neurosci. *30*, 8234–8244.

Schlosser, G. (2010). Making senses development of vertebrate cranial placodes. Int. Rev. Cell Mol. Biol. *283*, 129–234.

Schwander, M., Kachar, B., and Müller, U. (2010). Review series: The cell biology of hearing. J. Cell Biol. *190*, 9–20.

Shi, F., Kempfle, J.S., and Edge, A.S.B. (2012). Wnt-responsive Lgr5-expressing stem cells are hair cell progenitors in the cochlea. J. Neurosci. *32*, 9639–9648.

Shi, F., Hu, L., Jacques, B.E., Mulvaney, J.F., Dabdoub, A., and Edge, A.S.B. (2014). β-Catenin is required for hair-cell differentiation in the cochlea. J. Neurosci. *34*, 6470–6479.

Sienknecht, U.J., Köppl, C., and Fritzsch, B. (2014). Evolution and development of hair cell polarity and efferent function in the inner ear. Brain. Behav. Evol. *83*, 150–161.

Sprinzak, D., Lakhanpal, A., Lebon, L., Santat, L.A., Fontes, M.E., Anderson, G.A., Garcia-Ojalvo, J., and Elowitz, M.B. (2010). Cis-interactions between Notch and Delta generate mutually exclusive signalling states. Nature *465*, 86–90.

Tissir, F., and Goffinet, A.M. (2013). Shaping the nervous system: role of the core planar cell polarity genes. Nat. Rev. Neurosci. *14*, 525–535.

Turner, N., and Grose, R. (2010). Fibroblast growth factor signalling: from development to cancer. Nat. Rev. Cancer *10*, 116–129.

Wada, H., Ghysen, A., Asakawa, K., Abe, G., Ishitani, T., and Kawakami, K. (2013). Wnt/Dkk negative feedback regulates sensory organ size in zebrafish. Curr. Biol. *23*, 1559–1565.

Wang, V.Y., Hassan, B.A., Bellen, H.J., and Zoghbi, H.Y. (2002). Drosophila atonal Fully Rescues the Phenotype of Math1 Null Mice. Curr. Biol. *12*, 1611–1616.

Whitfield, T.T. (2002). Zebrafish as a model for hearing and deafness. J. Neurobiol. *53*, 157–171.

Whitfield, T.T., and Hammond, K.L. (2007). Axial patterning in the developing vertebrate inner ear. Int. J. Dev. Biol. *51*, 507–520.

Wu, D.K., and Kelley, M.W. (2012). Molecular mechanisms of inner ear development. Cold Spring Harb. Perspect. Biol. *4*, a008409.

Figure 1.1. Hair cells and vertebrate mechanosensory systems.
(A) Mechanosensory hair cell. (B) Simplified schematics of a sensory epithelia (macular organ). Hair cells show opposite polarities. (C) The inner ear is a sensory system located in the head of every vertebrate. The lateral line mechanosensory organs (blue dots) are distributed across the surface of aquatic vertebrates. (D) Main sensory organs within the vertebrate inner ear (Red dots). (E-F) Lateral line neuromast. (E) Horizontal view. (F) Lateral view.

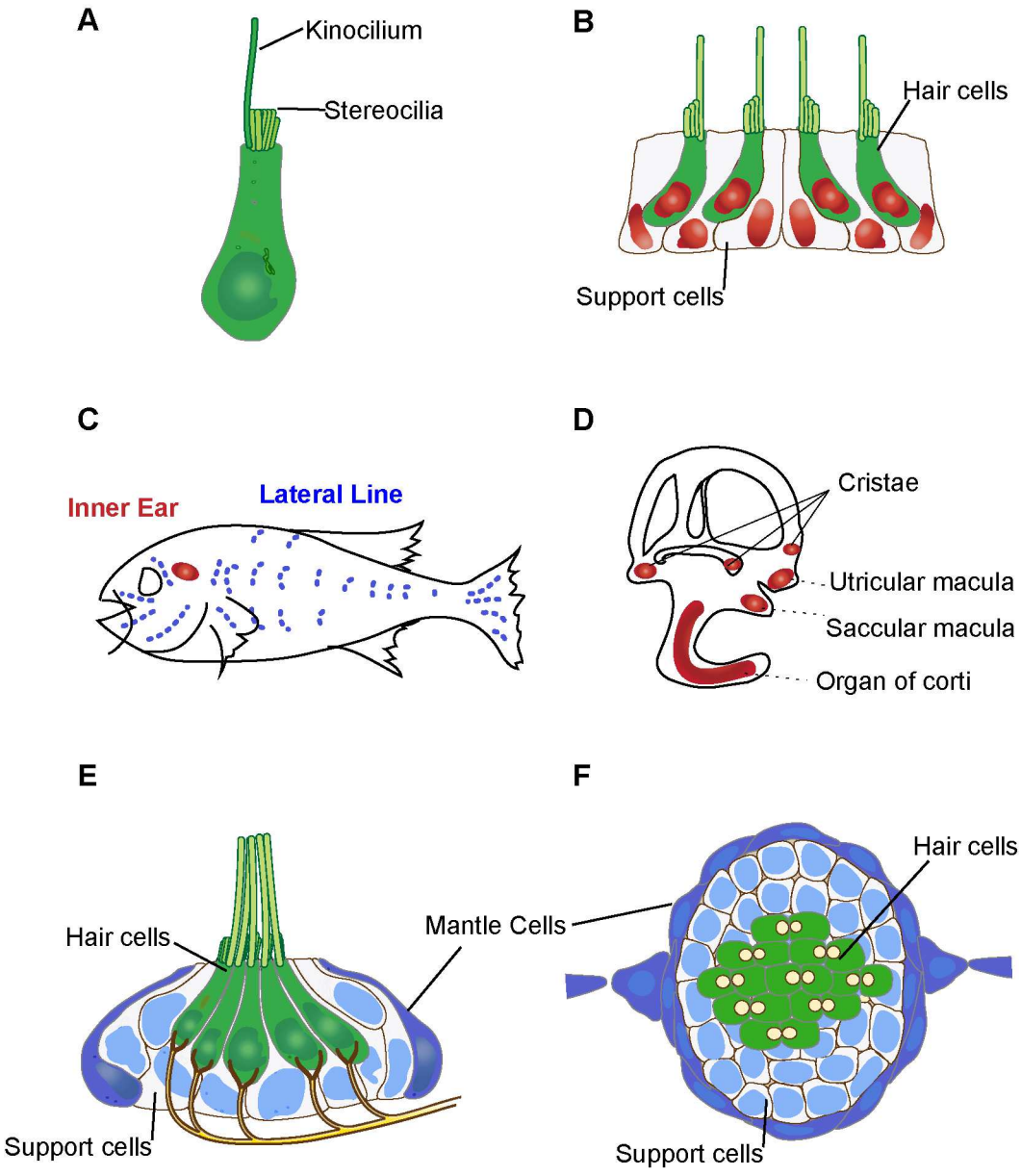
A
Kinocilium
Stereocilia
B
Hair cells
Support cells
C
Inner Ear
Lateral Line
D
Cristae
Utricular macula
Saccular macula
Organ of corti
E
Hair cells
Mantle Cells
Support cells
F
Hair cells
Support cells

Figure 1.2. General mechanism of hair cell differentiation from a neurosensory placode.
Wnt can induce *atoh1a* expression in early sensory development, and also proliferation in the pro-sensory cells. The interaction between Wnt and Notch during hair cell formation is still unknown.

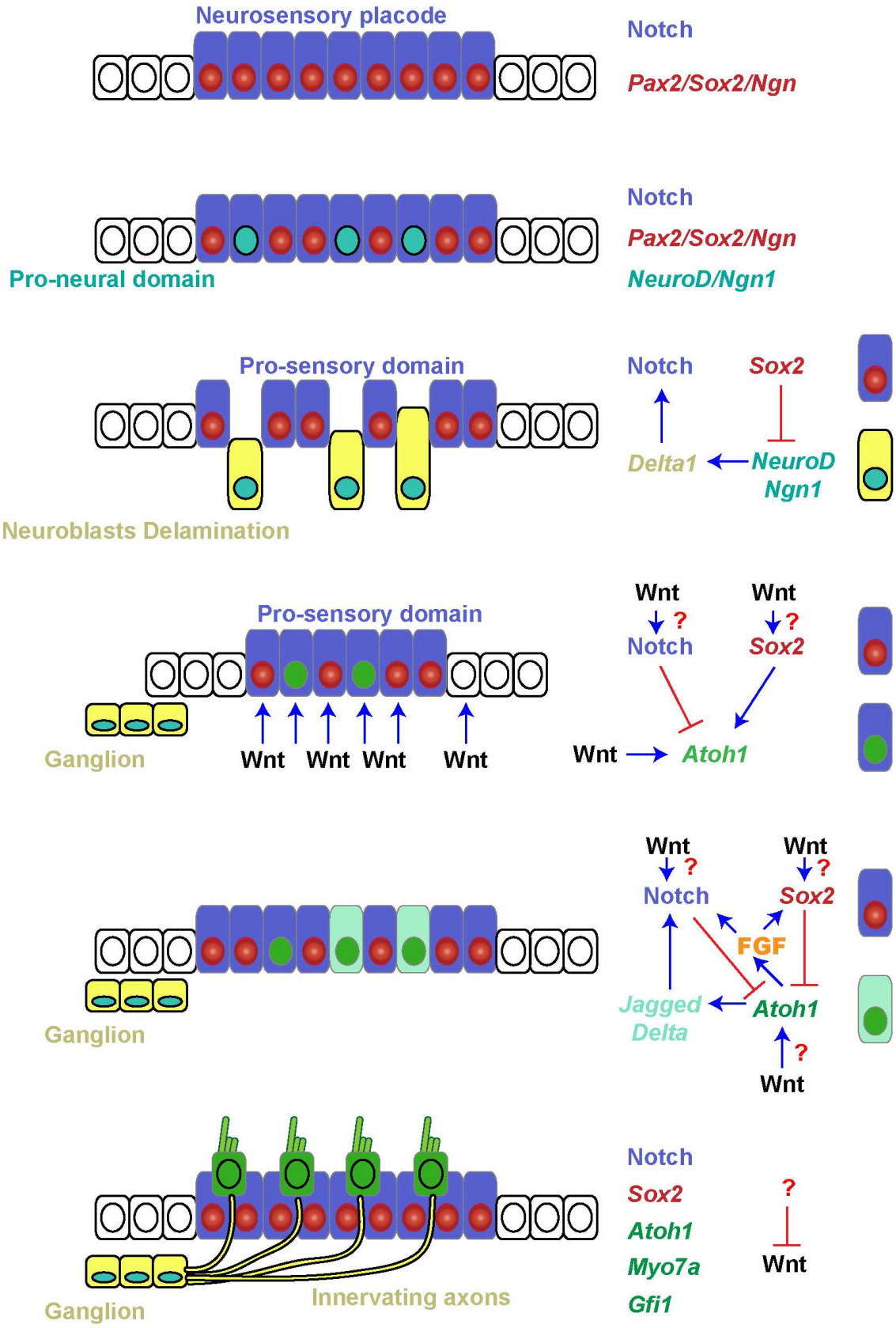
Neurosensory placode
Notch
Pax2/Sox2/Ngn
Notch
Pax2/Sox2/Ngn
Pro-neural domain
NeuroD/Ngn1
Pro-sensory domain
Notch
Sox2
Delta1
NeuroD
Ngn1
Neuroblasts Delamination
Pro-sensory domain
Wnt
Wnt
?
?
Notch
Sox2
Ganglion
Wnt
Wnt
Wnt
Wnt
Wnt
Atoh1
Wnt
Wnt
?
?
Notch
Sox2
FGF
Ganglion
Jagged
Delta
Atoh1
?
Wnt
Notch
Sox2
Atoh1
Myo7a
Gfi1
?
Wnt
Ganglion
Innervating axons

Figure 1.3. Hair cell development in the zebrafish lateral line
(A) The otic placode (red) and the lateral line placode (blue) are induced in separate domains at the cranial ectoderm. (B) The posterior lateral line neuromast develop from a migrating placode called primordium (C). (D) Schematics illustrating the main expression domains in the migrating primordium. Although the leading region is mostly composed of mesenchymal cells and the trailing region is mostly composed of forming rosettes, the actual boundaries of the expression domains are unknown and the colors only illustrate approximate expression patterns. The Wnt target gene and secreted FGF ligand *fgf3* (together with *fgf10*) activates FGF signaling in the trailing region. The Wnt target gene and FGF inhibitor *sef* inhibits FGFR activation in the leading region and maintains the leading-trailing boundaries. The FGF target gene and Wnt inhibitor *dkk1b* is expressed approximately in the leading-trailing boundary and restricts Wnt signaling to the leading region (Aman and Piotrowski, 2008). Notch and FGF signaling can modulate *atoh1a* in central cells of the primordium, where hair cells possibly develop (Matsuda and Chitnis, 2010). (E-F) Although the origin of the Wnt activating signal is unknown, it has been proposed that hair cell formation and differentiation require Wnt signaling. Hair cells on the other hand express *dkk2* which would block hair cell differentiation (Wada et al., 2013).

A

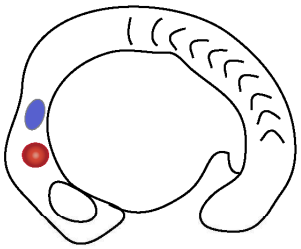

B

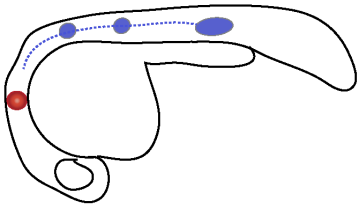

C

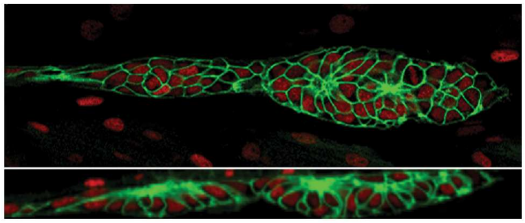

cldnB:lynGFP;cldnB:H2A-mCherry

D

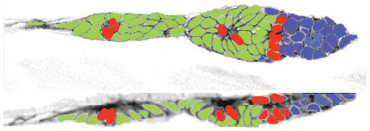

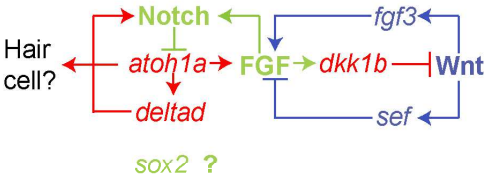

Matsuda and Chitnis, 2010

Aman and Piotrowski, 2008

E

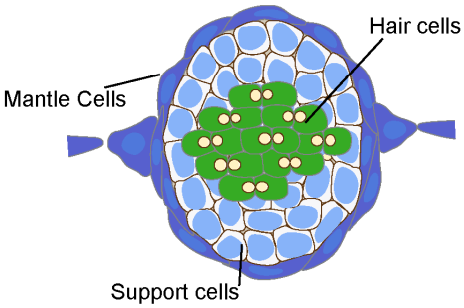

F

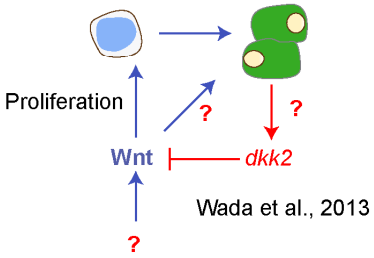

Wada et al., 2013

CHAPTER 2

SUPPORT CELL EARLY RESPONSES TO HAIR CELL DEATH AND THE ROLE OF *SPALT-LIKE 1B* IN HAIR CELL REGENERATION

Abstract

Our current understanding about mechanosensory hair cell regeneration is limited. The zebrafish lateral line mechanosensory organs or neuromasts are an emerging model for the study of hair cell regeneration. These organs are composed of a central group of hair cells, a surrounding population of support cells and the outer mantle cells. Support cells regenerate hair cells through mitosis; however, the molecular mechanisms that trigger this response are unknown. We performed a microarray analysis using RNA samples from a mantle cell-specific transgenic line 1 hr post hair cell death. The analysis shows a striking down-regulation of the Notch signaling pathway and many transcription factors involved in lateral line development, and particularly, pluripotency markers from the SoxB1 family evidencing role of transcription in the regenerative response. The transcriptional repressor *spalt-like1b (sall1b)* is one of the most up-regulated genes in the microarray and is expressed in central cells of the lateral line primordium and in mature neuromasts. Silencing of *sall1b* by using splice-blocking morpholinos affects the number of deposited

neuromasts without affecting cell migration and may also play a role in hair cell and rosette formation during neuromast development. A gene expression analysis of morphant embryos showed that silencing of *sall1b* induces upregulation of Wnt and Fgf target genes, both interdependent pathways involved in primordium migration and neuromast development. *sall1b* silencing also enhances *sox2* expression, an inner support cell marker that is not expressed in hair cells.

Introduction

Regenerative capabilities differ among taxa and have become very restricted in higher vertebrates. Mammals are incapable of regenerating the mechanosensory hair cells in the inner ear epithelium, which in the case of humans bears high biomedical and public health importance. Given the power and amenability of the zebrafish for genetics and developmental biology, combined with the accessibility of the lateral line organs for analysis in vivo, the zebrafish posterior lateral line system has become an enlightening tool for the study of mechanosensory hair cell function and sensory organ regeneration (Brignull et al., 2009; Lush and Piotrowski, 2014a).

Hair cell death

Like other post-mitotic sensory cells, hair cells are prone to cell death. The main causes of hair cell death are ageing, chronic or acute exposure to high-intensity stimuli, and chemical-induced hair cell toxicity (ototoxins). These events

generate reactive oxygen species (ROS) and trigger apoptosis, necrosis, and scaring in the sensory epithelia (Furness, 2015). Ageing causes mitochondrial dysfunction and oxidative stress, possibly following a miRNA-mediated senescence program (McFadden et al.; Zhang et al., 2013). Age-related loss of hair cells has only been analyzed in mammals where hair cells are expected to survive during the animal's life time. On the contrary, hair cells in chicken or zebrafish have much shorter lifespans and they are constantly replaced (Cruz et al., 2015; Kil et al., 1997). High-intensity noise produce physical damage or toxic effects to inner ear hair cells in most studied vertebrates including fish (Cotanche, 1999; Monroe et al., 2015). Noise cellular toxicity is tonotopic and related to the expression of calcium sensing proteins and channels which will alter calcium metabolism and ultimately activate inflammation, extrinsic apoptotic signals, and ROS (Esterberg et al., 2013; Furness, 2015). Ototoxins are chemical compounds that, selectively or not, can kill hair cells. Water pollutants like Copper, aminoglycosides like neomycin, kanamycin or streptomycin, and heavy metal-based chemotherapeutic agents like cisplatin are all known ototoxins. The toxicity of these compounds is often related to the cellular structure of hair cells, which explains hair sensitivity to multiple environmental insults. In fact, hair cell mechanotransducer channels are required for aminoglycoside toxicity and hair cell specific large-ion channels facilitate the toxic effect of copper or cisplatin (Alharazneh et al., 2011; Thomas et al., 2013).

Regeneration in the inner ear and lateral line

Most of the adult support cells in the mammalian inner ear are post-mitotic. Therefore, the main response after hair cell death is the formation of a scar by the surrounding support cells. Although the damage does not leave an acellular scar, the surrounding support cells do not proliferate in response to hair cell death but rather displace and cover the wound site, closing the epithelium without replacing hair cells (Raphael and Altschuler, 1991; Raphael et al., 2007). Although the support cells share the same developmental origin with hair cells, the gene expression profile of the scar cells is currently unknown, nor is the reason why these cells do not undergo differentiation. Importantly, *Sox2* is expressed in the damaged sensory epithelium, and the forced induction of *Atoh1* in this cells does not guarantee hair cell formation (Oesterle et al., 2008; Yang et al., 2012). In addition, Notch and Wnt signaling pathways are not active in the mature mammalian support cells (Maass et al., 2015). This might be the reason why the activation of β-catenin, the inhibition of Notch signaling, or even the silencing of cell cycle inhibitors like *Cdkn1* do not induce proliferation in the mature sensory epithelium of mammals and only have an effect in the early post-natal days (Bramhall et al., 2014; Jeon et al., 2011; Li et al., 2014; Shi et al., 2012, 2013; Walters et al., 2014). The lack of mammalian regeneration suggests adult support cells have an independent genetic program that still needs to be unraveled. Indeed, other signaling pathways and its interactions might also be involved in the hair cell differentiation process, and further understanding of the mechanisms is sorely needed.

In contrast, the ability to regenerate mechanosensory hair cells is widespread among nonmammalian vertebrates. Hence, the study of hair cell regeneration in regenerative species may bring to light new insights in the field of hair cell regeneration (Brignull et al., 2009). In the avian inner ear, hair cells are regenerated from the support cells through two main mechanisms: cell division and trans-differentiation. Mitosis after hair cell death occurs immediately after injury in the avian utricle but is delayed in the cochlea where trans-differentiation occurs first (Roberson et al., 2004). Transdifferentiating cells are post-mitotic cells that become hair cells without cell division. The mitotic events in the cochlea are mostly to replace the support cell population by generating a pair of support cells. However, mitosis can also produce a pair of hair cells, or a hair cell and a support cell, possibly through asymmetric cell division (Stone and Cotanche, 2007).

The molecular mechanisms of regeneration in the avian inner ear are still being uncovered and clearly resemble the mechanisms of hair cell development. After injury, *Atoh1* expression is upregulated in most of the injured epithelium, but the Atoh1 protein is only detected in the nucleus of the support cells that will differentiate (Stone and Cotanche, 2007; Stone and Rubel, 2000). Multiple signaling pathways seem to play an active role in the processes of proliferation and differentiation. Notch signaling is present in the mature epithelium and the inhibition of Notch signaling promotes excessive hair cell differentiation by trans-differentiation or mitosis, but only after injury (Daudet et al., 2009). A subsequent RNAseq analysis of regenerating cultured utricles found *Hes5* is downregulated

48hrs after hair cell ablation, a timepoint where *Atoh1* and other hair cell markers start to accumulate. The regulation of *Hes5* among other Notch target genes seems to be oscillatory (Ku et al., 2014). In contrast, Wnt target genes did not show significant changes during the regeneration timecourse, in spite of the fact that in a previous siRNA screen, it was discovered that the Wnt and Jnk-AP1 signaling pathways are required for proliferative response in cultured utricles (Alvarado et al., 2011). In addition to changes in Notch signaling, FGF signaling also responds to hair cell death. FGF activation has a negative role over proliferation and occurs progressively through regeneration (Ku et al., 2014). The dynamic changes in Notch gene expression and its important role in regulating *Atoh1* gene expression pinpoint this pathway as a major regulator of the regenerative process. However, the number of Notch ligands and receptors important for regeneration, its oscillatory nature, and the mechanism of controlled notch activation and suppression are completely unknown due to the lack of experimental analysis. In addition, other signaling pathways are active during the regenerative process and most likely interact with Notch. It is also unknown how the above described mechanisms coordinate the cellular proliferative response and the differentiation events.

In the mature zebrafish neuromasts, mitosis is required for hair cell regeneration and there is no evidence of hair cell transdifferentiation (Wibowo et al., 2011). The support cells exhibit increased BrdU incorporation as early as 12 hrs post hair cell death compared to the outer support cells, which show reduced BrdU incorporation and regeneration is complete within 72 hrs (Harris et al.,

2003; Ma et al., 2008; Mackenzie and Raible, 2012). Therefore, support cells might have different responses during regeneration. Indeed, although there has been great progress in developing strategies for generating new hair cells from a pool of progenitors, the cellular and molecular mechanism for restoring the sensory epithelium are less known. Previously, it has been suggested that the mantle cells are multipotent progenitors (Ghysen and Dambly-Chaudière, 2007; Jones and Corwin, 1993; Steiner et al., 2014; Williams and Holder, 2000). Mantle cells and the interneuromast cells share the transgenic marker *sqet20* (Parinov et al., 2004). The interneuromast cells are known multipotent cells since they generate complete neuromasts during post-embryonic development (Grant et al., 2005; Lush and Piotrowski, 2014b). Accordingly, mantle cells should be able to self-renew and also generate inner support cells and hair cells. This hypothesis is supported by previous observations that some peripheral support cells have different proliferative capacity compared to central support cells (Williams and Holder, 2000). Still, the role of these nondifferentiating mitotic events remains elusive due to the lack of a clear lineage analysis of the different support cell populations of the neuromast. In addition, the potency of mantle cells to generate inner support cells or hair cells is still unknown.

Despite of the lack of transdifferentiation, the molecular mechanisms of regeneration are very similar between the avian inner ear and the zebrafish neuromasts. In zebrafish, *atoh1* is also upregulated in the support cell population after hair cell death and Notch restricts the extent of hair cell regeneration (Ma et al., 2008). Since the ectopic activation of Notch signaling blocks regeneration

(Wibowo et al., 2011), Notch controlled downregulation and reactivation might be the main strategy for hair cell regeneration; still, the actual signals that respond to hair cell death and triggers the regenerative process are currently unknown. On the other hand, inhibiting notch signaling does not induce proliferation unless there is hair cell injury. Therefore, the signals for differentiation and proliferation might be uncoupled. Wnt signaling has also been implicated in neuromast hair cell regeneration since the use of the GSK3β inhibitors 1-Azakenpaullone (Head et al., 2013) or LiCl (Jacques et al., 2012) induce an increase in support cell proliferation and a mild increase in hair cell regeneration. Although it is clear that Wnt and Notch are required for tissue homeostasis, the mechanisms that activate these signals, and those that modulate them during regeneration, are yet to be discovered. Indeed, other pathways might be interacting with the above mentioned canonical signals. Previous gene expression analyses after noise-induced hair cell death in the zebrafish inner ear ambiguously pointed to cytokine-Stat signaling as important for hair cell regeneration. The growth hormone, *stat3* and *socs3* transcripts are upregulated at different timepoints after injury, and the addition of growth hormone enhances support cell proliferation (Schuck et al., 2011). Oddly, the inhibition of Stat phosphorylation caused a mild improvement in the regenerating response (Liang et al., 2012).

The experiments presented in this chapter are part of an initial effort to analyze early responses to hair cell death using RNA microarrays, and describe preliminary unpublished data. Through this approach, we were able to find evidence of Notch signaling downregulation 1 hr after hair cell death. We also

identified some new Wnt target genes that are upregulated after hair cell death, and performed some functional analysis to validate the role of *spalt-like 1b* (sall1b) in lateral line development. After sampling the first timepoint after hair cell death, and while validating the results of this microarray, another member of the laboratory performed a gene expression analysis in the regenerating lateral line using RNA sequencing with different cell dissociation and cell sorting protocols (Jiang et al., 2014). Through this approach, we were able to show that Wnt, Notch, Jak-Stat, and Bmp signaling suffer important changes in gene expression in the first 10 hrs after hair cell death. These results suggest a different regeneration strategy that may involve multiple signaling crosstalks and a higher complexity than what has been previously described. Importantly, a thorough comparison between the results of the microarray presented in this chapter and the early timepoint of the RNAseq data (not shown; Jiang et al., 2014) determined an overlapping dataset no higher than 40%, which is understandable, due to the drastic differences in methods and sample processing.

Preliminary results and future directions

Identification of early-response genes involved in hair cell regeneration.

The molecular mechanisms that determine if support cells self-renew or differentiate into hair cells in response to hair cell death in the neuromast are unknown. In order to address early transcriptional changes in response to hair cell death, we induced hair cell death in mature neuromasts by treating 5 days

post fertilization (dpf) *Et(krt4:EGFP)^{sqet20}* (*sqet20*) transgenic larvae with the aminoglycoside antibiotic neomycin (Harris et al., 2003). The *sqet20* transgene is an enhancer trap that drives GFP expression in the interneuromast cells, mantle cells and with less strength in support cells, and other tissues (Figure 2.1A). To analyze gene expression changes specific to the neuromast response, we reduced the amount of non-neuromast GFP+ tissue by using only the post-cloacal tail for cell dissociation, according to the protocol detailed in experimental procedure (Figure 2.1B-2.1E). RNA samples for GFP+ and GFP- cells, 1 hr after neo treatment and mock treated larvae, were hybridized on custom made 44K Agilent microarray chips. The chips were designed by Chris Seidel at the Stowers Institute for Medical Research (SIMR), and consisted of 24962 printed oligoprobes from the *Danio rerio* VEGA40 array (2011) plus 18691 oligoprobes of interest from the previously available *Danio rerio* AgilentV3 array (2009). Due to the constant curation of the zebrafish genome sequence, the probes from the initial array were re-blasted to the Zv9 version of the zebrafish genome, and 70% of the initially printed probes retrieved a perfect alignment. All the bioinformatics analyses were done on this new dataset, and the fold change was adjusted for the reduced number of probes. From the total collection of tested transcripts, 309 showed 1 fold changes or more with a confidence significance of $p < 0.05$ (Figure 2.1F-2.1H). To validate the results, I generated in situ hybridization probes from the 3'UTR of the first 10 up- and downregulated transcripts in the list plus some additional interesting genes (Table 2.1). Indeed, most of these genes were expressed in the inner ear, the posterior lateral line primordium, and in

mature neuromasts (Figures 2.2. and 2.3.). While most of the upregulated genes showed an ubiquitous expression and a barely legible response to neomycin, some of them showed striking expression patterns in the primordium central cells (*sall1b, bcl2l10, si:busm1-57f23.1, and A_15_P760286*) or in the cells that surround the primordium (*lima1*). On the other hand, most of the validated downregulated genes had very specific expression patterns in the migrating primordium, in the leading edge (*sox1a*), in the trailing region (*sox2*), and in central cells (*si:ch211-235e18.3*, *sox1b* and *sox3*) (Figure 2.3.). The neomycin response was difficult to address at 1 hr post neomycin; however, some transcripts did show important responses to hair cell death (Figure 2.4.). The in situ hybridization legibility of the response to neomycin depended highly on the quality of the probe and the amount of background during the alkaline-phosphatase developing reaction. Other downregulated transcripts were not expressed in the primordium but had specific expression patterns in the neuromast (*pvalb9*, *lad1* and *sost*). *sost* together with other genes like *wnt2* and *deltaa*, also present in the early response gene list, show polarized expression in the dorso-ventral cells of the neuromast. The fact that such genes have a restricted expression pattern within the support cell population suggests that support cells in the neuromast are not a homogeneous population, which is compelling evidence to search for heterogeneities in the cellular response to hair cell death and regeneration. The results of this project are described in Chapter 3.

Notch signaling is downregulated 1 hr after hair cell death

To test for the enrichment of pathways or biological processes controlled by the transcripts responding to hair cell death, we performed a GO term enrichment analysis (Table 2.2.). Strikingly, multiple transcripts from the Notch signaling pathway are downregulated 1 hr after hair cell death (Table 2.2.). These transcripts were distributed across various significantly enriched terms including “Notch signaling pathway” and “inner ear receptor cell differentiation”. This was the first piece of evidence that pinpointed important changes in Notch signaling after hair cell death and a possible role in the regeneration process. This result was confirmed by RNAseq and in-situ hybridization analysis of gene expression 1 hr, 3 hrs, and 5 hrs after hair cell death (Jiang et al., 2014). The hypothesis of a possible functional importance of the early downregulation of Notch signaling was tested in Chapter 3.

It was also surprising to find that the list of downregulated transcripts is significantly enriched for regulators of transcription, and most of these transcription factors are involved in lateral line and or hair cell development. Importantly, the SoxB1 transcription factors *sox1a, sox1b, sox2,* and *sox3* are among the top 10 most downregulated genes plus several pluripotency markers including *klf4, foxd3, pax2b, six2a, barhl1.2,* and *pou2f1* (Table 2.3).

The list of upregulated transcripts might be enriched for Wnt-target genes

The list of upregulated genes did not show enrichment for any GO term and the transcript list is composed of ubiquitously expressed transcripts, often unannotated and with unknown function (Figure 2.2). During *sall1b* probe validation by in situ hybridization, I used a batch of in-crossed of *apc*$^{mcr/+}$ mutant embryos and 25% of the stained embryos at 35 hours post fertilization (hpf) showed increased *sall1b* staining which was no longer in central cells but intensely expressed in every cell of the primordium (Figure 2.5C). *apc*^{mcr} is a non-sense mutation in the *adenomatous polyposis coli* gene that encodes the Wnt inhibiting protein APC, part of the β-catenin destruction complex (Hurlstone et al., 2003), and *apc*$^{mcr/mcr}$ embryos show Wnt upregulation in multiple tissues including the migrating primordium (Aman and Piotrowski, 2008). The mutant primordium also has an abnormal shape compared to the wild-type, which helped to confirm that the *sall1b* upregulation phenotype only occurred in *apc*$^{mcr/mcr}$ mutant primordia. Strikingly, most of the validated transcripts from the upregulated list showed increased gene expression in the *apc*$^{mcr/mcr}$ mutant primordium except for *irg1l* and *timp2b* which showed increased expression everywhere (Figure 2.5C). In contrast, transcripts from the downregulated set did not show any response in *apc*$^{mcr/mcr}$, aside from *sox2,* which maintained its expression in the trailing region, but still looked upregulated (Figure 2.5D). To confirm that this observation is due to Wnt activation, I used the FGFR inhibitor drug SU5402 to simultaneously block FGF signaling (hyperactive in *apc*$^{mcr/mcr}$),

and activate Wnt signaling (FGF signaling restricts Wnt signaling to the leading region of the primordium through *dkk1*; Figure 1.3. and 2.5B). This treatment indeed induced upregulation of most of the upregulated transcripts except *ugdh* and *lima1* (possible FGF signaling targets), and only induced upregulation of *sox1a* and *sox2* (possible targets of a different pathway inhibited by FGF). In all, this serendipitous experiment proved there is a potential enrichment of Wnt signaling targets in the transcripts that respond to hair cell death and that Wnt signaling might be active during the regeneration process. This was confirmed by RNAseq experiments, were Wnt targets and a Wnt reporter are activated during the regeneration process (Jiang et al., 2014). A functional analysis of wnt signaling and its interaction with Notch signaling during regeneration are described in Chapter 3.

The enrichment of Wnt target genes expressed in the lateral line primordium also suggested that the genes responding to hair cell death are actively playing a role in lateral line development, and that the regenerative response to hair dell death might be the reenactment of hair cell development, which occurs during the lateral line primordium migration. To address this point, I decided to do a functional analysis of candidate genes to dissect their role in lateral line development. I was particularly interested in multiple genes that showed expression in the central cells of the lateral line primordium.

The role of the primordium central cells in hair cell differentiation

The expression pattern of *sall1b* and other transcripts is restricted to the central cells of the migrating primordium and immature neuromast (Figure 2.6A and, 2.6B). On the contrary, *sox2* is a downregulated transcript expressed in the trailing region of the primordium with reduced expression in central cells (Figure 2.6C-2.6F). In mature neuromasts, *sall1b* signal is often not present, but is strongly upregulated early after hair cell death, in single cells, possibly support cells. *sox2,* in contrast, is clearly downregulated in most support cells (Figure 2.4B and 2.4C).

The central cells of the primordium are known to express the hair cell precursor marker *atoh1a* (Matsuda and Chitnis, 2010) and *deltad* (Figure 2.6E-2.6F). Hence, these cells might be possible hair cell progenitors. In order to test this, I manually traced back the first two formed hair cells of a deposited neuromast to their original position in the migrating primordium. Indeed the central cells of the second rosette were the origin of the 4 hair cells traced (Figure 2.6G-2.6H). The result suggests that *sall1b* might have a potential role in hair cell progenitor specification or differentiation.

The role of sall1b in lateral line development

sall1b is one of the vertebrate orthologues of the *Drosophila* zinc-finger transcription factor codified by the gene *spalt* (*sal*). *sal* is a known transcriptional repressor, which in *Drosophila* and in vertebrates is able to repress transcription through recruitment of the HDAC complex (Kiefer et al., 2002; Sánchez et al.,

2011). Notably, *sal* and *sal-related* are both required for differentiation of the mechanosensory neurons (insect hair cells) and binary decisions during the insect hearing organ (Johnston organ) development. These genes are co-expressed with the *atoh1* orthologue *atonal* in *Drosophila* (Boekhoff-Falk, 2005; Dong et al., 2003; Elstob et al., 2001). The role of *sall1* in vertebrates is yet to be elucidated; however, *sall1* expression is restricted within multiple tissues, including the inner ear, and mutations in this gene causes the Townes-Brocke syndrome which among other anomalies, includes sensorineural hearing loss (Duncan and Fritzsch, 2012; Fritzsch et al., 2013; Kohlhase et al., 1998). These pieces of evidence suggest *sal* and its orthologs might be part of the metazoan conserved pathway that control mechanosensory hair cell differentiation. Other spalt proteins play some major roles in regulating stem cell pluripotency; for example, the mammalian homolog *Sall4* can downregulate *Oct4*, *Sox2, c-Myc,* and *Klf4* expression in mouse embryonic stem cells (Sweetman and Münsterberg, 2006).

To test the role of *sall1b* in lateral line development, I designed two splice blocking morpholinos against the first exon-intron (EX1IN1) or the fourth intron-exon (IN2EX3) boundaries (Figure 2.7A). Although both morpholinos induced similar effects on injected larvae, I could only validate the effects of IN2EX3 through RT-PCR (Figure 2.7B). *sall1b* morphant embryos have less deposited neuromasts (Figures 2.7C-2.7D). Primordium migration, however, was not affected, as seen by the deposition of interneuromast cells (Figure 2.7C and 2.7E). In fact, the morphant primordium still deposits small metameric clumps of

cells that will form neuromasts later on (Figure 2.7E). Though the phenotype was consistent in multiple batches of injected embryos, the morphant phenotype must be validated by improving the RT-PCR technique, by addressing toxic effects of the morpholino, and by other means of *sall1b* silencing. We have designed TALENs for this gene that need to be tested. In all, *sall1b* may be playing a role in rosette formation during neuromast development.

A gene expression analysis of morphant embryos showed that the silencing of *sall1b* induces upregulation of the Wnt target genes *lef1* and *fgf3* (Figure 2.7H-2.7K), and the FGF target *pea3* (Figure 2.7F-2.7K). Morphants also have reduced expression of *dkk1b,* which explain the Wnt upregulation phenotype (Figure 2.7L-2.7M; Aman and Piotrowski, 2008). In addition, the expression levels of some genes involved in Notch signaling are not affected in *sall1b* morphants: however, its pattern is and they no longer have a centralized expression. Finally, *sall1b* morphats have significantly more *sox2* expression compared to controls (Figure 2.7R-2.7S).

The reduced number of deposited neuromasts and the upregulation of Wnt signaling resemble the phenotype of the *mindbomb* mutation, which causes loss of Notch signaling and also loss of *dkk1b*. Hence, it is possible that *sall1b* might be acting downstream or in parallel with Notch signaling in the process of central cell specification during neuromast development. In fact, Notch-FGF interactions are required to establish the central cell phenotype (Matsuda and Chitnis, 2010). Still, it is currently unknown how from the mesenchymal leading region of the primordium only a few central cells are specified instead of the

classical salt-and pepper pattern formed by Notch mediated lateral inhibition in other systems. According to my results, *sall1b* is a Wnt target gene (Figure 2.5C); therefore, *sall1b* could be a centralizing signal independent of FGF (Figure 2.7T). This also raises the possibility of *sall1b* acting as a transcriptional effector of Notch or FGF signaling. The results also suggest a role in hair cell specification since *sall1b* silencing also enhances *sox2* expression. *sox2* is a support cell marker that is not expressed in hair cells or in the central cells of the primordium. It remains to be determined how *sall1b* expression is restricted during development and what the role of *sall1b* during hair cell regeneration.

Once the effects of the morpholinos are correctly validated, it is definitely necessary to improve the analysis of the effects of the *sall1b* morpholino using more Notch, FGF, and Wnt target genes and analyze the epistatic effects of *sall1b* loss of function over Wnt, FGF, and Notch loss of functions. It is also necessary to determine the effect of Notch loss of function in *sall1b* expression. To further define the targets of *sall1b*, I also propose the elaboration of gain-of-function transgenic lines.

Experimental procedures

Fish lines and regeneration experiments

Zebrafish lines used: *Tg(clndB:lynGFP)*^{zf106} (Haas and Gilmour, 2006), *Tg(cldnB:H2A-mCherry)*^{psi4} (Lush and Piotrowski, 2014b), *Et(krt4:EGFP)*^{sqet20} or *sqet20* (Parinov et al., 2004), *sqet4* or *Tg(atp2b1a-GFP)* (Go et al., 2010), *apc*^{mcr} (Hurlstone et al., 2003). Hair cell death for regeneration assays was induced by

treating 5 dpf larvae for 30 min with 300μM neomycin-sulfate (Fisher Bioreagents) in 0.5X E2. Larvae were then rinsed three times in E2 medium.

Cell dissociation and FACS

The following protocol was designed by Tatjana Piotrowski, Danielle Downey, Robert Duncan, and Jim Jenkins at the University of Utah. Zebrafish embryos were sorted for GFP from the *sqet20* transgene and raised to 5 dpf. Around 600 larvae were treated with 300 μM Neomycin for 30 min to kill hair cells. 600 larvae were not treated as a control experiment. After treatment, larvae were washed 3 times in 0.5X E2, sedated with Tricaine (200 mg/mL in 0.5X E2) and their tails were dissected off by making a section posterior to the cloaca. Fins were collected in 2 ml tubes. For cell dissociation, fins were mechanically disrupted in Trypsin solution (0.5 g/L Trypsin, 0.14 M NaCl, 0.05 M KCl, 5 mM Glucose, 7 mM Na(HCO_3), 0.7 mM EDTA) by pipetting up and down for 15 min. Once single cells are visible in a wet preparation, debris was filtered using a 70 μm cell strainer (Falcon) and rinsed. The filtrate was centrifuged for 10 min at 3000 rpm and the supernatant removed. The cell pellet was resuspended in 1X PBS and filtered using a 35 μm cell strainer and rinsed with PBS. Cells were stained with 5 μg/ml Propidium Iodide (PI) for 10 min before sorting. Fluorescence activated cell sorting (FACS) was performed using a Becton Dickinson FACSvantage sorter and a 2 gate strategy. The first gate was to sort out debris and dead cells by addressing cell particle size and PI staining (PI x FSC). The second gate sorted out the cells that passed the first gate by sorting GFP intensity (GFP x FSC). Sorted cells were centrifuged for 10 min at 3000

rpm and the supernatant removed. For RNA extraction, the Ambion Aqueous micro or Quiagen Rneasy micro kits were used (Table 2.1.).

Microarray analysis of gene expression

Chip design, sample hybridization, and bioinformatics analyses were performed by Chris Seidel and Ariel Paulson at SIMR on 2011. Samples were hybridized on custom designed Agilent 44K using a two-color strategy (Cy3 and Cy5). 4 control replicates were hybridized to 4 regeneration replicates.

In situ hybridization

Primers for the genes detailed in Table 2.1. were designed manually from the 3' UTR region of the gene. PCR products were cloned into PCRII-TOPO plasmids using the TOPO cloning strategy (Invitrogen). In situ hybridization was performed as described in (Kopinke et al., 2006) with modifications for 5-day-old fish described in Ma *et al.* (2008). In situ hybridization was performed using an Intavis InSituPro robot. Images of stained embryos were acquired on a Zeiss Axio Observer microscope using an Axiocam camera.

Immunohistochemistry

Larvae were fixed in 4% PFA for 3 days before staining. Fixed larvae were progressively dehydrated to methanol incubate overnight at -20C. Larvae were rehydrated to 0.8% PBT (Tween-20), washed and permeabilized in dH2O for 1hr, and in acetone (7 min at -20 C). For the deltad antibody, larvae were not

dehydrated in methanol. Larvae were washed 0.8% PBT and blocked 2 hrs in 0.8% PBT + 10%NGS. Antibodies used: polyclonal rabbit anti-Sox2 (1:500; Abcam), monoclonal mouse anti-deltaD (zdd2/ Abcam, 1:50) and rabbit anti-GFP (1:500; Invitrogen).

Morpholino injections

Two morpholinos were designed for the 5' Exon1-Intron1 boundary (EX1IN1_MO: AAAGTCCTACCAAACTTACCGAGGA) and the Intron2Exon3 boundary (IN2EX3_MO: GTGAACCTGGATGGACATTTAAGAA; Gene Tools LLC). Morpholinos were diluted in 0.1M KCl and 5% phenol red.

Pharmacological inhibitors

The GSK3 selective inhibitor BIO (Sigma-Aldrich) and the FGFR inhibitor SU5402 (Tocris) were kept in 10 mM aliquots in DMSO, and diluted to the desired concentrations in 0.5X E2 media with a final concentration of 1% DMSO. Control larvae were treated with 1% DMSO.

Author contributions

This project was designed by Tatjana Piotrowki, Danielle Downey, and Jim Jenkins. Chris Seidel (SIMR) designed the Microarray chips, performed the RNA chip hybridization, and produced the list of up and downregulated genes. Ariel Paulson (SIMR) preformed the GO term enrichment analysis and the comparison between the microarray and the RNAseq experiments. I performed all the

experiments. Rob Duncan performed initial standardizations and improved the cell dissociation protocol. Jim Jenkins performed the FACS sorting of samples.

Acknowledgements

We are grateful to Mark Lush, MinhTu Nguyen, Megan Senecal, Andy Aman, Rob Crosbie, Rob Duncan, and Marina Venero-Galanternik for their time and help obtaining *sqet20* larva and cutting tails for the FACS experiment. We also thank Dr. Judith Eisen for providing the *deltad* antibody.

References

Alharazneh, A., Luk, L., Huth, M., Monfared, A., Steyger, P.S., Cheng, A.G., and Ricci, A.J. (2011). Functional hair cell mechanotransducer channels are required for aminoglycoside ototoxicity. PLoS One *6*, e22347.

Alvarado, D.M., Hawkins, R.D., Bashiardes, S., Veile, R.A., Ku, Y.-C., Powder, K.E., Spriggs, M.K., Speck, J.D., Warchol, M.E., and Lovett, M. (2011). An RNA interference-based screen of transcription factor genes identifies pathways necessary for sensory regeneration in the avian inner ear. J. Neurosci. *31*, 4535–4543.

Aman, A., and Piotrowski, T. (2008). Wnt/beta-catenin and Fgf signaling control collective cell migration by restricting chemokine receptor expression. Dev. Cell *15*, 749–761.

Boekhoff-Falk, G. (2005). Hearing in Drosophila: development of Johnston's organ and emerging parallels to vertebrate ear development. Dev. Dyn. *232*, 550–558.

Bramhall, N.F., Shi, F., Arnold, K., Hochedlinger, K., and Edge, A.S.B. (2014). Lgr5-positive supporting cells generate new hair cells in the postnatal cochlea. Stem Cell Reports *2*, 311–322.

Brignull, H.R., Raible, D.W., and Stone, J.S. (2009). Feathers and fins: non-mammalian models for hair cell regeneration. Brain Res. *1277*, 12–23.

Cotanche, D.A. (1999). Structural recovery from sound and aminoglycoside damage in the avian cochlea. Audiol. Neurootol. *4*, 271–285.

Cruz, I.A., Kappedal, R., Mackenzie, S.M., Hailey, D.W., Hoffman, T.L., Schilling, T.F., and Raible, D.W. (2015). Robust regeneration of adult zebrafish lateral line hair cells reflects continued precursor pool maintenance. Dev. Biol.

Daudet, N., Gibson, R., Shang, J., Bernard, A., Lewis, J., and Stone, J. (2009). Notch regulation of progenitor cell behavior in quiescent and regenerating auditory epithelium of mature birds. Dev. Biol. *326*, 86–100.

Dong, P.D.S., Todi, S. V, Eberl, D.F., and Boekhoff-Falk, G. (2003). Drosophila spalt/spalt-related mutants exhibit Townes-Brocks' syndrome phenotypes. Proc. Natl. Acad. Sci. U. S. A. *100*, 10293–10298.

Duncan, J.S., and Fritzsch, B. (2012). Evolution of Sound and Balance Perception: Innovations that Aggregate Single Hair Cells into the Ear and Transform a Gravistatic Sensor into the Organ of Corti. Anat. Rec. Adv. Integr. Anat. Evol. Biol. *295*, 1760–1774.

Elstob, P.R., Brodu, V., and Gould, A.P. (2001). spalt-dependent switching between two cell fates that are induced by the Drosophila EGF receptor. Development *128*, 723–732.

Esterberg, R., Hailey, D.W., Coffin, A.B., Raible, D.W., and Rubel, E.W. (2013). Disruption of intracellular calcium regulation is integral to aminoglycoside-induced hair cell death. J. Neurosci. *33*, 7513–7525.

Fritzsch, B., Pan, N., Jahan, I., Duncan, J.S., Kopecky, B.J., Elliott, K.L., Kersigo, J., and Yang, T. (2013). Evolution and development of the tetrapod auditory system: an organ of Corti-centric perspective. Evol. Dev. *15*, 63–79.

Furness, D.N. (2015). Molecular basis of hair cell loss. Cell Tissue Res.

Ghysen, A., and Dambly-Chaudière, C. (2007). The lateral line microcosmos. Genes Dev. *21*, 2118–2130.

Go, W., Bessarab, D., and Korzh, V. (2010). atp2b1a regulates Ca(2+) export during differentiation and regeneration of mechanosensory hair cells in zebrafish. Cell Calcium *48*, 302–313.

Grant, K.A., Raible, D.W., and Piotrowski, T. (2005). Regulation of latent sensory hair cell precursors by glia in the zebrafish lateral line. Neuron *45*, 69–80.

Haas, P., and Gilmour, D. (2006). Chemokine signaling mediates self-organizing tissue migration in the zebrafish lateral line. Dev. Cell *10*, 673–680.

Harris, J.A., Cheng, A.G., Cunningham, L.L., MacDonald, G., Raible, D.W., and Rubel, E.W. (2003). Neomycin-induced hair cell death and rapid regeneration in

the lateral line of zebrafish (Danio rerio). J. Assoc. Res. Otolaryngol. *4*, 219–234.

Head, J.R., Gacioch, L., Pennisi, M., and Meyers, J.R. (2013). Activation of canonical Wnt/β-catenin signaling stimulates proliferation in neuromasts in the zebrafish posterior lateral line. Dev. Dyn. *242*, 832–846.

Hurlstone, A.F.L., Haramis, A.-P.G., Wienholds, E., Begthel, H., Korving, J., Van Eeden, F., Cuppen, E., Zivkovic, D., Plasterk, R.H.A., and Clevers, H. (2003). The Wnt/beta-catenin pathway regulates cardiac valve formation. Nature *425*, 633–637.

Jacques, B.E., Puligilla, C., Weichert, R.M., Ferrer-Vaquer, A., Hadjantonakis, A.-K., Kelley, M.W., and Dabdoub, A. (2012). A dual function for canonical Wnt/β-catenin signaling in the developing mammalian cochlea. Development *139*, 4395–4404.

Jeon, S.-J., Fujioka, M., Kim, S.-C., and Edge, A.S.B. (2011). Notch signaling alters sensory or neuronal cell fate specification of inner ear stem cells. J. Neurosci. *31*, 8351–8358.

Jiang, L., Romero-Carvajal, A., Haug, J.S., Seidel, C.W., and Piotrowski, T. (2014). Gene-expression analysis of hair cell regeneration in the zebrafish lateral line. Proc. Natl. Acad. Sci. E1383–E1392.

Jones, J.E., and Corwin, J.T. (1993). Replacement of lateral line sensory organs during tail regeneration in salamanders: identification of progenitor cells and analysis of leukocyte activity. J. Neurosci. *13*, 1022–1034.

Kiefer, S.M., McDill, B.W., Yang, J., and Rauchman, M. (2002). Murine Sall1 represses transcription by recruiting a histone deacetylase complex. J. Biol. Chem. *277*, 14869–14876.

Kil, J., Warchol, M.E., and Corwin, J.T. (1997). Cell death, cell proliferation, and estimates of hair cell life spans in the vestibular organs of chicks. Hear. Res. *114*, 117–126.

Kohlhase, J., Wischermann, A., Reichenbach, H., Froster, U., and Engel, W. (1998). Mutations in the SALL1 putative transcription factor gene cause Townes-Brocks syndrome. Nat. Genet. *18*, 81–83.

Kopinke, D., Sasine, J., Swift, J., Stephens, W.Z., and Piotrowski, T. (2006). Retinoic acid is required for endodermal pouch morphogenesis and not for pharyngeal endoderm specification. Dev. Dyn. *235*, 2695–2709.

Ku, Y.-C., Renaud, N.A., Veile, R.A., Helms, C., Voelker, C.C.J., Warchol, M.E., and Lovett, M. (2014). The transcriptome of utricle hair cell regeneration in the

avian inner ear. J. Neurosci. *34*, 3523–3535.

Li, W., Wu, J., Yang, J., Sun, S., Chai, R., Chen, Z.-Y., and Li, H. (2014). Notch inhibition induces mitotically generated hair cells in mammalian cochleae via activating the Wnt pathway. Proc. Natl. Acad. Sci. *112*, 201415901.

Liang, J., Wang, D., Renaud, G., Wolfsberg, T.G., Wilson, A.F., and Burgess, S.M. (2012). The stat3/socs3a pathway is a key regulator of hair cell regeneration in zebrafish. [corrected]. J. Neurosci. *32*, 10662–10673.

Lush, M.E., and Piotrowski, T. (2014a). Sensory hair cell regeneration in the zebrafish lateral line. Dev. Dyn. *243*, 1187–1202.

Lush, M.E., and Piotrowski, T. (2014b). ErbB expressing Schwann cells control lateral line progenitor cells via non-cell-autonomous regulation of Wnt/β-catenin. Elife *3*, e01832.

Ma, E.Y., Rubel, E.W., and Raible, D.W. (2008). Notch signaling regulates the extent of hair cell regeneration in the zebrafish lateral line. J. Neurosci. *28*, 2261–2273.

Maass, J.C., Gu, R., Basch, M.L., Waldhaus, J., Lopez, E.M., Xia, A., Oghalai, J.S., Heller, S., and Groves, A.K. (2015). Changes in the regulation of the Notch signaling pathway are temporally correlated with regenerative failure in the mouse cochlea. Front. Cell. Neurosci. *9*.

Mackenzie, S.M., and Raible, D.W. (2012). Proliferative regeneration of zebrafish lateral line hair cells after different ototoxic insults. PLoS One *7*, e47257.

Matsuda, M., and Chitnis, A.B. (2010). Atoh1a expression must be restricted by Notch signaling for effective morphogenesis of the posterior lateral line primordium in zebrafish. Development *137*, 3477–3487.

McFadden, S.L., Ding, D., Reaume, A.G., Flood, D.G., and Salvi, R.J. Age-related cochlear hair cell loss is enhanced in mice lacking copper/zinc superoxide dismutase. Neurobiol. Aging *20*, 1–8.

Monroe, J.D., Rajadinakaran, G., and Smith, M.E. (2015). Sensory hair cell death and regeneration in fishes. Front. Cell. Neurosci. *9*, 131.

Oesterle, E.C., Campbell, S., Taylor, R.R., Forge, A., and Hume, C.R. (2008). Sox2 and JAGGED1 expression in normal and drug-damaged adult mouse inner ear. J. Assoc. Res. Otolaryngol. *9*, 65–89.

Parinov, S., Kondrichin, I., Korzh, V., and Emelyanov, A. (2004). Tol2 transposon-mediated enhancer trap to identify developmentally regulated

zebrafish genes in vivo. Dev. Dyn. *231*, 449–459.

Raphael, Y., and Altschuler, R.A. (1991). Scar formation after drug-induced cochlear insult. Hear. Res. *51*, 173–183.

Raphael, Y., Kim, Y.-H., Osumi, Y., and Izumikawa, M. (2007). Non-sensory cells in the deafened organ of Corti: approaches for repair. Int. J. Dev. Biol. *51*, 649–654.

Roberson, D.W., Alosi, J.A., and Cotanche, D.A. (2004). Direct transdifferentiation gives rise to the earliest new hair cells in regenerating avian auditory epithelium. J. Neurosci. Res. *78*, 461–471.

Sánchez, J., Talamillo, A., González, M., Sánchez-Pulido, L., Jiménez, S., Pirone, L., Sutherland, J.D., and Barrio, R. (2011). Drosophila Sal and Salr are transcriptional repressors. Biochem. J. *438*, 437–445.

Schuck, J.B., Sun, H., Penberthy, W.T., Cooper, N.G.F., Li, X., and Smith, M.E. (2011). Transcriptomic analysis of the zebrafish inner ear points to growth hormone mediated regeneration following acoustic trauma. BMC Neurosci. *12*, 88.

Shi, F., Kempfle, J.S., and Edge, A.S.B. (2012). Wnt-responsive Lgr5-expressing stem cells are hair cell progenitors in the cochlea. J. Neurosci. *32*, 9639–9648.

Shi, F., Hu, L., and Edge, A.S.B. (2013). Generation of hair cells in neonatal mice by β-catenin overexpression in Lgr5-positive cochlear progenitors. Proc. Natl. Acad. Sci. U. S. A. *110*, 13851–13856.

Steiner, A.B., Kim, T., Cabot, V., and Hudspeth, A.J. (2014). Dynamic gene expression by putative hair-cell progenitors during regeneration in the zebrafish lateral line. Proc. Natl. Acad. Sci. U. S. A. *111*, E1393–E1401.

Stone, J.S., and Cotanche, D. a. (2007). Hair cell regeneration in the avian auditory epithelium. Int. J. Dev. Biol. *51*, 633–647.

Stone, J.S., and Rubel, E.W. (2000). Cellular studies of auditory hair cell regeneration in birds. Proc. Natl. Acad. Sci. U. S. A. *97*, 11714–11721.

Sweetman, D., and Münsterberg, A. (2006). The vertebrate spalt genes in development and disease. Dev. Biol. *293*, 285–293.

Thomas, A.J., Hailey, D.W., Stawicki, T.M., Wu, P., Coffin, A.B., Rubel, E.W., Raible, D.W., Simon, J.A., and Ou, H.C. (2013). Functional Mechanotransduction Is Required for Cisplatin-Induced Hair Cell Death in the Zebrafish Lateral Line. J. Neurosci. *33*, 4405–4414.

Walters, B.J., Liu, Z., Crabtree, M., Coak, E., Cox, B.C., and Zuo, J. (2014). Auditory hair cell-specific deletion of p27Kip1 in postnatal mice promotes cell-autonomous generation of new hair cells and normal hearing. J. Neurosci. *34*, 15751–15763.

Wibowo, I., Pinto-Teixeira, F., Satou, C., Higashijima, S., and López-Schier, H. (2011). Compartmentalized Notch signaling sustains epithelial mirror symmetry. Development *138*, 1143–1152.

Williams, J.., and Holder, N. (2000). Cell turnover in neuromasts of zebrafish larvae. Hear. Res. *143*, 171–181.

Yang, S.-M., Chen, W., Guo, W.-W., Jia, S., Sun, J.-H., Liu, H.-Z., Young, W.-Y., and He, D.Z.Z. (2012). Regeneration of stereocilia of hair cells by forced Atoh1 expression in the adult mammalian cochlea. PLoS One *7*, e46355.

Zhang, Q., Liu, H., McGee, J., Walsh, E.J., Soukup, G.A., and He, D.Z.Z. (2013). Identifying microRNAs involved in degeneration of the organ of corti during age-related hearing loss. PLoS One *8*, e62786.

Figure 2.1. Microarray-based gene expression analysis 1 hr after hair cell ablation in the zebrafish posterior lateral line neuromasts.
(A) 5 dpf zebrafish larva expressing the *Et(krt4:EGFP)*^{sqet20} transgene. This enhancer trap drives GFP expression in the lateral line neuromasts, interneuromast cells and with less extent, in muscle, and fin rays. The white arrows show the cut site. The pos-cloacal tail was used for cell dissociation and FAC sorting .
(B) 5 dpf neuromast show GFP expression in the outermost cell population, the mantle cells.
(C) Schematics of the protocol to obtain RNA from GFP+ neuromast cells in neo treated and control larvae.
(D-E) Fluorescence activated cell sorting protocol (FACS) to isolate *sqet20*+ cells for RNA extraction. (D) PI x FSC gate to sort out debris and dead cells by addressing cell particle size and Propidium Iodide staining. (E) GFP x FSC gate to sort cells by GFP intensity. The magenta shapes indicate the sampled cells from the GFP+ and GFP- populations
(F) Less than 200 genes showed differential gene expression after hair cell death as shown in an averaged MA plot (red =upregulation, green= downregulation).
(G) Individual MA plots for each RNA sample showing the consistency of reads of known transcripts (colored dots) across different replicates.
(H) Venn diagram illustrating the transcripts responding to hair cell death in GFP+ cells.

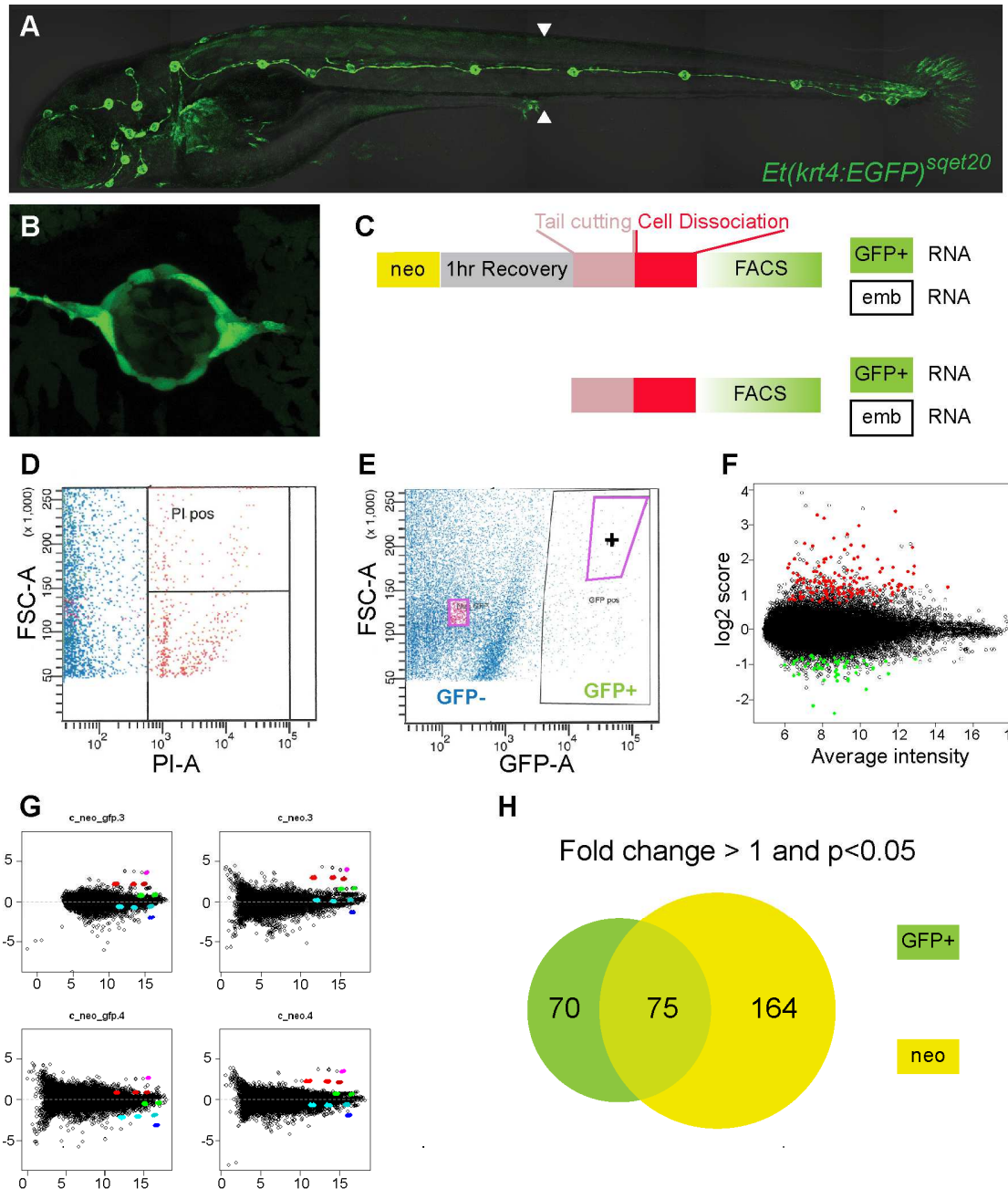
A
Et(krt4:EGFP)sqet20
B
C
Tail cutting
Cell Dissociation
neo
1hr Recovery
FACS
GFP+ RNA
emb RNA
FACS
GFP+ RNA
emb RNA
D
PI pos
FSC-A
PI-A
E
FSC-A
GFP-
GFP+
GFP-A
F
log2 score
Average intensity
G
c_neo_gfp.3
c_neo.3
c_neo_gfp.4
c_neo.4
H
Fold change > 1 and p<0.05
70
75
164
GFP+
neo

Figure 2.2. Whole mount in situ hybridization of the top upregulated genes.
Krt1-19d. Ubiquitously expressed in superficial keratinocytes.
sall1b. ventral region of the otic vesicle and in central cells of the primordium and neuromasts.
si:busm1-57f23.1. Ubiquitous in the otic vesicle. Central cells of the primordium and newly deposited neuromasts. Support cells of mature neuromasts.
irgl1. Ubiquitous in the otic vesicle. Not expressed in the primordium or 40 hpf neuromasts. In support cells of mature neuromasts.
timp2b. Strong expression in the anterior basal otic vesicle. Undetermined expressionin the primordium or 40 hpf neuromast. In support cells of mature neuromasts.
A_15_P760286. Strong expression in the anterior ventral otic vesicle. Undetermined expression in the primordium or 40 hpf neuromast. Support cells of mature neuromasts.
A_15_P701096. Strong expression in the ventral otic vesicle. Central cells of the primordium and newly deposited neuromasts. Support cells of mature neuromasts.
hfe2. Expression in the anterior-posterior poles and dorsal otic vesicle. Central cells of the primordium and newly deposited neuromasts. Support cells of mature neuromasts.
nlrc3. Ubiquitous expression across the embryo.
ugdh. Ubiquitous in the otic vesicle. Expressed in cells from the horizontal myoseptum. Only present in mature neuromast support cells.
lima1. Not expressed in the otic vesicle. Ubiquitous in basal keratinocytes with stronger expression around the primordium. Not expressed in neuromasts.
bcl2l10. Ubiquitous in the otic vesicle. Central cells of the migrating primordium and newly deposited neuromasts. In support cells of mature neuromasts.

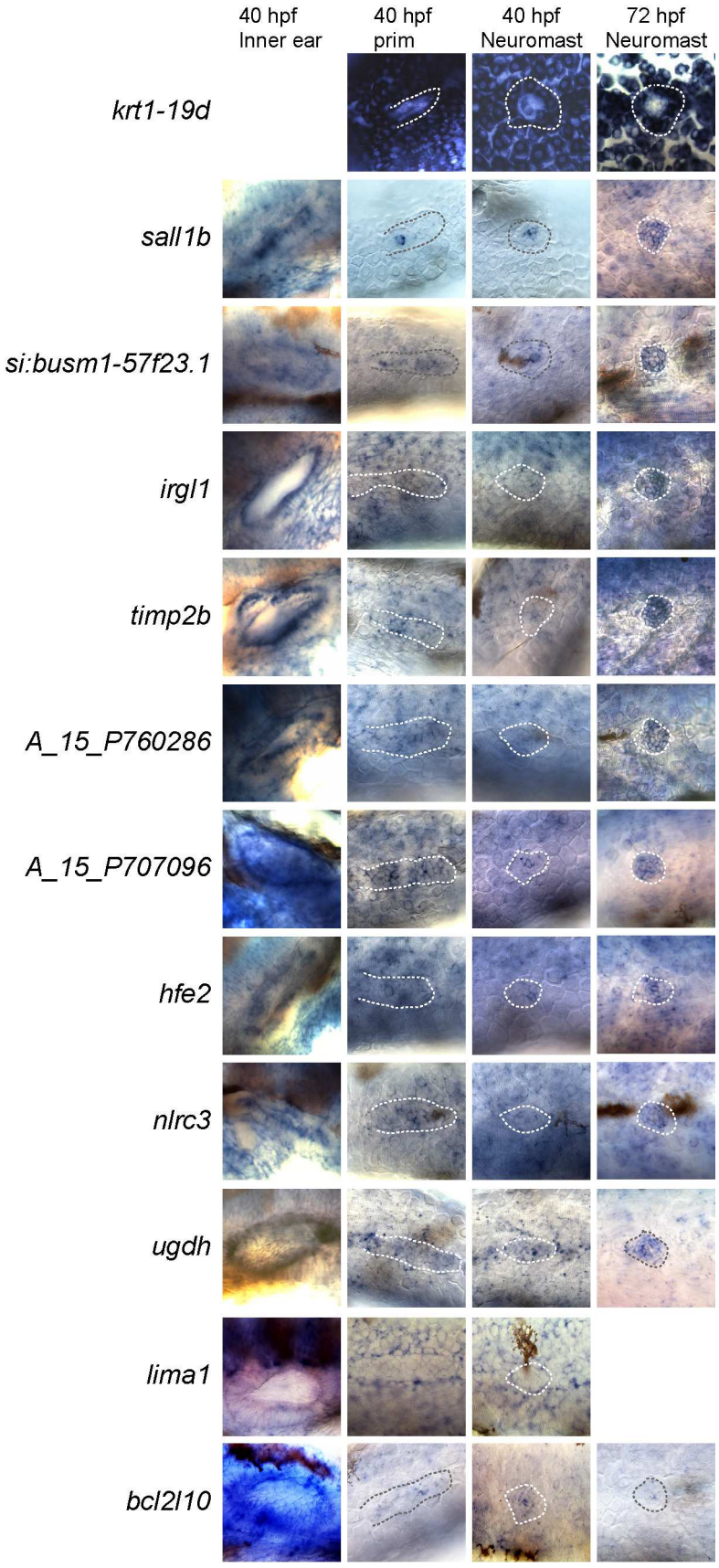
40 hpf
Inner ear
40 hpf
prim
40 hpf
Neuromast
72 hpf
Neuromast
krt1-19d
sall1b
si:busm1-57f23.1
irgl1
timp2b
A_15_P760286
A_15_P707096
hfe2
nlrc3
ugdh
lima1
bcl2l10

Figure 2.3. Whole mount in situ hybridization of the top downregulated genes.
sox1a. Ubiquitous in the otic vesicle. Specific expression in leading region of the primordium. Low expression in 40 hpf neuromasts, higher in mature neuromasts.
sost. Ubiquitous in the otic vesicle. Not expressed in the primordium. Specifically expressed in the dorso-ventral support cells of neuromasts.
si:ch211-235e18.3. Expressed in the anterior-posterior regions of the otic vesicle and in central cells of the primordium and neuromast.
sox1b. Expressed in the anterior-posterior regions of the otic vesicle and in central cells of the primordium and neuromast.
ptger4a. Expressed in the anterior region of the otic vesicle. Not present in the primordium. In central cells of neuromast support cells.
sox2. Expressed in the posterior-ventral region of the otic vesicle, in the trailing region of the prim, and support cells of neuromasts.
sox3. Expressed in the posterior-dorsal region of the otic vesicle, in central cells the prim, and in support cells of neuromasts.
lad1. Expressed in the ventral region of the otic vesicle, and ubiquitous in the larvae and neuromast support cells.
pvalb9. Strong expression in anterior-ventral otic vesicle, and mild expression in primordium and 40hpf neuromasts, strong in support cells.

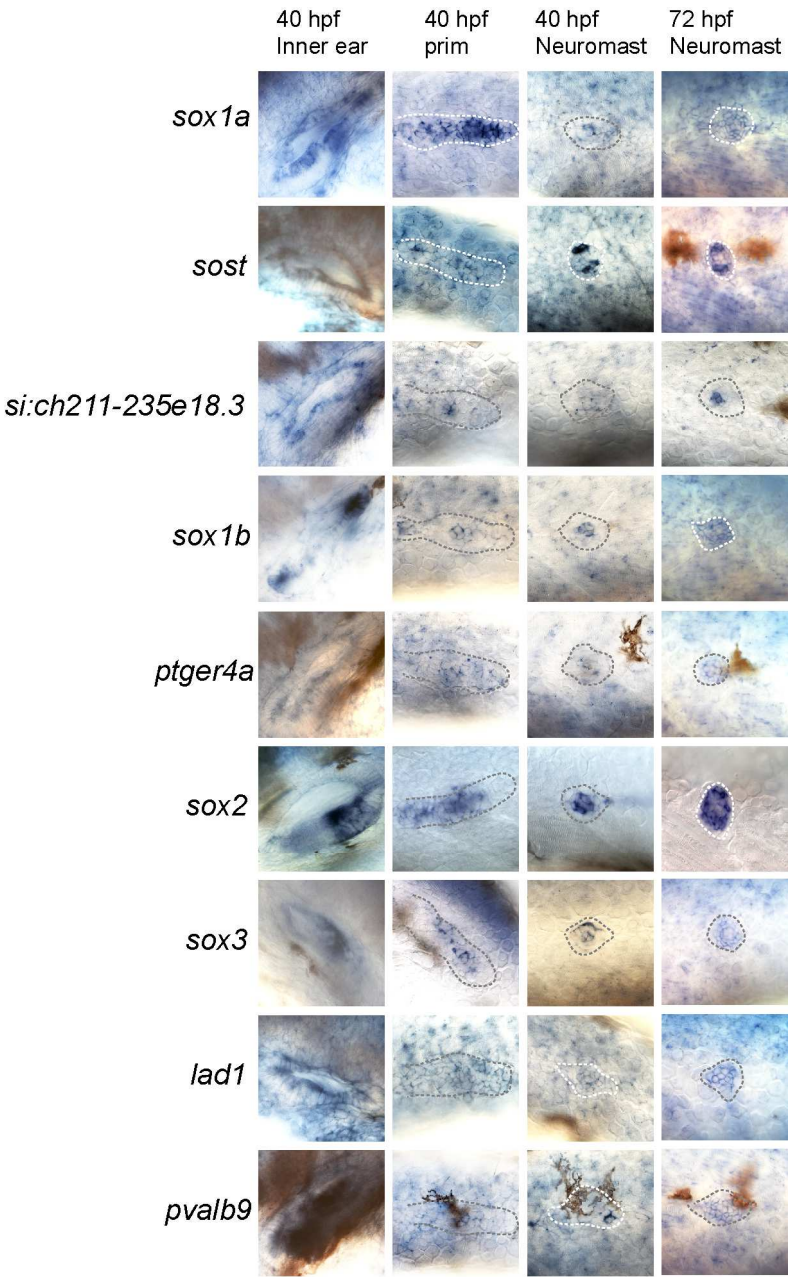
40 hpf
Inner ear
40 hpf
prim
40 hpf
Neuromast
72 hpf
Neuromast
sox1a
sost
si:ch211-235e18.3
sox1b
ptger4a
sox2
sox3
lad1
pvalb9

Figure 2.4. Up and downregulated genes respond no to hair cell death.
(A) *lima1* is not expressed in mature neuromast however is strongly upregulated after hair cell death.
(B) *sall1b* is expressed in central cells of mature neuromasts. After hair cell death, it is upregulated in single cells.
(C) *sox2* transcripts are drastically upregulated after hair cell death.
(D) *sclerostin* (*sost*) is downregulated one hour after hair cell death.

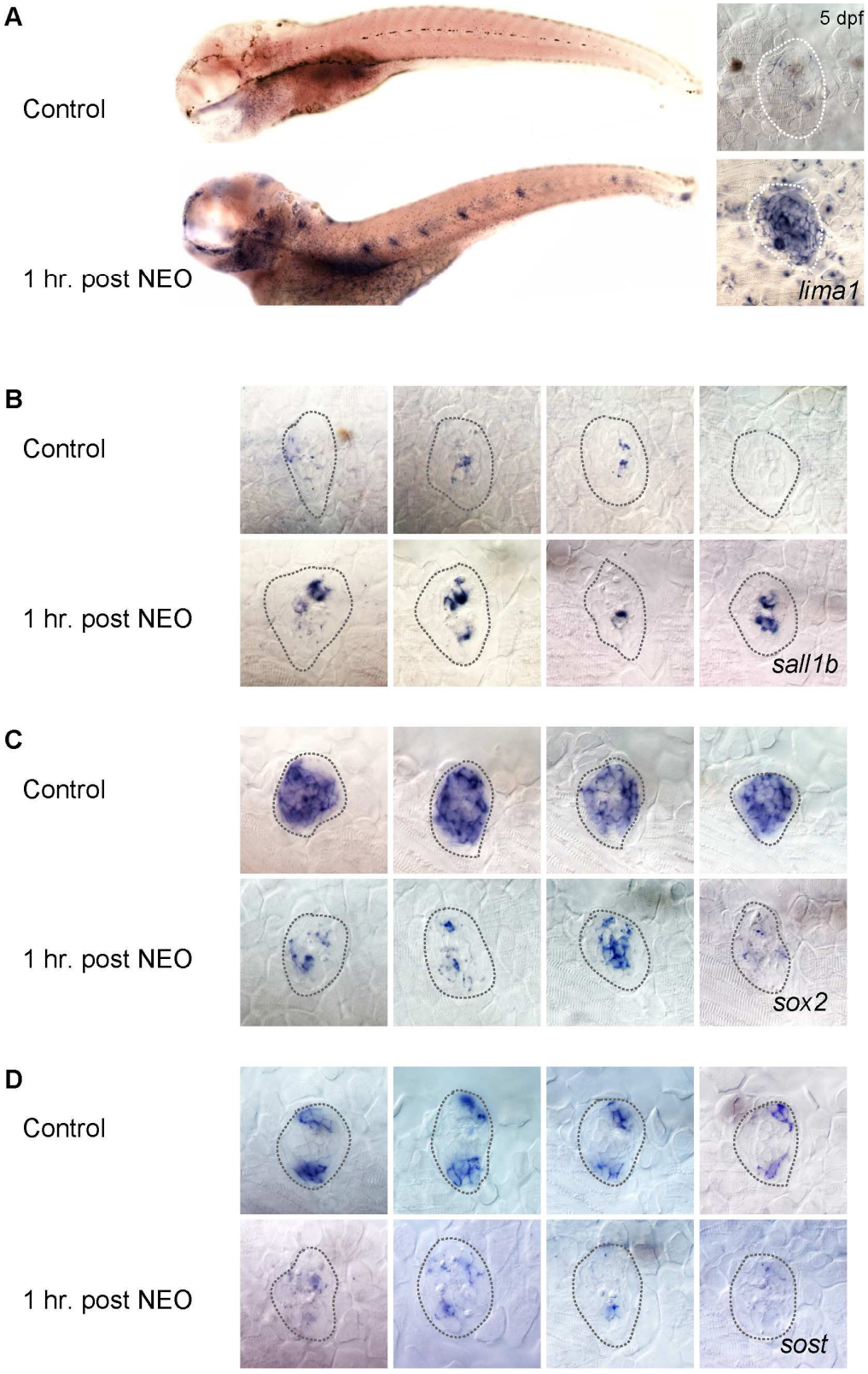
A
Control
1 hr. post NEO
5 dpf
lima1
B
Control
1 hr. post NEO
sall1b
C
Control
1 hr. post NEO
sox2
D
Control
1 hr. post NEO
sost

Figure 2.5. The list of upregulated transcripts might be enriched of Wnt target genes.
(A) Posterior lateral line primordium expressing GFP in the cell membranes and mCherry (Red) in the nuclei, both driven by the lateral line specific enhancer of the gene *claudinb.* The most posterior neuromast is detaching from the trailing region while new neuromasts are being formed in the primordium, as shown
(B) Schematics illustrating the main expression domains in the migrating primordium. Although the leading region is mostly composed of mesenchymal cells and the frailing region is mostly composed of forming rosettes, the actual boundaries of the expression domains are unknown and the colors only illustrate approximate expression patterns. The Wnt target gene and secreted FGF ligand *fgf3* (together with *fgf10*) activates FGF signaling in the trailing region. The Wnt target gene and FGF inhibitor *sef* inhibits FGFR activation in the leading region and maintains the leading-trailing boundaries. The FGF target gene and Wnt inhibitor *dkk1b* is expressed approximately in the leading-trailing boundary and restricts Wnt signaling to the leading region.
(C) apc^{mcr} is a Wnt gain-of-function mutation that activates transcription of the upregulated genes in the primordium. The inhibitor of FGF signaling SU5402 also enhance Wnt signaling by downregulating *dkk1b* expression. Most of the upregulated genes also respond to FGF signaling inhibition, confirming its role as Wnt target genes. *ugdh* and *lima1* are possible FGF target genes.
(D) The downregulated genes are mostly unresponsive to the apc^{mcr} mutation or SU5402

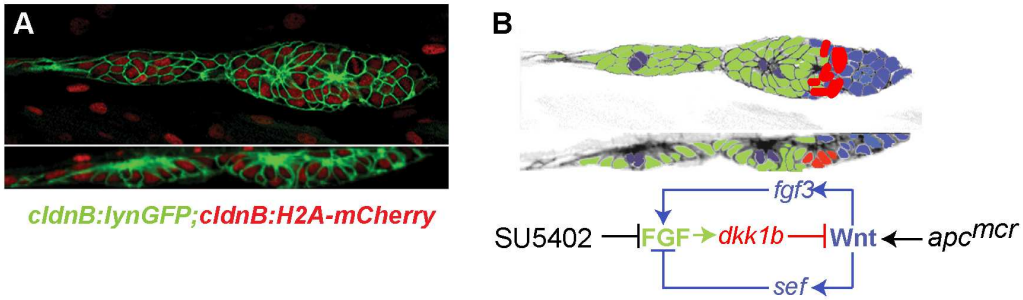
A
cldnB:lynGFP;cldnB:H2A-mCherry
B
fgf3
SU5402
FGF
dkk1b
Wnt
apc^mcr
sef

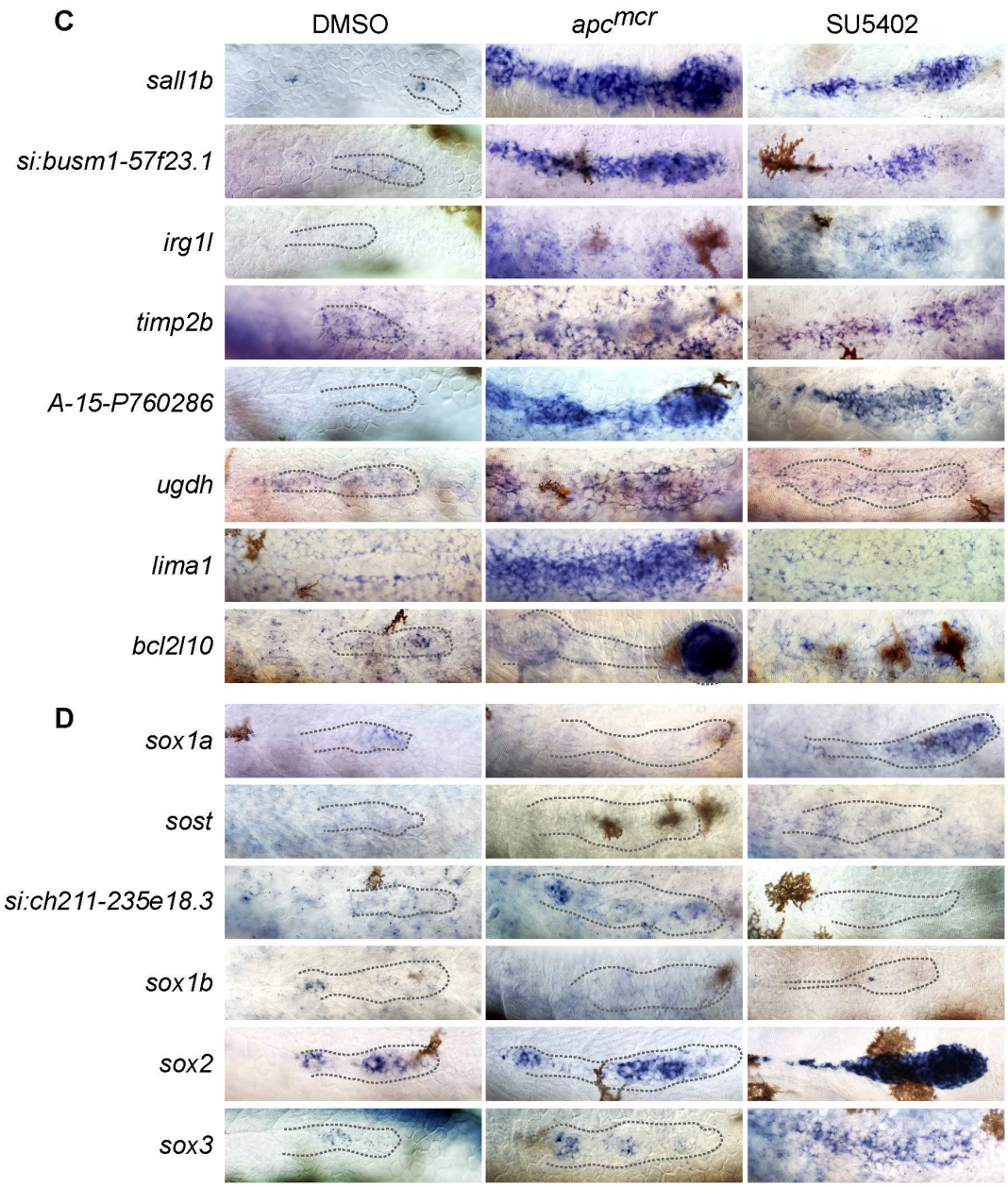
C
DMSO
apc^mcr
SU5402
sall1b
si:busm1-57f23.1
irg1l
timp2b
A-15-P760286
ugdh
lima1
bcl2l10
D
sox1a
sost
si:ch211-235e18.3
sox1b
sox2
sox3

Figure 2.6. The primordium central cells are hair cell progenitors.
(A-B) *sall1b* is expressed in central cells of the migrating primordium and newly deposited neuromasts.
(C-D) *sox2* is expressed in the trailing region of the primordium as shown by antibody staining. The expression is reduced in central cells of the neuromast and trailing region.
(E-F) *deltad* is a hair cell progenitor marker expressed specifically in central cells of deposited neuromasts (E) and in the primordium (F).
(G-H) Manual backtracking of hair cells to their progenitors located in the central cells of the migrating primordium. (E) Hair cell progenitors are labeled with arrow heads. White arrowheads label post-mitotic cells, the pink arrowhead labels a pre-mitotic progenitor. (F) Post –mitotic cells only differentiated into hair cells, the pre mitotic cell divided and formed a pair of hair cells. (G) Cell lineage tracking across 10 hrs of timelapse. The pre-mitotic progenitor divided at time = 00:40:00.

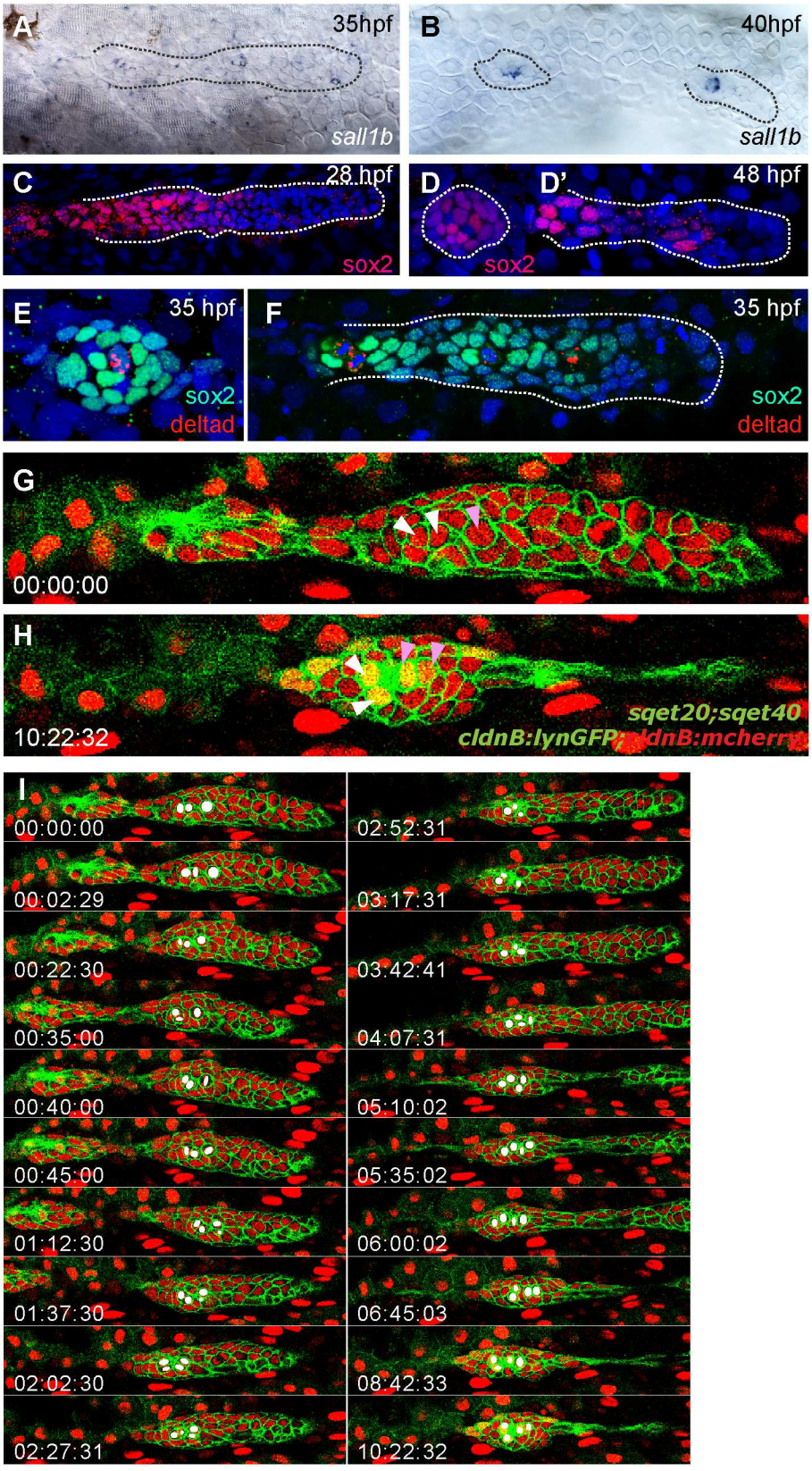
A
35hpf
sall1b
B
40hpf
sall1b
C
28 hpf
sox2
D
D'
48 hpf
sox2
E
35 hpf
sox2
deltad
F
35 hpf
sox2
deltad
G
00:00:00
H
10:22:32
sqet20;sqet40
cldnB:lynGFP;
I
00:00:00
00:02:29
00:22:30
00:35:00
00:40:00
00:45:00
01:12:30
01:37:30
02:02:30
02:27:31
02:52:31
03:17:31
03:42:41
04:07:31
05:10:02
05:35:02
06:00:02
06:45:03
08:42:33
10:22:32

Figure 2.7. *sall1b* might be important for lateral line morphogenesis by specifying central cells through *dkk1b* induction and *sox2* inhibition.
(A-B)Schematics of the *sall1b* gene showing the splice sites (red) for which morpholinos were designed. The arrows show the primers designed to address transcript silencing through RT-PCR (B)
(C-D) *sall1b* morphants primordium migration is not affected as seen by the deposited trail of interneuromast cells. However, neuromast deposition is highly affected with more than 50% of the injected embryos with 2 neuromast or less.
(E-E') *sall1b* morphant primordium deposit small clusters of cells with rosette conformation. These clusters will later form neuromasts possibly due to the morpholino washout.
(F-G) FGFsignaling is somewhat upregulated and no longer restricted to the trailing region as shown through *pea3* expression.
(H-M)Wnt signaling is upregulated in *sall1b* morphants as evidenced by *fgf3* and *lef1* expression and *dkk1b* downregulation; this, in spite of the maintenance of FGF signaling.
(N-Q) The *notch3* receptor and the *deltaa* ligand are misexpressed in *sall1b* morphants.
(R-S) *sall1b* morphants show global upregulation of *sox2* including the primordium where it is expressed also in the leading region.
(T) *sall1b* might be important for lateral line morphogenesis by specifying central cells through *dkk1b* induction and *sox2* inhibition. It is still unclear the effects of *sall1b* silencing over *atoh1a* and other central cell markers.

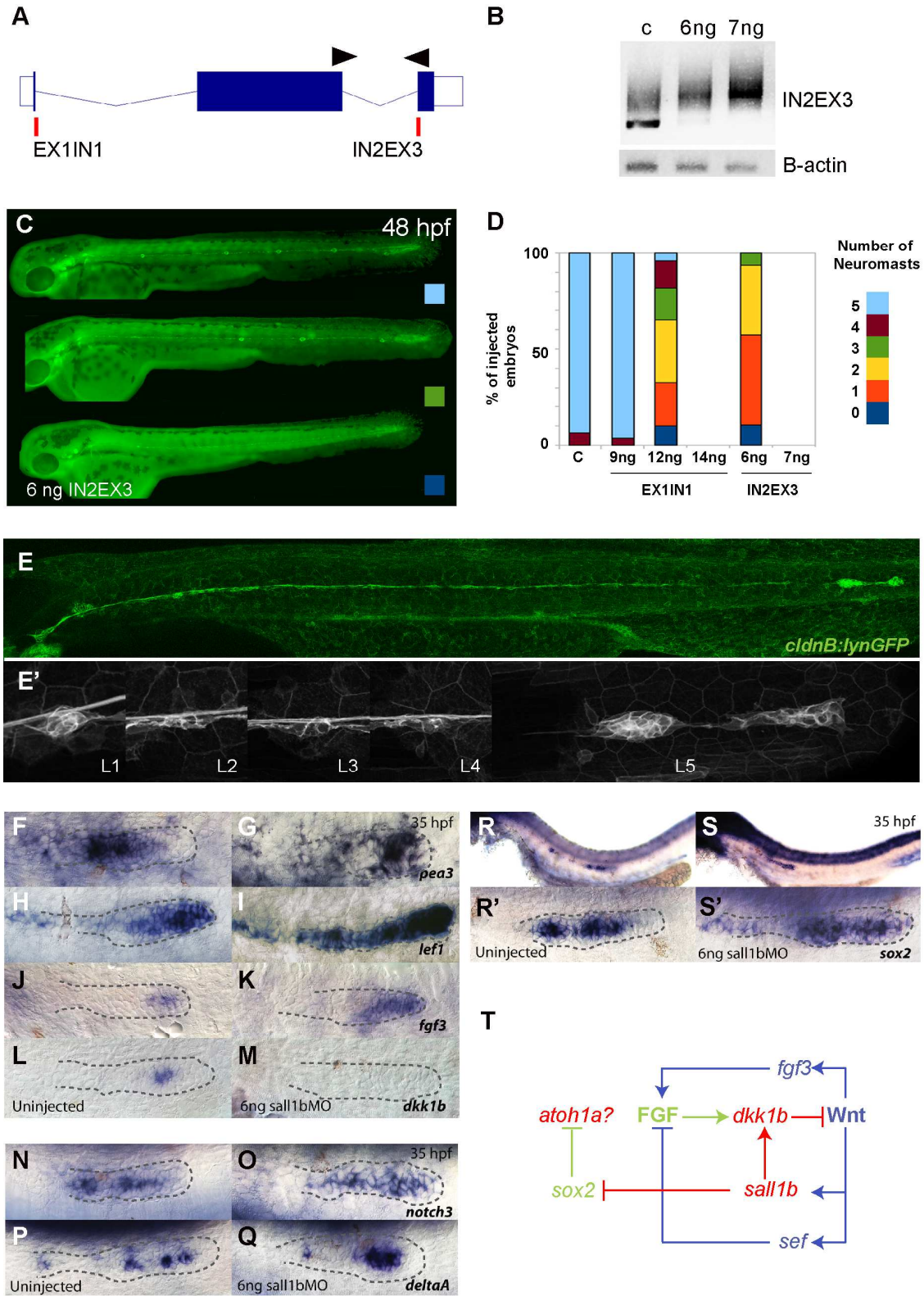
A
EX1IN1
IN2EX3
B
c
6ng
7ng
IN2EX3
B-actin
C
48 hpf
6 ng IN2EX3
D
% of injected embryos
100
50
0
C
9ng
12ng
14ng
6ng
7ng
EX1IN1
IN2EX3
Number of Neuromasts
5
4
3
2
1
0
E
cldnB:lynGFP
E'
L1
L2
L3
L4
L5
F
G
35 hpf
pea3
H
I
lef1
J
K
fgf3
L
Uninjected
M
6ng sall1bMO
dkk1b
R
S
35 hpf
R'
Uninjected
S'
6ng sall1bMO
sox2
N
O
35 hpf
notch3
P
Uninjected
Q
6ng sall1bMO
deltaA
T
fgf3
atoh1a?
FGF
dkk1b
Wnt
sox2
sall1b
sef

Table 2.1. List of up and downregulated genes cloned microarray validation of whole mount in situ hybridization

Fold Change	Gene	Gene ID	Description	Left primer	Right primer
	Upregulated				
2.19	*krt1-19d*	ENSDARG00000023082	keratin, type 1, gene 19d	ATCGAACTCCAGTCCCTCCT	CTGCGACTGTCAGACATGGT
1.96	*sall1b*	A_15_P762431	sal-like 1b	CGGGAAAACCTTCTCCTCTT	ATCGCTCAAGCCAAGGTAAA
1.93	*si:busm1-57f23.1*	ENSDARG00000074425	si:busm1-57f23.1	AAAAGCGGCCACATATTCAC	TGCACCTCATGGTCATCATT
1.8	*irg1l*	ENSDARG00000062788	immunoresponsive gene 1, like	CACAGCAACAGCAAACCAAG	ACGTGGGGCATAGTCTTCAT
1.71	*timp2b*	ENSDARG00000075261	tissue inhibitor of metalloproteinase 2b	TTTAGGGGTAATTGCGATGC	AAGCATTTGAACAGAGGAGCA
1.63	A_15_P760286	A_15_P760286	coiled-coil domain containing 48	GAAAACGTCAGGACGGAAAA	CTTCAACTCCGTCCAAGAGC
1.61	A_15_P701096	A_15_P701096	zinc finger, NFX-type containing 1	GAAAACTTGCGCTGACACAG	TGCGTTTAATCCATCCCATT
1.57	*hfe2*	ENSDARG00000030494	hemochromatosis type 2	ATCAAGCAAAACTGGGCAAC	CCGTTCCAGACAGCCTTTAC
1.53	*nlrc3*	ENSDARG00000061564	NLR family, CARD domain containing 3	ATCGCTGAAGCCATGAGAGT	AGCGCAGTCGCAATAAAGAT
1.51	*ugdh*	ENSDARG00000019838	UDP-glucose dehydrogenase	GACGTACGGTATGGGCAAAG	ACAGCGCAGAGATGGAGTTT
1.16	*lima1*	A_15_P624041	LIM domain and actin binding 1	AAAGCAGCTCTGGGAACATC	AGTCACAGCTGCCTGGTACA
0.68	*bcl2l10*	ENSDARG00000026766	BCL2-like 10 (apoptosis facilitator)	GCGGAGGACTACATCAGCTT	TCATGGAGGACTCCTGGTTC
	Downregulated				
-1.39	*sox1a*	ENSDARG00000069866	SRY-box containing gene 1a	AACGGAACTGTCCCACTGAC	TGTACAGCAGCAGTGACGTG
-1.4	*sost*	ENSDARG00000061259	sclerostin	AACCCGTGAAGGAACTTGTG	ACAGCGGACGTCTTTTCACT
-1.46	*si:ch211-235e18.3*	ENSDARG00000058606	salt-inducible kinase 1	CCGCACACACATAGCTGAAG	TCGCAGCTTTCTGGTATCCT
-1.67	*sox1b*	ENSDARG00000008131	SRY-box containing gene 1b	AACCGTTCCACTGACACACA	TTTTATCCCCTGGCAAATCC
-1.69	*ptger4a*	ENSDARG00000059236	prostaglandin E receptor 4 (subtype EP4) a	CAGTGGAGAAGCGTCTGGAT	CTGGACGCTGTCGTTAGTGA
-1.81	*sox2*	ENSDARG00000070913	SRY-box containing gene 2		
-1.85	*sox3*	ENSDARG00000053569	SRY-box containing gene 3	ACGACATATCGGGGACTTCA	CCGTCCCAGATAATGGGTTA
-2.31	*lad1*	ENSDARG00000022698	ladinin	TGGACTGCATTACAGCGTCT	AAATCCCTCTGGGCAGAAAC
-2.32	*pvalb9*	ENSDARG00000071601	parvalbumin 9	TCCATGGAGATGCTGTCATT	GGTGAATGTGGAACAACGAA

Table 2.2. GO term analysis shows significant enrichment of members of the Notch signaling pathway (bold letters).

Term	Term Name	Mapped Genes
GO:0001756	somitogenesis	*calcrla; cdh2;* ***her4.1;*** *hes6;* ***notch1a; rbpjb; zeb2a***
GO:0010605	negative regulation of macromolecule metabolic process	*enpp1; foxd3;* ***hes6;*** *klf4; nr0b1; pou2f1b;* ***rbpjb;*** *si:dkey-23c22.2; sirt3; taf9; wnt11*
GO:0035019	somatic stem cell maintenance	***notch3; sox2***
GO:0048468	cell development	***atoh1a;*** *cdh2;* ***dla;*** *dmd; foxd3;* ***her4.1;*** *id2a;* ***lfng;*** *meis1;* ***notch1a; notch3;*** *rnd1l; sec23b;* ***sox2;*** *zeb2a*
GO:0009063	cellular amino acid catabolic process	*amt; enosf1; gcshb; hgd*
GO:0030100	regulation of endocytosis	***notch1a; notch3****; wnt11*
GO:0043433	negative regulation of sequence-specific DNA binding transcription factor activity	*id2a; nr0b1; pbx1a; pycard; zgc:101056*
GO:0048332	mesoderm morphogenesis	*aplnrb; cdh2; notch1a; wnt11*
GO:0051091	positive regulation of sequence-specific DNA binding transcription factor activity	***pycard; sox1a; sox1b; sox2; sox3; wnt2***
GO:0060113	inner ear receptor cell differentiation	***atoh1a;*** *cdh2;* ***dla***
GO:0060898	eye field cell fate commitment involved in camera-type eye formation	*fzd8a; wnt11*
GO:0001840	neural plate development	***notch1a; notch3; wnt11***
GO:0007219	**Notch signaling pathway**	***dla;*** *gmds;* ***her4.1; lfng; notch1a; notch3; rbpjb***
GO:0021531	spinal cord radial glial cell differentiation	***fzd8a; notch1a***
GO:0048593	camera-type eye morphogenesis	*cdh2; cdh6; fzd8a; gmds; meis1; wnt11*
GO:0055016	hypochord development	***dla; lfng; notch1a***
GO:0045893	positive regulation of transcription, DNA-dependent	*foxd3; klf4; pea3;* ***rbpjb;*** *si:dkey-23c22.2;* ***sox2;*** *usf1; wnt11; zgc:165628*
GO:0048936	peripheral nervous system neuron axonogenesis	***her4.1; notch1a; notch3***
GO:0070301	cellular response to hydrogen peroxide	*cat; park7*

Table 2.3. List of transcription factors and transcription-related proteins up and downregulated after hair cell death. Bolded text shows genes know to be expressed in the lateral line.

Fold Change	Gene	Gene ID	Description
	Upregulated		
1.96	***sall1b***	A_15_P762431	sall1b
1.61	*NFX1_typecontaining1*	A_15_P701096	NFX1_typecontaining1
1.41	*olig3*	ENSDARG00000074253	oligodendrocyte transcription factor 3
1.35	*zgc:175128*	ENSDARG00000077799	early growth response 4
1.19	*mybl1*	ENSDARG00000030999	v-myb myeloblastosis viral oncogene homolog (avian)-like 1
0.974	*twistnb*	A_15_P114278	Twist-neighbor
0.876	*dkc1*	ENSDARG00000016484	dyskeratosis congenita 1, dyskerin
0.816	*eif2c3*	ENSDARG00000063079	eukaryotic translation initiation factor 2C
0.783	*si:dkey-91i17.1*	ENSDARG00000043304	NOP2 nucleolar protein homolog (yeast)
0.734	*twistnb*	ENSDARG00000024416	TWIST neighbor [Source:ZFIN;Acc:ZDB-GENE-041007-3]
0.709	*dkc1*	ENSDARG00000016484	dyskeratosis congenita 1, dyskerin
0.703	*mki67ip*	ENSDARG00000040666	mki67 (FHA domain) interacting nucleolar phosphoprotein
0.688	*egln1*	ENSDARG00000004632	egl nine homolog 1 (C. elegans)
0.675	*atxn1a*	ENSDARG00000061687	ataxin 1a
0.674	*mki67ip*	ENSDARG00000040666	mki67 (FHA domain) interacting nucleolar phosphoprotein
0.672	*mki67ip*	ENSDARG00000040666	mki67 (FHA domain) interacting nucleolar phosphoprotein
0.665	*gnl3*	ENSDARG00000006219	guanine nucleotide binding protein-like 3
0.632	*g3bp1*	ENSDARG00000017741	GTPase activating protein (SH3 domain) binding protein 1
0.614	*ddx18*	ENSDARG00000030789	DEAD (Asp-Glu-Ala-Asp) box polypeptide 18
0.612	*g3bp1*	ENSDARG00000017741	GTPase activating protein (SH3 domain) binding protein 1
0.608	*ddx49*	ENSDARG00000012899	DEAD (Asp-Glu-Ala-Asp) box polypeptide 49
0.573	*skib*	ENSDARG00000008034	nuclear oncoprotein skib
0.565	*polr1a*	ENSDARG00000029172	polymerase (RNA) I polypeptide A
0.563	*mphosph10*	ENSDARG00000012495	M-phase phosphoprotein 10 (U3 small nucleolar ribonucleoprotein)
0.528	*ddx56*	ENSDARG00000020913	DEAD (Asp-Glu-Ala-Asp) box polypeptide 56
0.525	***mycb***	ENSDARG00000007241	myelocytomatosis oncogene b
0.516	*dnttip2*	ENSDARG00000057648	deoxynucleotidyltransferase, terminal, interacting protein 2
0.514	*lin28a*	ENSDARG00000016999	lin-28 homolog A (C. elegans)
0.511		A_15_P241836	PREDICTED: Danio rerio zinc finger protein 521-like (LOC799182)
	Downregulated		
-0.513	*pou2f1b*	ENSDARG00000007996	POU class 2 homeobox 1b
-0.514	*msxd*	ENSDARG00000006982	muscle segment homeobox D
-0.523	*ZNF414*	ENSDARG00000079229	zinc finger protein 414
-0.532	*gata2b*	ENSDARG00000009094	GATA-binding protein 2b
-0.546	*zeb2a*	ENSDARG00000062338	zinc finger E-box binding homeobox 2a
-0.57	***pea3***	ENSDARG00000018303	ETS-domain transcription factor pea3
-0.58	*ssbp3b*	ENSDARG00000030155	single stranded DNA binding protein 3b
-0.59	*zeb2a*	ENSDARG00000062338	zinc finger E-box binding homeobox 2a

Table 2.3 (Continued)

Fold Change	Gene	Gene ID	Description
-0.591	***klf4***	ENSDARG00000038792	Kruppel-like factor 4
-0.613	*meis1*	ENSDARG00000012078	myeloid ecotropic viral integration 1
-0.618	*plagl2*	ENSDARG00000076657	pleiomorphic adenoma gene-like 2
-0.619	*nr0b1*	ENSDARG00000056541	nuclear receptor subfamily 0, group B, member 1
-0.622	*btg2*	ENSDARG00000020298	B-cell translocation gene 2
-0.629	*zeb2a*	ENSDARG00000062338	zinc finger E-box binding homeobox 2a
-0.632	*dpf3*	ENSDARG00000025309	D4, zinc and double PHD fingers, family 3
-0.66	***hoxb7a***	ENSDARG00000056030	homeo box B7a
-0.661	*grhl2b*	ENSDARG00000061974	grainyhead-like 2b
-0.686	*znf362-201*	ENSDARG00000060900	zinc finger protein 362
-0.697	*nr4a1*	ENSDARG00000000796	nuclear receptor subfamily 4, group A, member 1
-0.699	*si:ch211-202e12.3*	ENSDARG00000095715	Zebrafish DNA sequence from clone CH211-202E12 in linkage group 5 Contains a novel gene similar to the vertebrate MADS box transcription enhancer factor 2 (MEF2) family and the 5' end of a novel gene, complete sequence
-0.745	***eya2***	ENSDARG00000018984	eyes absent homolog 2
-0.747	*lmo1*	ENSDARG00000034504	LIM domain only 1
-0.752	*dacha*	OTTDART00000024134_108	
-0.756	*zgc:153317*	ENSDARG00000092903	chromosome 15 open reading frame 48
-0.76	*foxd3*	ENSDARG00000021032	forkhead box D3
-0.774	*msi1*	ENSDARG00000010710	musashi homolog 1
-0.758	*zfpm2b*	A_15_P656186	Danio rerio neural friend of GATA-B mRNA, complete cds
-0.801	*si:dkey-52h23.1*	ENSDARG00000094965	si:dkey-52h23.1
-0.823	***atoh1a***	ENSDARG00000055294	atonal homolog 1a
-0.838	***pax2b***	ENSDARG00000032578	paired box gene 2b
-0.864	*bcl11b*	ENSDARG00000062510	B-cell CLL/lymphoma 11Ba (zinc finger protein)
-0.886	*grhl2a*	A_15_P193401	grainyhead-like 2a
-0.897	***six2a***	ENSDARG00000058004	sine oculis-related homeobox 2a
-0.941	*si:dkey-12h9.13*	ENSDARG00000011445	chromosome 14 open reading frame 43
-0.944	*fos*	ENSDARG00000031683	v-fos FBJ murine osteosarcoma viral oncogene homolog
-1.02	***her4.1***	ENSDARG00000056732	hairy-related 4.1
-1.03	*hoxb8a*	ENSDARG00000056027	homeo box B8a
-1.03	*zgc:92851*	ENSDARG00000020133	Jun dimerization protein 2
-1.29	*six2b*	ENSDARG00000054878	sine oculis-related homeobox 2b
-1.34	*barhl1.2*	ENSDARG00000035508	BarH-like 1.2
-1.39	***sox1a***	ENSDARG00000069866	SRY-box containing gene 1a
-1.67	***sox1b***	ENSDARG00000008131	SRY-box containing gene 1b
-1.81	***sox2***	ENSDARG00000070913	SRY-box containing gene 2
-1.85	***sox3***	ENSDARG00000053569	SRY-box containing gene 3

CHAPTER 3

REGENERATION OF SENSORY HAIR CELLS REQUIRES LOCALIZED INTERACTIONS BETWEEN THE NOTCH AND WNT PATHWAYS

The following chapter was written in the format of a peer-reviewed publication and has been recently accepted for publication in *Developmental Cell*. 34, 1–16. To access the supplemental movies please access http://dx.doi.org/10.1016/j.devcel.2015.05.025

Summary

In vertebrates, mechano-electrical transduction of sound is accomplished by sensory hair cells. While mammalian hair cells are not replaced when lost, in fish, they constantly renew and regenerate after injury. In vivo tracking and cell fate analyses of all dividing cells during lateral line hair cell regeneration revealed that support and hair cell progenitors localize to distinct tissue compartments. Importantly, we find that the balance between self-renewal and differentiation in these compartments is controlled by spatially restricted Notch signaling and its

inhibition of Wnt-induced proliferation. The ability to simultaneously study and manipulate individual cell behaviors and multiple pathways in vivo transforms the lateral line into a powerful paradigm to mechanistically dissect sensory organ regeneration. The striking similarities to other vertebrate stem cell compartments uniquely place zebrafish to help elucidate why mammals possess such low capacity to regenerate hair cells.

Introduction

Mammalian adult tissues differ dramatically in their respective regenerative capacities. While the sensory cells of the olfactory epithelium and taste buds regenerate readily, the sensory hair cells of the mature inner ear cannot (Cox et al., 2014). Because sensory hair cells are crucial for hearing, their loss in mammals due to noise exposure, ageing, chemotherapeutic drugs, or antibiotics results in permanent loss (Furness, 2015). In contrast, the hair cells of the inner ear and lateral line system of nonmammalian vertebrates regenerate throughout the life of these animals (Rubel et al., 2013). The cellular and molecular basis of such striking difference between mammalian and nonmammalian vertebrates remains poorly understood. For instance, chicken and amphibian hair cells regenerate from dividing or transdifferentiating support cells (Balak et al., 1990; Corwin and Cotanche, 1988; Jones and Corwin, 1996); while fish lateral line hair cells regenerate from mitotic support cells (Lush and Piotrowski, 2014d; Ma et al., 2008; Wibowo et al., 2011; Williams and Holder, 2000). Nevertheless, the location and regulation of the stem cells and progeny

suspected to be involved in hair cell regeneration have yet to be fully characterized in any of the regenerating species. Likewise, our understanding of the molecular mechanisms controlling support cell behavior is limited. Here we take advantage of the superficially located and experimentally accessible zebrafish sensory lateral line system to study the cell behaviors and signaling events that lead to newly formed hair cells.

The lateral line system of aquatic vertebrates serves to detect water motion. The sensory organs are called neuromasts (NMs) and are distributed along lines over the body of the animal (Metcalfe et al., 1985; Northcutt et al., 1994). Each NM consists of mechanosensory hair cells that are surrounded by support cells and a ring of peripheral mantle cells (Figures 3.1A-3.1D). Lateral line hair cells are homologous to inner ear hair cells and mutations affecting lateral line hair cell function also cause deafness in humans (Nicolson, 2005; Whitfield, 2002). Previous studies of zebrafish lateral line regeneration described Notch-regulated proliferation patterns and localized quiescence in regenerating NMs; however, only differentiating divisions were described (Cruz et al., 2015; Ma et al., 2008; Wibowo et al., 2011). RNA-Seq analysis of regenerating NMs demonstrated that downregulation of Notch signaling is one of the earliest responses to hair cell death and therefore likely plays a crucial role in initiating regeneration (Jiang et al., 2014).

In neonatal mice, downregulation of Notch signaling also induces support cell proliferation, whereas in adults it leads to more hair cells via transdifferentiation (Mizutari et al., 2013). Similarly, canonical Wnt signaling

activates proliferation of support cells and causes an increase in hair cells in neonatal mice, but has no effect in adult animals (Shi et al., 2013). In regenerating chicken and zebrafish sensory epithelia, Wnt signaling increases proliferation and a modest increase in hair cell numbers (Head et al., 2013; Jacques et al., 2014). However, the interactions between Notch and Wnt signaling and their effect on distinct support cell fates have not been tested in regenerating species.

Because support cells look morphologically identical, we aimed to characterize NM cell populations by single cell lineage analyses. Manual tracking of every mantle and support cell, combined with spatial analysis of proliferating cells provides a potent and unbiased approach to distinguish lineages. We find that peripheral mantle cells are a quiescent cell population that only re-enters the cell cycle after severe injury to the sensory organs. We also discovered that during homeostasis and regeneration support cells make lineage decisions according to their location in the NM. This phenomenon is reminiscent of stem cell behaviors in the intestine and hair follicle where stem cell fate is determined by the location of the cells within the niche (Ritsma et al., 2014; Rompolas et al., 2013). Our results show that support cells self-renew in the dorso-ventral (D-V) poles, differentiate in the center and are relatively quiescent in the antero-posterior (A-P) poles. Importantly, the balance between self-renewal and differentiation is controlled by spatially restricted Notch signaling and its inhibition of Wnt-induced proliferation.

Results

Time-lapse and fate analyses define dynamics of cell division and differentiation in homeostatic and regenerating NMs

Dying lateral line hair cells are replaced in zebrafish by surrounding support cells throughout life (Cruz et al 2015). To determine if NMs possess a distinct stem cell population, we performed time-lapse analyses of homeostatic and regenerating NMs and recorded the fate of each dividing cell. We generated transgenic fish expressing four transgenes (Figures 3.1C-3.1H). *Et(krt4:EGFP)^{sqet20}*, (*sqet20*) labels mantle cells. *Tg(cldnb:lynGFP)* labels all lateral line cell membranes. *Tg(atp2b1a-GFP)*, or *sqet4* labels hair cells and their progenitors, and *Tg(cldnb:H2A-mCherry)* labels all cell nuclei.

We tracked cell lineages in 70 hour time-lapse recordings of 5 days post fertilization (dpf) control NMs during homeostasis (n=4; Figures 3.1I-3.1J, 3.S1B-3.S1E; Movie S1) and regeneration (n=3; Figures3.1K, 3.1L, 3.S1F-3.S1H, Movie S2). We determined the average number of cell types during regeneration in the first trunk NM (L1) at 0, 24, 48 and 72 hrs after hair cell loss (Figure 3.S1A). In a homeostatic NM we observed 3 support cell divisions (Movie S1; Figure 3.1I, 3.1J; Cell Divisions (CD) CD1-3) that we attribute to physiological hair cell turnover (Figure 3.S1A, black, dotted line). The first two progenitors divided symmetrically and produced two support cells each (CD1, CD2), while the third support cell (CD3) divided and the daughter cells differentiated into two GFP-positive hair cells (Figure 3.1J; Movie S1). The results of three other movies are described in Figures 3.S1C-3.S1E.

To induce hair cell regeneration, we immersed larvae in the antibiotic neomycin. Complete regeneration occurs after 72hrs (Figure 3.S1A, solid green line; Ma et al., 2008). Time-lapse imaging revealed that hair cell death significantly increases the number of mitoses (Figures 3.1K, 3.1L and 3.S1F-S1H; Movie 3.S2B). Tracking all cell divisions and daughter cells in three regenerating NMs over 70hrs revealed that support cells are a mixture of self-renewing multipotent stem cells and progenitor cells that give rise to hair cells (Figures 3.1L-3.1M). 42% of the observed cells divided and produced two undifferentiated support cells (Amplifying cell divisions; Figures 3.1L, CD2, 4, 6, Figures 3.S1F-3.S1H). This amplifying response led within 24hrs to a significant increase in support cell numbers that slowly returned to control levels by 72hrs, while other support cells continued to differentiate into hair cells (Figures 3.1N and 3.S1A, red lines). 45% of support cells produced two hair cells (Differentiating cell division; Figures 3.1L, CD3, 5, 8, 9, 3.S1F-3.S1H). 10% of the dividing support cells first gave rise to two support cells with one of the daughter cells dividing a second time to give rise to two hair cells (Figures 3.1L-3.1M, CD1; 3.S1G, CD10, CD11; Movie S2C). Therefore, support cells derived from symmetric, amplifying divisions have the potential to differentiate. Mantle cells, on the other hand, rarely divided (Figures 3.1L, CD7; 3.1M; 3.S1A, blue lines). These results show that support cells are the most likely source for stem cells, while mantle cells are unlikely to contribute to hair cell regeneration.

A prior study suggested that support cells migrate towards the D-V poles of the NMs to differentiate (Wibowo et al., 2011). In contrast, our time-lapse

recordings of regenerating NMs show that mitotic and quiescent cells maintain their relative positions and are not actively migrating during the course of regeneration (Figures 3.1O and Movie 3.S3). Neither amplifying, nor differentiating support cells were displaced by more than one cell diameter (5 pixels; Figure 3.S1I), which is not sufficient to move cells to the poles. When we analyzed the direction of cell movements before division, we observed that cells are displaced toward the center (Figure 3.1P). This movement is caused by the apical movement of dividing cells in NMs and the apical surface diameter being smaller than the basal surface. After division, cells move back down to their original position (Figure 3.1Q).

Our time-lapse recordings show that all cell divisions are symmetric, with approximately half of the daughters undergoing self-renewal or amplification, and the other half differentiating into hair cells. Our analyses define 5 cell behaviors during both homeostasis and regeneration: 1) differentiating cell divisions 2) amplifying cell divisions 3) support cells that divide a second time and gives rise to hair cells, 4) support cell quiescence, and 5) mantle cell quiescence.

Support cell lineages are restricted to different compartments

Given the limited cell movement, we tested whether support cell behaviors are spatially confined within the NMs. Time-lapse analyses suggested that cells in the poles self-renew, whereas cells in the center differentiate into hair cells (Figures S1J-S1J''). To confirm this observation, we performed 24hrs BrdU incorporation experiments in *sqet4;sqet20* homeostatic and regenerating larvae

(Figures 3.2A and 3.2D). We plotted the location of BrdU+ GFP+ hair cells (Figures 3.2B and 3.2E, differentiating cell divisions, green diamonds), BrdU+;GFP- support cells (amplifying cell divisions; red squares), and quiescent *sqet20*+ mantle cells (blue crosses). In homeostatic NMs, amplifying cell divisions cluster in the D-V poles (Figure 3.2B'). In contrast, differentiating divisions occur randomly in a circle and are not clustered (Figure 3.2B''). Quiescent support cells are located in the center and A-P poles of the NMs (unlabeled, white areas in Figure 3.2B). Within 24hrs, one support cell divides per pole to produce two support cells (amplifying division), while one central support cell gives rise to two hair cells (differentiating division, Figure 3.2C).

During regeneration, amplifying cell divisions increase but maintain their compartmentalized distribution in the D-V poles (Figures 3.2E and 3.2E' and 3.S2A). Differentiating divisions increase at the same rate as amplifying divisions but remain randomly distributed (Figures 3.2E-3.2E'' and 3.S2A). Also, differentiating divisions occur in previously quiescent, central support cells located immediately beneath the dying hair cells (Figure 3.2E). The schematic shows that approximately 4-5 amplifying and differentiating divisions occur per NM during regeneration (Figure 3.2F). Interestingly, amplifying divisions occur almost exclusively adjacent to mantle cells, whereas differentiating divisions occur toward the center (Figures 3.S2B-3.S2G).

To test if these localized cell behaviors correlate with hair cell orientation we studied neuromasts with a different developmental origin and epithelial planar cell polarity that is offset by 90^0 (primII-derived NMs; Figures 3.2A-3.2F and

3.S2H-3.S2M; López-Schier et al., 2004). We observed that amplifying support cell divisions in primII-derived NMs are restricted to the A-P poles (Figures 3.S2I-3.S2I' and 3.S2L-3.S2L'; A-P) mirroring the polar bias of amplifying cell divisions in primI-derived NMs.

We conclude from the dramatic and consistent spatial restriction of cell lineages uncovered by our studies that attendant and similarly restricted molecular cues must exist to induce amplifying support cell divisions in the poles and hair cell differentiating divisions closer to the center.

Notch and Wnt pathway members are expressed in complementary compartments during homeostasis

Notch and Wnt signaling control progenitor cell behavior and hair cell numbers in the lateral line (Head et al., 2013; Jacques et al., 2014; Ma et al., 2008; Wibowo et al., 2011). We discovered that members of these two signaling pathways are expressed in different NM compartments. *wnt2* and the Notch ligand *deltaa* show clear restrictions to the D-V or A-P poles in primI- and primII-derived NMs, respectively (Figures 3.2G-3.2J). *deltab, deltac* and *deltad* and the hair cell precursor marker *atoh1a* are expressed in single cells resembling the localization of differentiating hair cells (Ma et al., 2008). On the other hand, the ligand *jagged2b* is expressed broadly in the NM center (Figure 3.3A1-3.3A5). Notch receptors also show heterogeneous expression patterns. *notch3* is expressed in most support cells, with weaker expression in the D-V poles (Wibowo et al., 2011). *notch1a* is expressed robustly in all support cells, whereas

notch1b is expressed only in a few cells (Figures 3.3A6-3.3A8). In contrast, the Wnt inhibitor *dkk2* and the Notch target gene *her4* are restricted to central support cells beneath hair cells (Figures 3.3B-3.3C’’’).

The heterogeneous expression patterns of *notch* receptors and ligands suggest that different combinations may regulate progenitor proliferation or cell fate determination, as in the zebrafish CNS (Alunni et al., 2013; Okigawa et al., 2014). To determine in which cells Notch signaling is active, we analyzed the expression pattern of the Notch reporter *Tg(Tp1bglob:eEGFP)* crossed with *Tg(atoh1a:dTomato)* that labels hair cells. The Notch reporter expresses GFP in central support cells beneath the hair cells (Figures 3.2K-3.2K’), but is significantly biased toward the anterior poles of the NMs (Figure 3.2L-3.2L’, blue dots). Likewise, mRNA expression of the Notch reporter is shifted toward the anterior poles (Figure 3.2M). This bias in gene expression possibly corresponds to the slight bias of amplifying divisions towards the posterior poles in homeostatic and regenerating control NMs (Figures 3.2B’, 3.2E’; Cruz et al., 2015)), suggesting that Notch signaling keeps support cells quiescent across the central region and in the anterior pole.

Even though *wnt2* is strongly expressed in homeostatic NMs, we did not detect expression of the Wnt reporter *Tg(6xTcf/LefBS-miniP:d2EGFP)* or the Wnt target *wnt10a* (Lush and Piotrowski, 2014a) in the poles (Figures 3.3D1-3.3D3). However, *wnt10a* is transiently upregulated in central support cells during regeneration correlating with the downregulation of the Notch reporter (Figures 3.3E1-3.3F4). In contrast, the Wnt reporter is activated in only a few central cells

during regeneration suggesting that the reporter requires high levels of Wnt signaling for activation (Figure 3.3F1-3.3I1; Head et al., 2013). The inhibition of *wnt10a* and the Wnt reporter during homeostasis is likely due to co-expression of the Wnt inhibitor *dkk2* (Figures 3.3J7-3.3J10; Wada et al., 2013b). The compartmentalized expression of Notch and Wnt pathway members and their expression changes during regeneration suggest that they might be involved in controlling proliferation and differentiation in distinct regions of homeostatic and regenerating NMs.

Inhibition of Notch signaling mimics expression changes observed during regeneration

To test if the Notch and Wnt pathways regulate each other we determined how Notch downregulation affects Notch and Wnt pathway genes using the γ-secretase inhibitor LY411575, referred to as 'LY' (Mizutari et al., 2013). As Notch signaling exhibits dose-dependent effects we treated larvae with 10 and 50μM of LY (Chapouton et al., 2010; Ninov et al., 2012).

We first tested the effects on the transcription of Notch and Wnt pathway genes (Figures 3.3J-3.3L). Both doses of LY inhibit expression of the Notch reporter and the Notch target gene *her4* and lead to the upregulation of *deltad* and *atoh1a* that are normally inhibited by Notch signaling (Figures 3.3K1-3.3K5 and 3L1-3L5; Itoh and Chitnis, 2001). In homeostatic NMs, the cyclin-dependent kinase inhibitor *cdkn1bb (p27)* is expressed in a central region similar to where Notch signaling is active (Figure 3.3J6). In mammals, *Cdkn1b* keeps support

cells quiescent (Chen et al., 2003). *cdkn1bb* is only downregulated by the high dose of LY (Figure 3.3L6). Likewise, the Wnt targets *wnt2* and *wnt10a* are only upregulated after treatment with 50μM LY (Figures 3.3L8-3.3L10), correlating with loss of the Notch target and Wnt inhibitor *dkk2* (Figure 3.3L7).

The expression changes induced by a 16hr exposure to 50μM LY closely mimic changes during the first few hours after hair cell death (Figures 3.3L-3.3M; Jiang et al., 2014). 3hrs after neo exposure Notch pathway genes are downregulated and *deltaa, deltad and atoh1a* are upregulated (Figures 3.3M1-3.3M5). In contrast, *wnt2* and *wnt10a* are transiently upregulated in the center of the NM, correlating with the downregulation of *dkk2* (Figures 3.3M7-3.3M10). *cdkn1bb* is also transiently downregulated but its expression recovers by 16hrs post hair cell death (Figures 3.3M6 and 3.3N6).

A 16hr treatment with 50μM LY also leads to gene expression changes that are not observed 3 or 16hrs after neo treatment, such as a complete loss of the Notch reporter and *her4* and upregulation of Wnt target genes (Figures 3.3L). These differences are likely due to the sustained downregulation of Notch after LY treatment, whereas Notch is reactivated 5hrs after neo treatment (Figure 3.3G4).

We conclude from these data that Notch inhibits Wnt signaling in a dose dependent manner and that the expression changes observed during the first hours of regeneration can largely be attributed to the transient downregulation of Notch signaling. This interpretation is supported by the finding that the expression changes 3hrs after neo are very similar to the expression changes

after 3hrs neo and LY (Figures 3.3M and 3.3O).

Notch inhibits proliferation and differentiation through different mechanisms

To quantify the effect of Notch downregulation on proliferation and differentiation, we performed 24hr BrdU experiments on LY-treated larvae (Figures 3.4A and 3.4F). Downregulation of Notch signaling with 10 and 50μM LY doses has no significant effect on the total proliferation rate during homeostasis (Figures 3.4B-3.4E and 3.4K, TOTAL; Ma et al., 2008). However, the polar distribution of amplifying divisions is disrupted (Figures 3.4B-3.4B'' and 3.4D-3.4D'').

During regeneration the two doses of LY have different effects on total proliferation. 10μM LY does not increase the proliferation rate above the level of regenerating control NMs (Figures 3.4G and 3.4L), whereas 50μM increases total proliferation two-fold (Figures 3.4I and 3.4L). On the other hand, treatment with both doses of LY during regeneration causes loss of the D-V compartments and an increase in differentiation at the expense of amplifying divisions (Figures 3.4G-3.4J). Thus, upon Notch downregulation the majority of proliferating support cells differentiate into hair cells (Ma et al., 2008; Wibowo et al., 2011). These experiments show that Notch maintains neuromast size and the progenitor pool by inhibiting proliferation and differentiation during homeostasis. During regeneration, Notch is transiently downregulated, which triggers proliferation and differentiation (Figure 3.3J1 and 3.3M1). The finding that a low dose of the Notch

inhibitor has no effect on total proliferation but promotes differentiation demonstrates that Notch signaling inhibits these two processes via independent mechanisms.

Notch signaling inhibits proliferation via inhibition of Wnt and by a Wnt-independent mechanism

Wnt signaling induces proliferation in lateral line NMs (Head et al., 2013; Jacques et al., 2014). We confirmed this finding by treating NMs with the GSK3β inhibitor 1-Azakenpaullone (AZK) (Figures 3.5A and 3.S3A). During homeostasis and regeneration AZK treatment significantly increases the BrdU index (Figures 3.5B-3.5C, 3.5J, 3.S5B-3.S3C, 3.S5J). To test how loss of Wnt signaling affects proliferation, we generated *wnt10a* and *wnt2* mutations using TALENS that did not produce any phenotypes, likely due to redundancy with other Wnt ligands (T.P. unpublished). We therefore inhibited Wnt signaling with *hs:dkk2* that blocks the binding of Wnt ligands to their Lrp co-receptor, and we observed a significant decrease in proliferation (Figures 3.5F-3.5G, 3.5K, 3.S5F-3.S5G, 3.S5K). Thus, Notch and Wnt signaling exert opposite effects on support cell proliferation.

The finding that Wnt pathway genes are upregulated after downregulation of Notch suggests that Notch inhibits Wnt signaling via *dkk2* induction (Figures 3.3L7-3.3L10 and 3.6B6-3.6B9). To determine if the increase in proliferation after Notch inhibition during regeneration is due to upregulation of Wnt signaling, we performed epistasis experiments and treated *hs:dkk2* larvae with 50μM LY (Figures 3.5H-3.5I and 3.5K). Indeed, the LY-induced increase in total

proliferation is reduced to below normal levels, indicating that the majority of extra hair cells formed after LY treatment are likely due to an increase in Wnt signaling. This conclusion is supported by AZK-induced Wnt activation in myc-tagged *hs:nicd* larvae, in which the Notch pathway is constitutively active. Even though only 20% of cells show c-Myc expression after heat shock (data not shown), *hs:nicd* induction causes a reduction in support cell proliferation that is reverted by simultaneous activation of Wnt with AZK (Figures 3.5D-3.5E, 3.5J, 3.S5D-3.S5E, 3.S5J).

Notch signaling also inhibits some degree of proliferation independently of Wnt signaling, as in LY treated *hs:dkk2* larvae cell proliferation is not as severely reduced as in *hs:dkk2* larvae (Figures 3.5I and 3.5K). Likewise, in the presence of NICD, AZK-induced proliferation is lower than if treated with AZK alone implying that Notch signaling also inhibits other proliferative signals (Figures 3.5E and 3.5J).

We also tested the effects of Notch and Wnt on the expression of the cell cycle inhibitor *cdkn1bb*. 50μM LY downregulates *cdkn1bb* (Figures 3.3L6, 3.6A5, 3.6B5, 3.6D5, and 3.6F5) and Notch activation by *hs:nicd* enhances *cdkn1bb* expression (Figures 3.6G5, 3.6H5). However, LY does not inhibit *cdkn1bb* completely and possibly other signals also control its expression. In contrast, AZK or *hs:dkk2* do not affect *cdkn1bb* expression showing that *cdkn1bb* expression is not Wnt-dependent (Figures 3.6B5, 3.6C5, 3.6E5, 3.6F5 and 3.6H5). Together with the BrdU analyses, these data suggest that Notch signaling inhibits proliferation both in a Wnt-dependent fashion via the induction

of *dkk2* and independently of Wnt, possibly via the induction of *cdkn1bb*.

Wnt and Notch signaling control proliferation in overlapping and distinct compartments

AZK treatment specifically increases amplifying divisions in the poles and in other quiescent support cells without affecting differentiation in the center (Figures 3.6I, 3.6J, 3.6N, 3.6O, 3.6M and 3.6R). Hence, we hypothesized that central differentiating divisions are not affected by AZK, because Notch signaling is still present (Figure 3.6C). Indeed, Notch inhibition in AZK treated larvae induces central cell amplification (Figures 3.6K-3.6L and 3.6P-3.6Q). In contrast, loss of Wnt signaling significantly reduces amplifying divisions in the poles, periphery and center of the NMs (Figures 3.5F-3.5I, 3.S5F-3.S5I). Importantly, Notch inhibition in *hs:dkk2* NMs only induces differentiating divisions in the center (Figures 3.5I and 3.S5I). Combined, these analyses support the notion that Notch inhibits proliferation and differentiation in the center of the NMs independently of Wnt signaling, putatively via activation of *cdkn1bb* (Figure 3.6C5).

Even though *wnt2* is expressed in the poles (Figure 3.2G-3.2H), the Wnt reporter, when activated, is expressed only in central cells. We did not detect polar Wnt reporter expression during regeneration or after AZK treatment (Figures 3.3D1-3.3I4, and 3.6A7-3.6H7). Still, Wnt signaling has a clear activating effect on proliferation of the polar cells (Figure 3.6J). Therefore, we postulate that during regeneration, Notch downregulation in center cells activates Wnt signaling cell autonomously, which then non-cell autonomously upregulates

proliferation in the periphery via an unknown mechanism. The role *wnt2* plays in support cell behavior is unknown.

Wnt does not affect hair cell differentiation during hair cell regeneration

Notch signaling inhibits hair cell differentiation during development via *atoh1a* inhibition (Itoh and Chitnis, 2001). However, Wnt is required for hair cell differentiation in the developing mouse inner ear, as the *Atoh1* promoter possesses β-Catenin binding sites and downregulation of β-Catenin causes loss of *Atoh1*-positive cells (Jacques et al., 2014; Jacques et al., 2012; Shi et al., 2014; Shi et al., 2012). We therefore asked if Wnt signaling upregulates *atoh1a* expression in mature NMs, suggesting that Notch might affect *atoh1a* via Wnt signaling. However, *atoh1a* is only upregulated after Notch downregulation (Figures 3.3K5-3.3L5, 3.6B4, 3.6D4, 3.6F4) and *atoh1a* is not affected by either AZK-induced Wnt activation or *hs:dkk2* induction (Figures 3.6C4, 3.6E4 and 3.6H4). Also, differentiation is not enhanced in the poles after AZK treatment (Figures 3.6J and 3.6O). Only 72hr treatments with AZK modestly increase the number of hair cells, while most dividing cells remain support cells (Figures 3.S6A-3.S6C; Head et al., 2013; Jacques et al., 2014). Therefore, AZK leads to a proportional increase of hair cell numbers because more support cells divide. Either Wnt signaling interacts with *atoh1a* only during NM development, or the disparate findings in mouse and zebrafish reflect species-specific differences. Future experiments are needed to identify the signal(s) that activate *atoh1a* and drive differentiation in mature NMs. Our results show that in NMs Wnt signaling

activates support cell amplification, but is not sufficient to induce hair cell differentiation, which is induced by Notch downregulation.

Mantle cells can re-enter the cell cycle

Mantle cells do not respond to neo-induced hair cell death (Figures 3.4L and 3.7A-3.7B, 3.7D and 3.7F). However, mantle cells serve as stem cells for restoring NMs on regenerating tail tips (Dufourcq et al., 2006; Jones and Corwin, 1993). Hence, we tested if loss of support cells, in addition to hair cells would trigger mantle cell proliferation. We depleted the support cell pool by inhibiting Notch during regeneration to convert more support cells into hair cells, followed by a second dose of neomycin (neo) (Figures 3.7A, 3.S7I). Indeed, 6hrs after the second neo treatment, NMs collapse and mainly consist of GFP+ mantle cells (Figures 3.S7D-3.S7F'). NMs regain some of their shape by 10hrs but the number of mantle cells is reduced demonstrating that mantle cells were also killed (Figures 3.7H, 3.S7D-3.S7D'). By 24hrs the mantle cell number has recovered (Figure 3.7H, 3.S7F-F').

BrdU incorporation between 0-10hrs after the second neo treatment shows an increase in the BrdU index of GFP+ mantle cells that further increases between 10-24hrs (Figures 3.7E and 3.7I). As the mantle cell population recovers 24hrs after the second neo treatment, we also performed BrdU incorporation experiments between 24-36hrs. The BrdU index of mantle cells is still significantly increased, suggesting that mantle cells divide, possibly to restore the support cell population (Figures 3.7G and 3.7I). The cell cycle re-entry of mantle

cells also correlates with the disappearance of mKO2 fluorescence in *Tg(cldnb:mKO2-zCdt1); sqet20* larvae (Figures 3.7J-3.7O). mKO2-zCdt1 labels quiescent cells in the G1 phase of the cell cycle (Sugiyama et al., 2009) and is highly expressed in mantle cells (Figures 3.7L-3.7O).

Because we experimentally transformed most support cells into hair cells using LY (Figures 3.S7G-3.S7I), we wondered whether Notch downregulation was sufficient to activate mantle cell proliferation. However, LY-treatment does not cause a significant change in mantle cell proliferation (Figures 3.4K-3.4L). It remains to be demonstrated if mantle cells are stem cells and can differentiate into hair cells.

Discussion

In many animals, differences in regenerative capacities depend on the ability of tissues to maintain or induce a population of progenitor cells. In species that regenerate hair cells, support cells self-renew and give rise to new hair cells or they transdifferentiate into hair cells. In mammals, this ability is lost after birth leading to the hypothesis that mammalian support cells are highly differentiated (Burns and Corwin, 2014; Warchol, 2011). Yet, even in regenerating species support cells are not well characterized due to a dearth of molecular markers and the lack of distinct cytological characteristics. It is still unknown if support cells consist of different populations and which among them act as self-renewing stem cells (Groves, 2010; Ronaghi et al., 2012). One way to overcome these limitations is to track cell behavior in vivo and in real time. Previous studies

observed that support cells give rise to two hair cells without assessing amplifying divisions or mantle cells (López-Schier and Hudspeth, 2006; Ma et al., 2008; Wibowo et al., 2011). In adult zebrafish, anterior and posterior NM cells are label-retaining and support cells divide more often in the D/Vpoles (Cruz et al 2015). However, the identity and potency of the proliferating cells and the molecular underpinnings of their behavior could not be addressed.

Self-renewal and differentiation occur in distinct compartments and are regulated by Notch/Wnt interactions

Our analyses of regenerating neuromasts revealed a striking spatial compartmentalization of cell behaviors and we identified at least three support cell populations: 1) self-renewing cells located immediately adjacent to peripheral mantle cells in the D-V poles; 2) cells located in the center and A-P poles that proliferate and differentiate and 3) quiescent peripheral mantle cells that only respond to severe injury.

We determined that the Notch and Wnt signaling pathways balance progenitor maintenance with hair cell differentiation during homeostasis and regeneration (Figures 8A-8B). The activation of Notch and Wnt pathways in the center of the NM, and *deltaa* and *wnt2* expression in the poles, correlate with these different cell behaviors. Prior functional tests had determined that Notch signaling regulates hair cell differentiation in the center via the downregulation of *atoh1a* (Itoh and Chitnis, 2001; Ma et al., 2008).

Importantly, downregulation of Notch signaling in center support cells also

activates Wnt signaling (*wnt10a, wnt2*), as in murine inner ear development (Li et al., 2015). In addition, we show that the Wnt inhibitor *dkk2* is a Notch target in center cells beneath hair cells and that its downregulation after loss of Notch is involved in the upregulation of Wnt signaling (Figures 3.3B and 6, rows 6 and 7). The regulation of *dkk2* by Notch could be direct, as the human *DKK2* enhancer possesses RBP-Jκ binding sites (Katoh and Katoh, 2007). Subsequently, Wnt signaling also activates proliferation non-cell autonomously in polar cells, as polar cells do not show signs of canonical Wnt pathway activation. The nature of this Wnt-induced signal to polar cells remains unknown. These data show that the activation of Wnt-induced proliferation and hair cell regeneration is controlled by the prior downregulation of Notch signaling. Our previous RNA-Seq analysis of regenerating support cells supports this conclusion. After hair cell death, Notch signaling is transiently downregulated before Wnt signaling is activated and we propose that loss of Notch signaling is triggering regeneration upstream of Wnt signaling (Jiang et al., 2014).

Expression of Notch pathway genes

Notch signaling cannot be equally active in all central cells, as it would prevent hair cell differentiation. To identify cells where the Notch-active cells, we performed in situ analyses with candidate ligands and receptors. The heterogeneous expression patterns of three Notch receptors (*notch1a, notch1b, notch3*) and four ligands (*deltaa, deltab, deltac, deltad, jagged2b*) in NMs (Figures 3.3A1-3.3A8) suggest that hair cell differentiation cannot simply be

explained by lateral inhibition, where ligand expression predicts which cells differentiate (Eddison et al., 2000; Kageyama et al., 2008). For example, *deltaa* is strongly expressed in NM poles, where no hair cell differentiation occurs (Figures 3.2I-3.2J). Recent studies showed that different ligand/ receptor combinations regulate either progenitor proliferation or cell fate determination in the CNS and spinal cord (Alunni et al., 2013; Okigawa et al., 2014). In addition, Notch targets oscillate in neural progenitors, which can only be detected using live imaging techniques (Kageyama et al., 2008). As a result, the expression pattern of Notch pathway members is not sufficient to deduce in which cells Notch signaling is active (Perdigoto and Bardin, 2013; Petrovic et al., 2014).

We therefore relied on the expression of a Notch reporter that is active in the center and A-P poles. Because of the large number of ligands and receptors that are expressed in NMs and the lack of combinatorial mutants, a dissection of different combinations of ligand-receptor pairs, their effect on Notch signaling and lateral line cell behavior awaits to be performed.

Different dosages of Notch affect differentiation and proliferation

An effect of Notch dosage on cell quiescence, renewal, and cell differentiation occurs in the chick inner ear, mammary epithelial cells, fly intestine and pancreatic endocrine progenitors (Perdigoto and Bardin, 2013). Such dosage-dependency has been attributed to the fact that different ligands have different abilities to activate Notch signaling (Ninov et al., 2012; Petrovic et al.,

2014). Interestingly, we also observed a correlation between Notch signaling strength and different cell behaviors in the NMs. A higher dose of the Notch inhibitor causes hair cell differentiation as well as induction of proliferation, whereas a lower dose only affects hair cell differentiation. These results suggest that different target genes regulate these two processes independently. We conclude that cell differentiation is inhibited by Notch cell-autonomously in center cells of the NM, whereas the inhibition of the majority of proliferation is mediated via the regulation of Wnt signaling.

Why is the Notch-regulated restriction of amplifying divisions to the poles important?

The significance of restricting amplifying divisions to the poles and keeping the anterior pole more quiescent than the posterior pole is not apparent. In other tissues, such as the fly midgut, stem cells are mosaically distributed throughout the epithelium (Ohlstein and Spradling, 2007). The observation that Notch signaling is linked to the establishment of mirror-symmetric planar cell polarity of the two daughter hair cells may provide an explanation (López-Schier and Hudspeth, 2006; Wibowo et al., 2011). A reduction in Notch leads to hair cell pairs that are polarized primarily in the same direction, rather than a 1:1 distribution of opposite polarities (Mirkovic et al., 2012; Wibowo et al., 2011). As such, identifying the signal(s) that activate the Notch pathway in the NM center, defining the mechanism underpinning the enrichment of Notch signaling in the anterior side of the NM and keeping it out of the poles (Figure 3.2K) will be quite

informative. Likewise, we also have not yet identified the molecules that may be activating Wnt signaling in NMs.

Support cells throughout the NM are multipotent

NM support cells are cytologically undistinguishable, raising the question as to whether all support cells are stem cells, only a few stem cells are intermingled between progenitor cells, or if stem cells could be localized in discrete compartments such as the NM poles.

To regenerate an average of 14 hair cells in a 5 dpf NM, approximately 7 center support cells divide and produce two hair cells each, and 3-4 support cells per pole divide to maintain the progenitor pool (Figures 3.2F and 3.S2A). We do not believe that these 3-4 cells constitute a special population of stem cells because a downregulation of Notch or ubiquitous activation of Wnt signaling abolishes the bias of amplifying divisions to the poles and posterior side of the NM. Thus, support cells throughout the NM are responsive to the Notch and Wnt signaling pathways and are capable to either amplify or give rise to hair cells. These findings are strikingly similar to hair follicle and intestinal stem cells, where the position within the niche determines the fate of the cells, as passive displacement exposes them to differentiation signals (Ritsma et al., 2014; Rompolas et al., 2013).

Mantle cells are quiescent but proliferate in response to severe injury

Transection of axolotl tails and zebrafish fins causes peripheral cells to proliferate and migrate onto the regenerating tail tips, where they form new sense organs (Jones and Corwin, 1993; Stone, 1937). Mantle cells also give rise to postembryonic NMs suggesting that mantle cells are multipotent progenitors (Wada et al., 2013a). We were surprised that mantle cells do not react to neo-induced hair cell death. However, given that inner support cell amplification and differentiation are balanced during regeneration, a mantle cell response is not required (Figure 3.4L). Our finding that mantle cells re-enter the cell cycle after more severe damage to the NM suggests that mantle cells might represent a quiescent pool of progenitor cells that respond to signals triggered by severe injury. Quiescence is characteristic of a variety of stem cell populations in the liver, hair follicles, intestine and hematopoietic system (Li and Clevers, 2010; Tetteh et al., 2014). Alternatively, mantle cells could be specialized support cells that only proliferate to maintain the mantle cell population. We will distinguish between these possibilities by generating transgenic lines that permit us to lineage-trace proliferating mantle cells. Interestingly, support cell amplification almost exclusively occurs in cells that are in contact with mantle cells (Figures S2B-S2G), raising the possibility that mantle cells might constitute a niche for support stem cells.

Conclusion

We report a comprehensive, systematic in vivo analysis of progenitor cell lineages during homeostasis and regeneration. We also demonstrate how this approach can be used to investigate the function of signaling pathways at the single cell level during the poorly understood process of hair cell regeneration. Our combined methods have allowed to precisely identify different progenitor cell types that are restricted to particular tissue compartments, follow their behavior in real time and define a Notch-driven inhibition of Wnt-induced cell proliferation. These findings set the stage for a detailed characterization of signals that control progenitor cell maintenance versus differentiation in a vertebrate sensory organ. Our results stand to inform and contribute to our understanding of the biology and population dynamics of adult stem cells in multiple systems, including mammals.

Experimental procedures

Fish lines and regeneration experiments

Zebrafish lines used: *Tg(cldnb:lynGFP)^{zf106}* (Haas and Gilmour, 2006), *Tg(cldnB:H2A-mCherry)^{psi4}* (Lush and Piotrowski, 2014a), *Et(krt4:EGFP)^{sqet20}* or *sqet20* (Parinov et al., 2004), *sqet4* or *Tg(atp2b1a-GFP)* (Go et al., 2010), *Tg(Tp1bglob:eGFP)^{um13}* (Parsons et al., 2009), *Tg(atoh1a:dTomato)^{nns8}* (Wada et al., 2010), *Tg(6xTcf/LefBS-miniP:d2EGFP)^{kyu1}* (Shimizu et al., 2012), *Tg(hsp70l:Gal4-VP16)*^{VU22} (Shin et al., 2007), *Tg(UAS:myc-Notch1a-intra)^{kca3}* (*hs:nicd*; Scheer et al., 2001), *Tg(UAS:dkk2-RFP)^{zf424}* (*hs:dkk2*; Wada et al.,

2013b). To generate the *Tg(cldnb:mKO2-zCdt1)* line, the zCdt1-mKO2 (Sugiyama et al., 2009) motif was cloned into a pDest vector containing the -*8.0claudinb* promoter. To induce hair cell regeneration 5 dpf larvae were treated for 30min with 300μM neo in 0.5 E2 (Fisher Bioreagents).

Time-lapse imaging and image acquisition

Quadruple transgenic fish were obtained by crossing *Tg(cldnb:lynGFP); Tg(cldnb:H2A-mCherry)* and *sqet20; sqet4.* Before neo treatment, larvae were immobilized with tricaine (MS-222) up to 150 mg/L (100μL of 4g/L tricaine every 20min for 2 to 3hrs). Larvae were mounted in 1% low melting point agarose in 0.5X E2 with 100 mg/L tricaine on glass bottom dishes (Mat-Tek, USA). Images were acquired at 28ºC on a Zeiss LSM780 confocal microscope using a 40X water objective and with appropriate Z-sampling for three-dimensional reconstruction and 4D-stacks. Except for Figure S2, only primI-derived pL1, pL2 or pL3 NMs were imaged. After neo treatment, single NMs were imaged every 6min for more than 70hrs. Three-dimensional rendering and image analysis of confocal z-stacks of single NMs were done using Imaris (Bitplane). Please, see Supplemental Experimental Procedures for specifics of the Spatial and cell movement analyses.

Pharmacological inhibitors and BrdU incorporation

The γ-secretase inhibitor LY411575 (Selleckchem) and the GSK3β inhibitor 1-Azakenpaullone (Sigma-Aldrich) were diluted to their desired

concentrations in 0.5X E2 media with a final concentration of 1% DMSO. Control larvae were treated with 1% DMSO. Bromodeoxyuridine (Sigma Aldrich) was diluted to 10mM in embryo medium containing 1%DMSO with or without the pharmacological inhibitors.

Heat-shock experiments

Tg(hsp70l:Gal4);Tg(sqet4) fish were crossed with either *Tg(UAS:myc-Notch1a-intra)* or *Tg(UAS:dkk2-RFP).* GFP+ larvae were used for proliferation assays, and in situ hybridization was performed on GFP- siblings. To activate and sustain the expression driven by a heat shock-activated Gal4, 5 dpf larvae were heat shocked (HS) every other hour (1hr HS then 1hr at 28.5ºC). Before drug treatments, larvae were heat shocked six times at 39ºC (first HS at 37ºC) in a water bath. After this initial activation, larvae were treated with neo or DMSO and transferred to E2 medium containing pharmacological inhibitors as described above. To maintain Gal4-activated expression, larvae were heat shocked every other hour for 24hrs in a 37ºC incubator. Larvae were fixed in 4% paraformaldehyde at 4ºC for 3 days. Activated *Tg(UAS:dkk2-RFP)* embryos were sorted after fixation by RFP fluorescence. *Tg(UAS:myc-Notch1a-intra)* fish were sorted after anti c-Myc antibody staining.

Immunohistochemistry

BrdU immunodetection was done according to Ma et al. (2008) with the following modifications: larvae were permeabilized for 15min using 20µg/ml

proteinase-K and treated for 1hr in 2N hydrochloric acid. Antibodies used: monoclonal rat anti-BrdU (1:500; Accurate Chemical & Scientific Corp), rabbit anti-GFP (1:500; Invitrogen), monoclonal mouse anti c-myc (Santa Cruz). DAPI (Invitrogen) was used as counterstain. BrdU indexes were calculated as the number of BrdU+ cells over the total NM cell number. We compared samples by ANOVA and Tukey post-Hoc tests using the SAS 9.3 statistical software. The indexes were transformed using the formula arsin (sqrt(percentage/100)) to ensure the assumption of normality.

In situ hybridization

In situ hybridization was performed as described in by (Kopinke et al., 2006) with modifications for 5 dpf fish described in (Ma et al., 2008). See Supplemental Experimental Procedures for probes used.

Author contributions

A.R.-C. and T.P. designed the study, analyzed and interpreted data, and wrote the paper.

A.R.-C., J.N.A., L.J. and A.K.-G. performed experiments.

H.L. performed the statistical analyses.

R.A. developed and performed the cell movement analyses.

Acknowledgments

We are grateful to Drs. A. Sánchez Alvarado, L. Li, M. Lush, J. Kniss and M. Venero Galanternik for valuable comments on the manuscript, and Drs. V. Korzh, N. Lawson, T. Ishitani, H. Wada, K. Kawakami, B. Appel and P. Kulesa for strains and reagents. We are also thankful to R. Duncan and E. Young for preliminary experiments, members of the Piotrowski lab, and Dr. T. Xie for insightful discussions. We would also like to thank D. Fekete for suggesting the neo-LY-neo experiment. We thank the U. of Utah Zebrafish Core and the Aquatics Facility at the Stowers Institute for excellent fish care, J. Unruh and B. Rubinstein for support with the spatial analysis, J. Lange, S. McKinney and the Microscopy Core for imaging support and M. Miller for help with graphic design. This work was funded by an NIH (NIDCD) award RC1DC010631 to T.P, the Hearing Health Foundation, and by institutional support from the Stowers Institute for Medical Research.

References

Alunni, A., Krecsmarik, M., Bosco, A., Galant, S., Pan, L., Moens, C.B., and Bally-Cuif, L. (2013). Notch3 signaling gates cell cycle entry and limits neural stem cell amplification in the adult pallium. Development *140*, 3335-3347.

Balak, K.J., Corwin, J.T., and Jones, J.E. (1990). Regenerated hair cells can originate from supporting cell progeny: evidence from phototoxicity and laser ablation experiments in the lateral line system. J Neurosci *10*, 2502-2512.

Burns, J.C., and Corwin, J.T. (2014). Responses to cell loss become restricted as the supporting cells in mammalian vestibular organs grow thick junctional actin bands that develop high stability. J Neurosci *34*, 1998-2011.

Chapouton, P., Skupien, P., Hesl, B., Coolen, M., Moore, J.C., Madelaine, R.,

Kremmer, E., Faus-Kessler, T., Blader, P., Lawson, N.D.*, et al.* (2010). Notch activity levels control the balance between quiescence and recruitment of adult neural stem cells. J Neurosci *30*, 7961-7974.

Chen, P., Zindy, F., Abdala, C., Liu, F., Li, X., Roussel, M.F., and Segil, N. (2003). Progressive hearing loss in mice lacking the cyclin-dependent kinase inhibitor Ink4d. Nat Cell Biol *5*, 422-426.

Corwin, J.T., and Cotanche, D.a. (1988). Regeneration of sensory hair cells after acoustic trauma. Science (New York, NY) *240*, 1772-1774.

Cox, B.C., Chai, R., Lenoir, A., Liu, Z., Zhang, L., Nguyen, D.-H., Chalasani, K., Steigelman, K.A., Fang, J., Rubel, E.W.*, et al.* (2014). Spontaneous hair cell regeneration in the neonatal mouse cochlea in vivo. Development *141*, 816-829.

Cruz, I.A., Kappedal, R., Mackenzie, S.M., Hailey, D.W., Hoffman, T.L., Schilling, T.F., and Raible, D.W. (2015). Robust regeneration of adult zebrafish lateral line hair cells reflects continued precursor pool maintenance. Dev Biol.

Dufourcq, P., Roussigné, M., Blader, P., Rosa, F., Peyrieras, N., and Vriz, S. (2006). Mechano-sensory organ regeneration in adults: the zebrafish lateral line as a model. Mol Cell Neurosci *33*, 180-187.

Eddison, M., Le Roux, I., and Lewis, J. (2000). Notch signaling in the development of the inner ear: lessons from Drosophila. Proc Natl Acad Sci U S A *97*, 11692-11699.

Furness, D.N. (2015). Molecular basis of hair cell loss. Cell Tissue Res.1-13

Go, W., Bessarab, D., and Korzh, V. (2010). atp2b1a regulates Ca(2+) export during differentiation and regeneration of mechanosensory hair cells in zebrafish. Cell Calcium *48*, 302-313.

Groves, A.K. (2010). The challenge of hair cell regeneration. Exp Biol Med (Maywood) *235*, 434-446.

Haas, P., and Gilmour, D. (2006). Chemokine signaling mediates self-organizing tissue migration in the zebrafish lateral line. Dev Cell *10*, 673-680.

Head, J.R., Gacioch, L., Pennisi, M., and Meyers, J.R. (2013). Activation of canonical Wnt/β-catenin signaling stimulates proliferation in neuromasts in the zebrafish posterior lateral line. Dev Dyn *242*, 832-846.

Itoh, M., and Chitnis, A.B. (2001). Expression of proneural and neurogenic genes in the zebrafish lateral line primordium correlates with selection of hair cell fate in neuromasts. Mech Dev *102*, 263-266.

Jacques, B.E., Montgomery, W.H., Uribe, P.M., Yatteau, A., Asuncion, J.D., Resendiz, G., Matsui, J.I., and Dabdoub, A. (2014). The role of Wnt/β-catenin signaling in proliferation and regeneration of the developing basilar papilla and lateral line. Dev Neurobiol *74*, 438-456.

Jacques, B.E., Puligilla, C., Weichert, R.M., Ferrer-Vaquer, A., Hadjantonakis, A.-K., Kelley, M.W., and Dabdoub, A. (2012). A dual function for canonical Wnt/β-catenin signaling in the developing mammalian cochlea. Development *139*, 4395-4404.

Jiang, L., Romero-Carvajal, A., Haug, J.S., Seidel, C.W., and Piotrowski, T. (2014). Gene-expression analysis of hair cell regeneration in the zebrafish lateral line. Proc Natl Acad Sci U S A *111*, E1383-1392.

Jones, J.E., and Corwin, J.T. (1993). Replacement of lateral line sensory organs during tail regeneration in salamanders: identification of progenitor cells and analysis of leukocyte activity. J Neurosci *13*, 1022-1034.

Jones, J.E., and Corwin, J.T. (1996). Regeneration of sensory cells after laser ablation in the lateral line system: hair cell lineage and macrophage behavior revealed by time-lapse video microscopy. J Neurosci *16*, 649-662.

Kageyama, R., Ohtsuka, T., Shimojo, H., and Imayoshi, I. (2008). Dynamic Notch signaling in neural progenitor cells and a revised view of lateral inhibition. Nat Neurosci *11*, 1247-1251.

Katoh, M., and Katoh, M. (2007). WNT antagonist, DKK2, is a Notch signaling target in intestinal stem cells: Augmentation of a negative regulation system for canonical WNT signaling pathway by the Notch-DKK2 signaling loop in primates. Int J Mol Med *19*, 197-201.

Kopinke, D., Sasine, J., Swift, J., Stephens, W.Z., and Piotrowski, T. (2006). Retinoic acid is required for endodermal pouch morphogenesis and not for pharyngeal endoderm specification. Dev Dyn *235*, 2695-2709.

Li, L., and Clevers, H. (2010). Coexistence of quiescent and active adult stem cells in mammals. Science (New York, NY) *327*, 542-545.

Li, W., Wu, J., Yang, J., Sun, S., Chai, R., Chen, Z.Y., and Li, H. (2015). Notch

inhibition induces mitotically generated hair cells in mammalian cochleae via activating the Wnt pathway. Proc Natl Acad Sci U S A *112*, 166-171.

López-Schier, H., and Hudspeth, A.J. (2006). A two-step mechanism underlies the planar polarization of regenerating sensory hair cells. Proc Natl Acad Sci U S A *103*, 18615-18620.

López-Schier, H., Starr, C.J., Kappler, J.A., Kollmar, R., and Hudspeth, A.J. (2004). Directional cell migration establishes the axes of planar polarity in the posterior lateral-line organ of the zebrafish. Dev Cell *7*, 401-412.

Lush, M.E., and Piotrowski, T. (2014a). ErbB expressing Schwann cells control lateral line progenitor cells via non-cell-autonomous regulation of Wnt/β-catenin. eLife *3*, e01832.

Lush, M.E., and Piotrowski, T. (2014d). Sensory hair cell regeneration in the zebrafish lateral line. Dev Dyn *243*, 1187-1202.

Ma, E.Y., Rubel, E.W., and Raible, D.W. (2008). Notch signaling regulates the extent of hair cell regeneration in the zebrafish lateral line. J Neurosci *28*, 2261-2273.

Metcalfe, W.K., Kimmel, C.B., and Schabtach, E. (1985). Anatomy of the posterior lateral line system in young larvae of the zebrafish. J Comp Neurol *233*, 377-389.

Mirkovic, I., Pylawka, S., and Hudspeth, A.J. (2012). Rearrangements between differentiating hair cells coordinate planar polarity and the establishment of mirror symmetry in lateral-line neuromasts. Biology open *1*, 498-505.

Mizutari, K., Fujioka, M., Hosoya, M., Bramhall, N., Okano, H.J., Okano, H., and Edge, A.S.B. (2013). Notch inhibition induces cochlear hair cell regeneration and recovery of hearing after acoustic trauma. Neuron *77*, 58-69.

Nicolson, T. (2005). The Genetics of Hearing and Balance in Zebrafish Teresa. Annu Rev Genet *39*, 9-22.

Ninov, N., Borius, M., and Stainier, D.Y.R. (2012). Different levels of Notch signaling regulate quiescence, renewal and differentiation in pancreatic endocrine progenitors. Development *139*, 1557-1567.

Northcutt, R.G., Catania, K.C., and Criley, B.B. (1994). Development of lateral line organs in the axolotl. J Comp Neurol *340*, 480-514.

Ohlstein, B., and Spradling, A. (2007). Multipotent Drosophila intestinal stem cells specify daughter cell fates by differential notch signaling. Science (New York, NY) *315*, 988-992.

Okigawa, S., Mizoguchi, T., Okano, M., Tanaka, H., Isoda, M., Jiang, Y.-J., Suster, M., Higashijima, S.-I., Kawakami, K., and Itoh, M. (2014). Different combinations of Notch ligands and receptors regulate V2 interneuron progenitor proliferation and V2a/V2b cell fate determination. Dev Biol *391*, 196-206.

Parinov, S., Kondrichin, I., Korzh, V., and Emelyanov, A. (2004). Tol2 transposon-mediated enhancer trap to identify developmentally regulated zebrafish genes in vivo. Dev Dyn *231*, 449-459.

Parsons, M.J., Pisharath, H., Yusuff, S., Moore, J.C., Siekmann, A.F., Lawson, N., and Leach, S.D. (2009). Notch-responsive cells initiate the secondary transition in larval zebrafish pancreas. Mech Dev *126*, 898-912.

Perdigoto, C.N., and Bardin, A.J. (2013). Sending the right signal: Notch and stem cells. Biochim Biophys Acta *1830*, 2307-2322.

Petrovic, J., Formosa-Jordan, P., Luna-Escalante, J.C., Abelló, G., Ibañes, M., Neves, J., and Giraldez, F. (2014). Ligand-dependent Notch signaling strength orchestrates lateral induction and lateral inhibition in the developing inner ear. Development *141*, 2313-2324.

Ritsma, L., Ellenbroek, S.I.J., Zomer, A., Snippert, H.J., de Sauvage, F.J., Simons, B.D., Clevers, H., and van Rheenen, J. (2014). Intestinal crypt homeostasis revealed at single-stem-cell level by in vivo live imaging. Nature *507*, 362-365.

Rompolas, P., Mesa, K.R., and Greco, V. (2013). Spatial organization within a niche as a determinant of stem-cell fate. Nature *502*, 513-518.

Ronaghi, M., Nasr, M., and Heller, S. (2012). Concise review: Inner ear stem cells--an oxymoron, but why? Stem cells (Dayton, Ohio) *30*, 69-74.

Rubel, E.W., Furrer, S.A., and Stone, J.S. (2013). A brief history of hair cell regeneration research and speculations on the future. Hear Res *297*, 42-51.

Scheer, N., Groth, A., Hans, S., and Campos-Ortega, J.A. (2001). An instructive function for Notch in promoting gliogenesis in the zebrafish retina. Development *128*, 1099-1107.

Shi, F., Hu, L., and Edge, A.S.B. (2013). Generation of hair cells in neonatal mice by β-catenin overexpression in Lgr5-positive cochlear progenitors. Proc Natl Acad Sci U S A *110*, 13851-13856.

Shi, F., Hu, L., Jacques, B.E., Mulvaney, J.F., Dabdoub, A., and Edge, A.S.B. (2014). β-Catenin is required for hair-cell differentiation in the cochlea. J Neurosci *34*, 6470-6479.

Shi, F., Kempfle, J.S., and Edge, A.S.B. (2012). Wnt-responsive Lgr5-expressing stem cells are hair cell progenitors in the cochlea. J Neurosci *32*, 9639-9648.

Shimizu, N., Kawakami, K., and Ishitani, T. (2012). Visualization and exploration of Tcf/Lef function using a highly responsive Wnt/β-catenin signaling-reporter transgenic zebrafish. Dev Biol *370*, 71-85.

Shin, J., Poling, J., Park, H.C., and Appel, B. (2007). Notch signaling regulates neural precursor allocation and binary neuronal fate decisions in zebrafish. Development *134*, 1911-1920.

Stone, L.S. (1937). Further experimental studies of the development of lateral-line sense organs in amphibians observed in living preparations. J Comp Neurol *68*, 83-115.

Sugiyama, M., Sakaue-Sawano, A., Iimura, T., Fukami, K., Kitaguchi, T., Kawakami, K., Okamoto, H., Higashijima, S.-i., and Miyawaki, A. (2009). Illuminating cell-cycle progression in the developing zebrafish embryo. Proc Natl Acad Sci U S A *106*, 20812-20817.

Tetteh, P.W., Farin, H.F., and Clevers, H. (2014). Plasticity within stem cell hierarchies in mammalian epithelia. Trends Cell Biol *25*, 100-108.

Wada, H., Dambly-Chaudiere, C., Kawakami, K., and Ghysen, A. (2013a). Innervation is required for sense organ development in the lateral line system of adult zebrafish. Proc Natl Acad Sci U S A *110*, 5659-5664.

Wada, H., Ghysen, A., Asakawa, K., Abe, G., Ishitani, T., and Kawakami, K. (2013b). Wnt/Dkk negative feedback regulates sensory organ size in zebrafish. Curr Biol *23*, 1559-1565.

Wada, H., Ghysen, A., Satou, C., Higashijima, S.-I., Kawakami, K., Hamaguchi, S., and Sakaizumi, M. (2010). Dermal morphogenesis controls lateral line patterning during postembryonic development of teleost fish. Dev Biol *340*, 583-594.

Warchol, M.E. (2011). Sensory regeneration in the vertebrate inner ear: differences at the levels of cells and species. Hear Res *273*, 72-79.

Whitfield, T.T. (2002). Zebrafish as a model for hearing and deafness. J Neurobiol *53*, 157-171.

Wibowo, I., Pinto-Teixeira, F., Satou, C., Higashijima, S.-i., and López-Schier, H. (2011). Compartmentalized Notch signaling sustains epithelial mirror symmetry. Development *138*, 1143-1152.

Williams, J.A., and Holder, N. (2000). Cell turnover in neuromasts of zebrafish larvae. Hear Res *143*, 171-181.

Supplemental experimental procedures

Spatial analysis

The relative position (X_n,Y_n) of cells within the neuromast in a z-stack file was obtained using the Imaris spots function. The coordinates of the neuromast center point (X_c,Y_c) were obtained by manually drawing the neuromast outline using the surface function. To establish a horizontal reference axis, the relative positions of the left and right interneuromast cells were recorded: (X_{Linc} ; Y_{Linc}) and (X_{Rinc}; Y_{Rinc}). The scatter plots of multiple neuromasts were superimposed and aligned for statistical analysis, first by translating the coordinates to an absolute center point ($X=(X_n - X_c)$; $Y=(Y_n - Y_c)$), and then by rotating each neuromast to a common X axis. Neuromast rotation was possible by calculating the neuromast tilt angle (α) from the left and right interneuromast coordinates $\alpha=\text{atan}((Y_{Linc}-Y_{Rinc})/X_{Linc}-X_{Rinc}))$. This angle was used to rotate the cell nuclei positions of a given neuromast to a common X axis using the formulas $X_r=(X*\cos(-\alpha))-(Y*\sin(-\alpha))$,$Y_r =(Y*\cos(-\alpha))-(X*\sin(-\alpha))$. The total ($X_r$;Y_r) recorded

positions were used to generate scatterplots in MS Excel. The distribution of angular position was represented using rose diagrams generated in R (RCoreTeam, 2013). The enrichment of a specific population in any of the quarters formed between 45°, 135°, 225° and 315° angles was addressed using Binomial analysis. The distribution of radii was analyzed using ANOVA.

Cell movement analysis

Every neuromast mitotic event observed in the time-lapse movies within the first 24hrs was manually back tracked to the origin of cell division at time 0 (1hr post neomycin treatment) and classified as a hair cell or support cell progenitor using Imaris' spots function. To account for larval movement and image drift, we also tracked the center of the neuromast throughout the movie. This created a new stabilized center point from which we calculated the relative position of a progenitor and its progeny at every time point until 26hrs using the method described above. We then used this new coordinate system to calculate the distance each cell traveled during the time course relative to the neuromast center point. To visualize the results, we created a Java program in ImageJ to plot the positions of each cell over time. The plotted positions were superimposed onto a z-projection of the stabilized movie.

In order to test whether cells migrate before division, we created a vector plot of the cell's location before division. We used the same center stabilized data in order to overlay the vectors onto a single plot. The vector was drawn from the cell location at the beginning of the timelapse ($X(t_0),Y(t_0)$) to the cell location one

frame before division ($X(t_{D-1}),Y(t_{D-1})$). To analyze movement after division, a vector plot was made using the same method as described above. The vector was drawn from the cell location at the time of the first division ($X(t_D),Y(t_D)$) to the cell location 25 frames later ($X(t_{D+25}),Y(t_{D+25})$). Since some cells divide again, the time t_{D+25} was chosen to make sure only the cell behavior immediately after the first division was captured, and not behavior before the next division. For clarity we randomly selected a single daughter cell to plot since daughter cells stay very close after division.

In situ hybridization

The following probes were used: *atoh1a, gfp, deltad, cdkn1bb, notch3, her4.1,* (Jiang et al., 2014)*, wnt10a* (Lush and Piotrowski, 2014)*, lef1* (Aman and Piotrowski, 2008)*, dkk2* (Wada et al., 2013)*, wnt2* (Poulain and Ober, 2011) and *deltaa, deltab, deltac* (Itoh and Chitnis, 2001). PCRII-TOPO cloning was used to synthesize probes for *notch1a* (ACGGCTAAAGTCCTGCTTGA, GAAGGCGGAGTCAGAAACTG) and *notch1b* (ACAACCTAGTGCGCAGTCCT, GGCACTTGAAGTTGGTGGTT). *jagged2b* (TTTTGAGTCGTTCGCAAGTG, CATTACCATCCCGTTTTGAGTCGTTCGCAAGTG) was cloned into pPR-T4P for probe synthesis using AA18 and PR244 primers. In situ hybridization was performed using an Intavis InSituPro robot. Images of stained embryos were acquired on a Zeiss Axio Observer microscope using an Axiocam camera.

Supplemental references

Aman, A., and Piotrowski, T. (2008). Wnt/beta-catenin and Fgf signaling control collective cell migration by restricting chemokine receptor expression. Developmental cell *15*, 749-761.

Itoh, M., and Chitnis, A.B. (2001). Expression of proneural and neurogenic genes in the zebrafish lateral line primordium correlates with selection of hair cell fate in neuromasts. Mechanisms of Development *102*, 263-266.

Jiang, L., Romero-Carvajal, A., Haug, J.S., Seidel, C.W., and Piotrowski, T. (2014). Gene-expression analysis of hair cell regeneration in the zebrafish lateral line. Proc Natl Acad Sci U S A *111*, E1383-1392.

Lush, M.E., and Piotrowski, T. (2014). ErbB expressing Schwann cells control lateral line progenitor cells via non-cell-autonomous regulation of Wnt/β-catenin. eLife *3*, e01832.

Poulain, M., and Ober, E.A. (2011). Interplay between Wnt2 and Wnt2bb controls multiple steps of early foregut-derived organ development. Development (Cambridge, England) *138*, 3557-3568.

RCoreTeam (2013). R: A language and environment for statistical computing. (Vienna, Austria, R Foundation for Statistical Computing).

Wada, H., Ghysen, A., Asakawa, K., Abe, G., Ishitani, T., and Kawakami, K. (2013). Wnt/Dkk negative feedback regulates sensory organ size in zebrafish. Curr Biol *23*, 1559-1565.

Figure 3.1. Support cells are multipotent progenitors.
(A) Horizontal and (B) lateral views of a NM.
(C-H) Quadruple transgenic larvae express the mantle cell marker *sqet20* (F, green), the hair cell marker *sqet4* (G, cytoplasmic green), the cell membrane marker *cldnb:lynGFP* (G) and the nuclear maker *cldnb:H2A-mCherry* (H).
(I) Still images of a time-lapse of a homeostatic NM (Movie S1). Time stamp in hours and minutes. Split images show different focal planes. Numbers in NMs label the progenitors shown in (J).
(J) Lineage analysis of the mitotic events in (I) and Movie S1.
(K) Time-lapse of a regenerating NM (Movie S2B). CD1 is shown in Movie S2C.
(L) Lineage analysis in a regenerating NM (Figure 1K; Movie S2).
(M) Support cells self-renew or differentiate into two hair cells: Quantification of lineages of three time-lapse movies of regenerating NMs from Figures S1F-S1H.
(N) Proliferation dynamics during regeneration. Amplifying divisions occur first ($p<0.0001$, Fisher's exact test).
(O) Proliferating cells and their progeny do not actively move in a regenerating NM. Lineages from Figure 1L are color-coded: red: amplifying cell divisions, green: differentiation, blue: mantle cell divisions (Movie S3). mCherry nuclei are in grey.
(P) Vectors show directions and distances of cell displacement before mitosis (metaphase) for every cell division recorded during the first 24hrs in Figures S1F-S1H). Central hair cell progenitors are not displaced.
(Q) Vectors show cell displacements of one of the daughter support cells back to their original positions. Displacements for P and Q are quantified in Figure S1I.
Scale bars = 10μm.
See also Figure S1, Movie S1, Movie S2, Movie S3

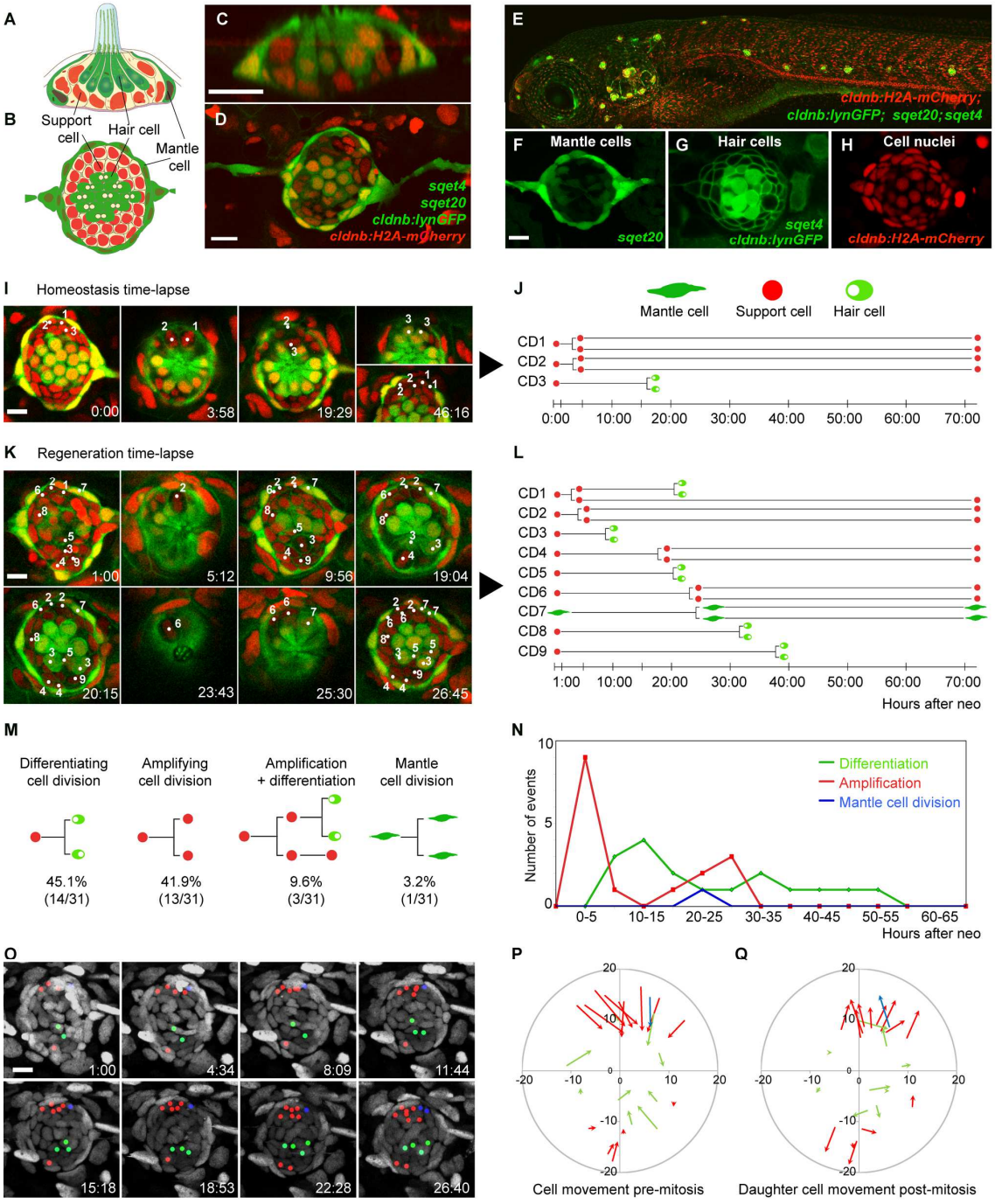
A
B
Support cell
Hair cell
Mantle cell
C
D
sqet4
sqet20
cldnb:lynGFP
cldnb:H2A-mCherry
E
cldnb:H2A-mCherry;
cldnb:lynGFP; sqet20;sqet4
F Mantle cells
sqet20
G Hair cells
sqet4
cldnb:lynGFP
H Cell nuclei
cldnb:H2A-mCherry
I Homeostasis time-lapse
0:00
3:58
19:29
46:16
J
Mantle cell
Support cell
Hair cell
CD1
CD2
CD3
0:00 10:00 20:00 30:00 40:00 50:00 60:00 70:00
K Regeneration time-lapse
1:00
5:12
9:56
19:04
20:15
23:43
25:30
26:45
L
CD1
CD2
CD3
CD4
CD5
CD6
CD7
CD8
CD9
1:00 10:00 20:00 30:00 40:00 50:00 60:00 70:00
Hours after neo
M
Differentiating cell division
Amplifying cell division
Amplification + differentiation
Mantle cell division
45.1% (14/31)
41.9% (13/31)
9.6% (3/31)
3.2% (1/31)
N
Differentiation
Amplification
Mantle cell division
Number of events
0-5 10-15 20-25 30-35 40-45 50-55 60-65
Hours after neo
O
1:00
4:34
8:09
11:44
15:18
18:53
22:28
26:40
P
Cell movement pre-mitosis
Q
Daughter cell movement post-mitosis

Figure S1. Support cells are multipotent progenitors. Related to Figure 3.1.
(A) Number of support and hair cells in first trunk neuromasts (L1, N=7) at 4 time points after hair cell death. Dotted lines show cell numbers in homeostatic neuromasts and solid lines show cell numbers in regenerating neuromasts. Error bars indicate the 95% confidence interval (CI).
(B-E) Lineage analyses of 4 time-lapse movies of homeostatic neuromasts. (B) is also shown in Figure 1J.
(F-H) Lineage analyses of 4 time-lapse movies of regenerating neuromasts. (F) is also shown in Figure 1L. (I) Cell displacement from the initial position of the progenitor and its daughter cells during the first 26hrs after hair cell death. Average displacement (not shown) and standard deviation of displacement were measured from the lineages traced in Movie S3 (colored dots; Figures 1L and 1O) and Figures S1F-S1H. The red circles and green diamonds show the positions of progenitors relative to the center of the NMs (in pixels) when the time-lapses started. Black asterisks indicate four tracked quiescent cells. The error bars show the standard deviation of the displacement at each timepoint from t=1:00 to t=26:40, indicating how much all progeny moved relative to the progenitors' initial position. The average diameter of 1 cell nucleus is 5 pixels.
(J) Positions of support or hair cell progenitors shown in F, G and H, superimposed on the same X,Y plane. The rose diagrams show the distribution of the angular position. Bipolar clustering (A-P or D-V) and directional bias were statistically analyzed using the Binomial test (***$p<0.001$).
See also Movie 3.S1, Movie 3.S2, Movie 3.S3

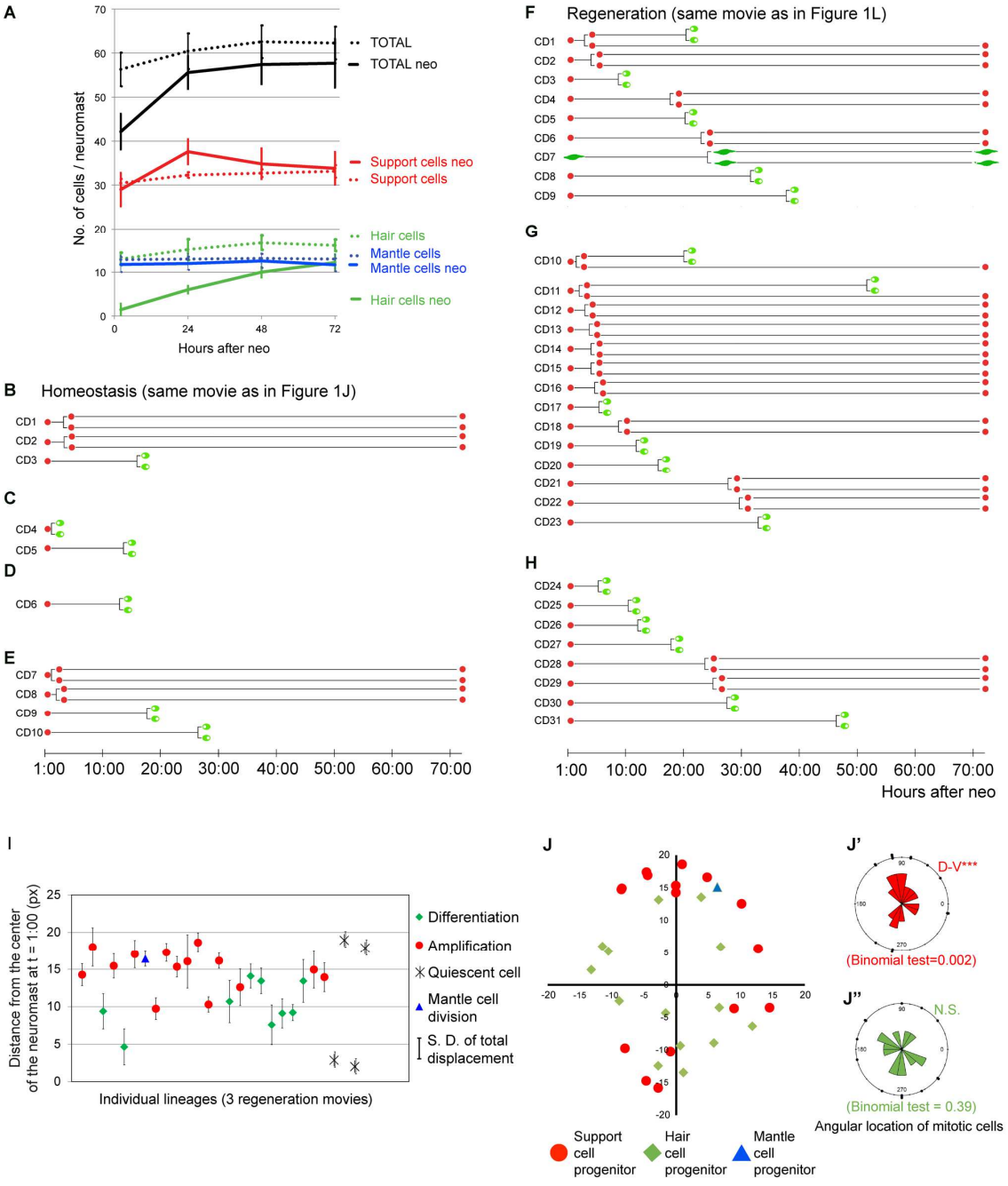
A
No. of cells / neuromast
Hours after neo
TOTAL
TOTAL neo
Support cells neo
Support cells
Hair cells
Mantle cells
Mantle cells neo
Hair cells neo
B Homeostasis (same movie as in Figure 1J)
C
D
E
F Regeneration (same movie as in Figure 1L)
G
H
Hours after neo
I
Distance from the center of the neuromast at t = 1:00 (px)
Individual lineages (3 regeneration movies)
Differentiation
Amplification
Quiescent cell
Mantle cell division
S. D. of total displacement
J
Support cell progenitor
Hair cell progenitor
Mantle cell progenitor
J'
D-V***
(Binomial test=0.002)
J"
N.S.
(Binomial test = 0.39)
Angular location of mitotic cells

Figure 3.2. Support cell amplification is restricted to polar compartments during homeostasis and regeneration.
(A, D) 24hr BrdU incorporation in primI-derived NMs during homeostasis and regeneration. Scale bar = 10μm.
(B, E) Amplifying cell divisions are clustered in the D/V compartments of NMs. BrdU plots show the positions of BrdU+ nuclei of 18 NMs superimposed on the same XY plane. Red squares indicate amplifying divisions; green diamonds indicate BrdU+ cells that differentiated into *sqet4*+ hair cells. Blue crosses indicate quiescent mantle cells. Axes units are in pixels.
(B', B'', E', E'') Rose diagrams for the angular position of BrdU+ support cells (red), BrdU+ hair cells (green). Bipolar clustering (D-V) and directional bias to the posterior (red arrow) were statistically analyzed using the Binomial test (***$p<0.001$).
(C, F) Number and location of progenitors that divide within 24hrs in a single NM.
(G-J) *wnt2* and *deltaa* are expressed in poles. Arrowheads label primI-derived NMs. Asterisks label primII-derived NMs. Dashed line indicates the NM outline. Scale bar in (G) =100μm; in (H)=60μm.
(K-K') EGFP expression in the Notch reporter *Tg(Tp1bglob:eGFP)* shows that Notch signaling occurs in central cells beneath the red hair cells labeled with *Tg(atoh1a:dTomato)*. The Atoh1a reporter is mosaic, leaving some cells unlabeled. (K') Orthogonal view of K. Scale bar = 10 μm
(L-L') Superimposed EGFP+ Notch reporter cells of 15 NMs (blue squares) are biased toward the anterior side of the NM, as seen in rose diagram.
(M) In situ hybridization of *gfp* mRNA in *Tg(Tp1bglob:eGFP).* Scale bar = 10 μm.
See also Figure S2.

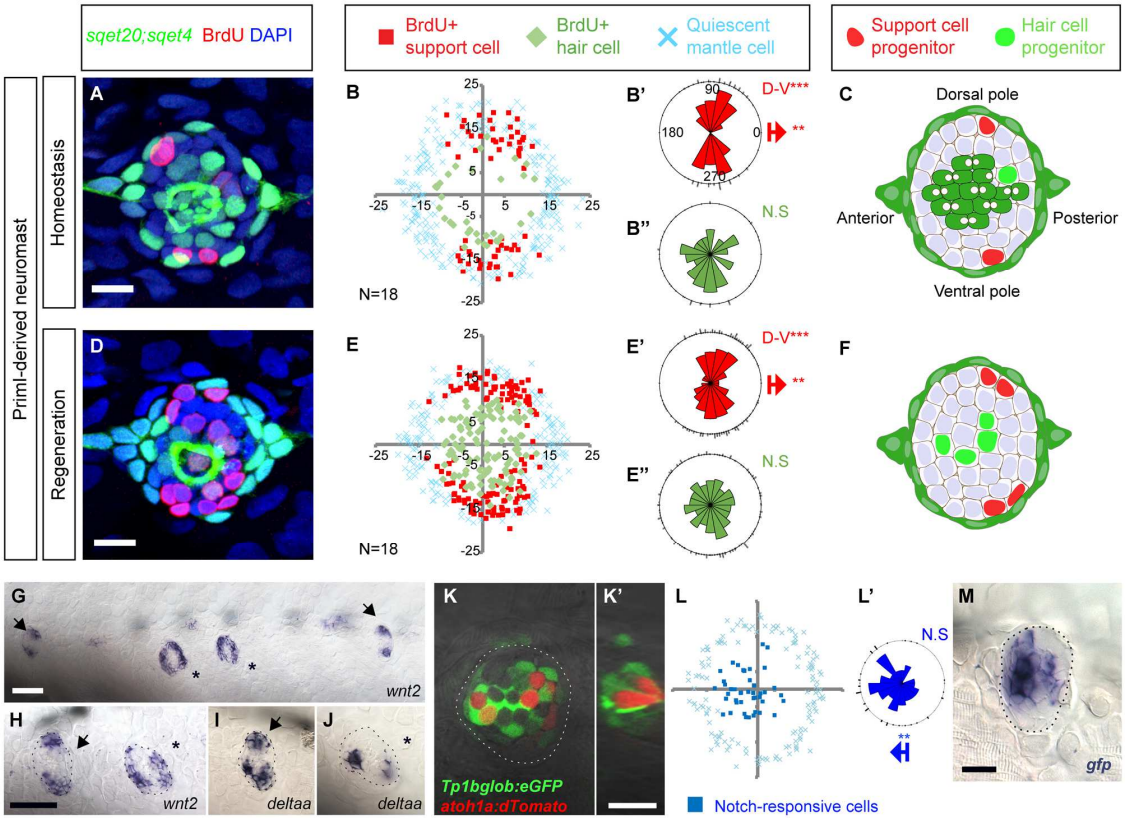
sqet20;sqet4 BrdU DAPI
BrdU+ support cell
BrdU+ hair cell
Quiescent mantle cell
Support cell progenitor
Hair cell progenitor
Primi-derived neuromast
Homeostasis
Regeneration
A
B
B'
B''
C
D
E
E'
E''
F
N=18
N=18
D-V***
**
N.S
Dorsal pole
Anterior
Posterior
Ventral pole
G
H
I
J
K
K'
L
L'
M
wnt2
wnt2
deltaa
deltaa
Tp1bglob:eGFP
atoh1a:dTomato
Notch-responsive cells
gfp

Figure 3.S2. Amplifying divisions occur in the A-P poles in close proximity to mantle cells in primII-derived neuromasts. Related to Figure 3.2.
(A) PrimI and primII-derived neuromasts show similar proliferation dynamics within 24hrs after hair cell death. Error bar = 95% CI.
(B) Schematic showing the two methods to analyze cell positions from the center of the neuromasts. We measured the distance in pixels of cells from the center (black arrows, C) and identified in which cell row away from mantle cells proliferating cells are located (red numbers, D-G).
(C) Differentiating cell divisions occur closer to the center of the neuromast in primI and primII derived neuromasts. The box plot shows the radii of BrdU+ hair cells (green) and support cells (red). Error bar = 1.5 * Interquartile range.
(D-G) Amplifying cell divisions occur next to mantle cells. The bars indicate the number of BrdU+ support cells (red) or BrdU+ hair cells (green) that are located in the different, concentric cell rows away from mantle cells (B) (n=18 neuromasts).
(H, K) BrdU incorporation in primII-derived neuromasts. Scale bars = 10 μm.
(I, L) Amplifying cell divisions are clustered in the A-P compartments of the neuromast; therefore, they have a polarity offset by 90° compared to primI-derived neuromasts. The BrdU plots show the positions of BrdU+ nuclei from 18 neuromasts superimposed on the same X,Y plane. Red squares indicate amplifying divisions, green diamonds indicate BrdU+ cells that differentiated into *sqet4+* hair cells.
(I', L') Rose diagrams for the angular position of BrdU+ cells (red), BrdU+ hair cells (green). Bipolar clustering (A-P) and directional bias were statistically analyzed using the Binomial test (***$p<0.001$).
(J, M) The number and location of progenitors that divide within 24hrs.

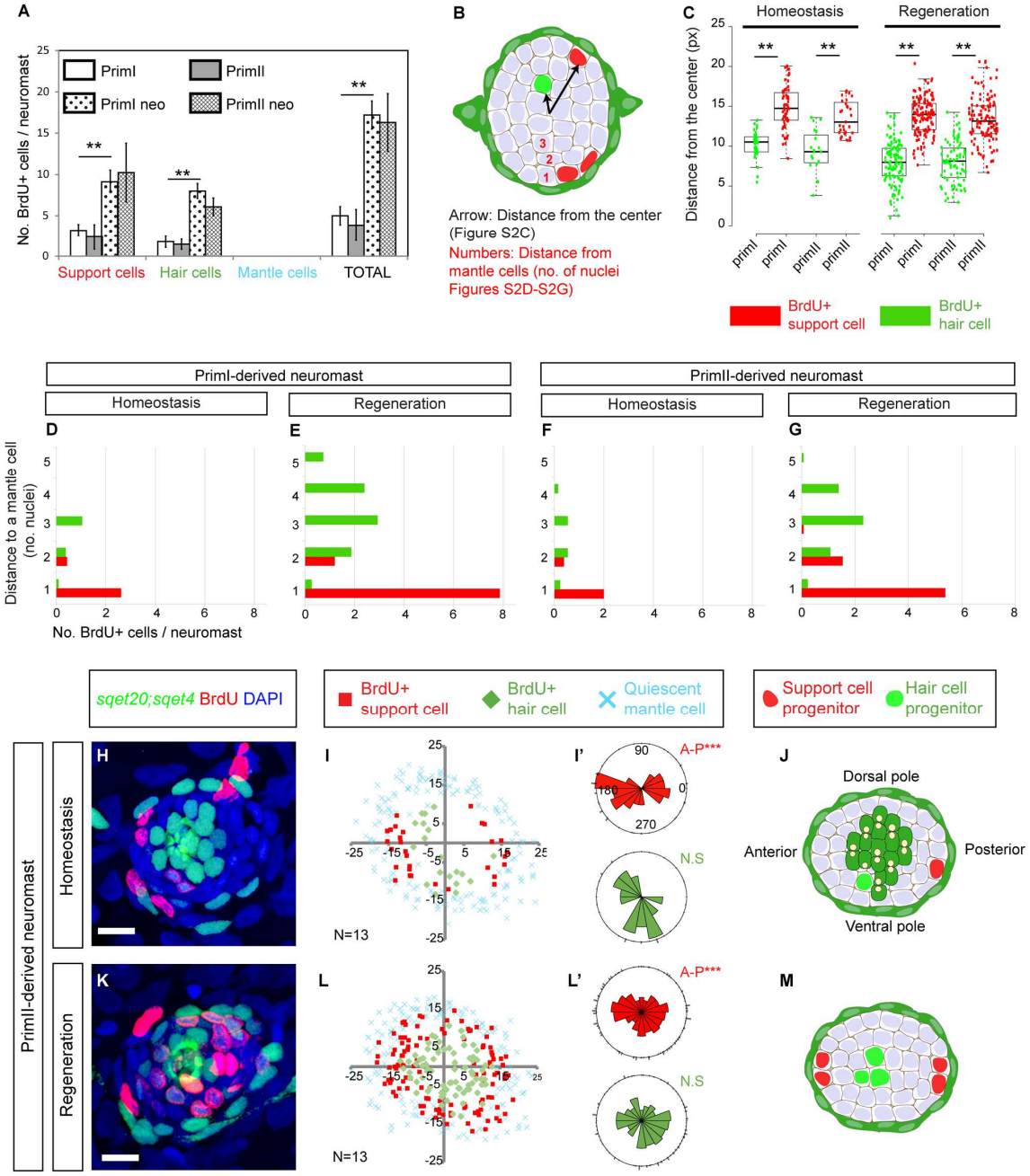
A
No. BrdU+ cells / neuromast
PrimI
PrimII
PrimI neo
PrimII neo
Support cells
Hair cells
Mantle cells
TOTAL
B
Arrow: Distance from the center (Figure S2C)
Numbers: Distance from mantle cells (no. of nuclei Figures S2D-S2G)
C
Homeostasis
Regeneration
Distance from the center (px)
BrdU+ support cell
BrdU+ hair cell
PrimI-derived neuromast
PrimII-derived neuromast
D
E
F
G
Distance to a mantle cell (no. nuclei)
No. BrdU+ cells / neuromast
sqet20;sqet4 BrdU DAPI
BrdU+ support cell
BrdU+ hair cell
Quiescent mantle cell
Support cell progenitor
Hair cell progenitor
H
I
I'
J
K
L
L'
M
N=13
A-P***
N.S
Dorsal pole
Anterior
Posterior
Ventral pole

Figure 3.3. Downregulation of Notch mimics gene expression changes during regeneration.
(A) Notch pathway genes have heterogeneous mRNA expression patterns in 5 dpf neuromasts. Dashed line outlines the neuromast.
(B-C) *dkk2* and *her4* are expressed in central support cells below hair cells as shown by confocal imaging of the in situ hybridization signal. B and B', C and C' are different focal planes. B'' and B''', C'' and C''' are orthogonal views. Hair cells are labeled with white arrows.
(D-I) Time course of mRNA expression of the Wnt reporter *Tg(6xTcf/LefBS-miniP:d2EGFP)* in row 1, the Wnt target genes *wnt10a* (row 2) and *wnt2* (row3), and the Notch reporter *Tg(Tp1bglob:EGFP*) (row4) at different time points after neomycin treatment shows that Notch is downregulated first, followed by the activation of Wnt signaling.
(Row 2) The Wnt target *wnt10a* is not active in control neuromasts but is activated between 3- 8hrs after hair cell death.
(Row 3) *wnt2* is present in the poles of homeostatic neuromasts but is upregulated 3h after hair cell death.
(Row 4) mRNA of the Notch reporter shows that Notch downregulation occurs between 1-3hrs after hair cell death.
(J-O) Notch inhibition using the γ-secretase inhibitor LY411575 mimics gene expression changes that occur during the first 16hrs of regeneration. Larvae were pre-treated with LY or DMSO for 6hrs before starting the timecourse (Figure 4A and 4F)
(J-K) Lower doses of LY (10μM) induce downregulation of the Notch target genes *her4* (K2) and the Notch reporter (shown by EGFP expression; K1), the cell cycle inhibitor *cdkn1bb* (K6), and the Wnt inhibitor *dkk2* (K7). Also, 10μM LY activates the expression of hair cell differentiation markers *deltad* (K4) and *atoh1a* (K5). The polar marker *deltaa* is also upregulated (K3).
(L) At 50μM LY, *dkk2* is absent (L7) and Wnt target genes *wnt2 and wnt10a* are activated (L8-L10).
(M-N) Although at different times, *deltaa* (M3), *deltad* (M4), and *atoh1a* (M5) are upregulated after neo-induced hair cell death. The Notch reporter (M1), *her4* (M2), *wnt2* (M9), *wnt10a* (M10) and *cdkn1bb* (M7, N7) show that Notch downregulation is transient during the first 16hrs after hair cell death.
(O) Notch downregulation during regeneration mimics changes in expression during regeneration. Larvae were pre-treated 6hrs in 50μM LY before neo.

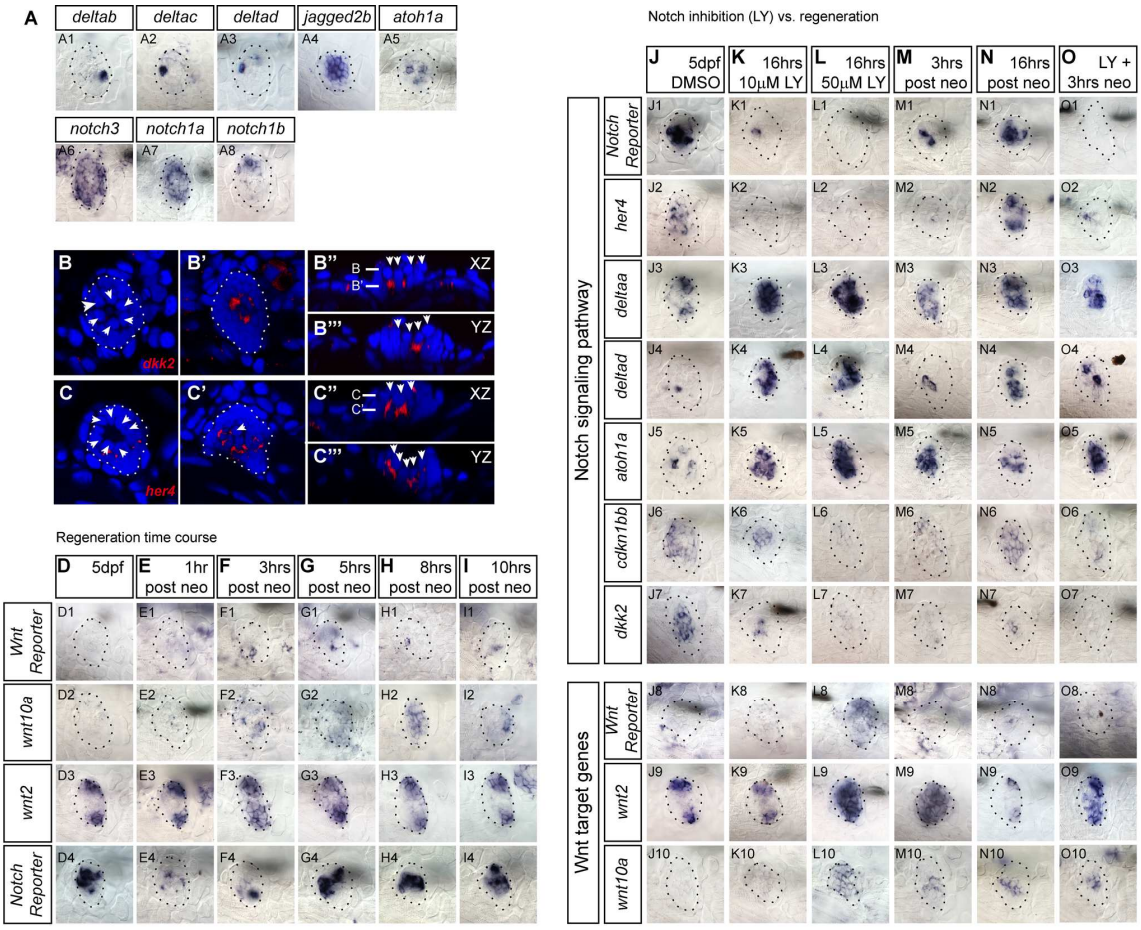
A
deltab
deltac
deltad
jagged2b
atoh1a
notch3
notch1a
notch1b
B
B'
B''
B'''
XZ
YZ
dkk2
C
C'
C''
C'''
her4
Regeneration time course
D 5dpf
E 1hr post neo
F 3hrs post neo
G 5hrs post neo
H 8hrs post neo
I 10hrs post neo
Wnt Reporter
wnt10a
wnt2
Notch Reporter
Notch inhibition (LY) vs. regeneration
J 5dpf DMSO
K 16hrs 10μM LY
L 16hrs 50μM LY
M 3hrs post neo
N 16hrs post neo
O LY + 3hrs neo
Notch signaling pathway
Notch Reporter
her4
deltaa
deltad
atoh1a
cdkn1bb
dkk2
Wnt target genes
Wnt Reporter
wnt2
wnt10a

Figure 3.4. Notch inhibits proliferation and differentiation in a dose-dependent manner.
(A, F) *sqet4;sqet20* larvae were treated for 30hrs with the γ-secretase inhibitor LY411575 (LY). After 6hrs in drug, BrdU was added for 24hrs. DMSO treated controls shown in Figures 2B and 2E.
(B-E) Notch inhibition disrupts the proliferative compartments. After 10μM LY, amplifying cell divisions are no longer clustered in the dorso-ventral poles.
(G-J) During regeneration, Notch inhibition enhances differentiating divisions in the central region of the NM and in the normally quiescent anterior and posterior compartments.
(K) Notch inhibition does not affect proliferation rates (BrdU index) during homeostasis.
(L) During regeneration 10μM LY does not affect total proliferation rates but induces differentiation at the expense of amplifying cell divisions. 50μM LY induces hyper-proliferation and an increase in differentiation.
Error bars show the 95% confidence interval (CI).

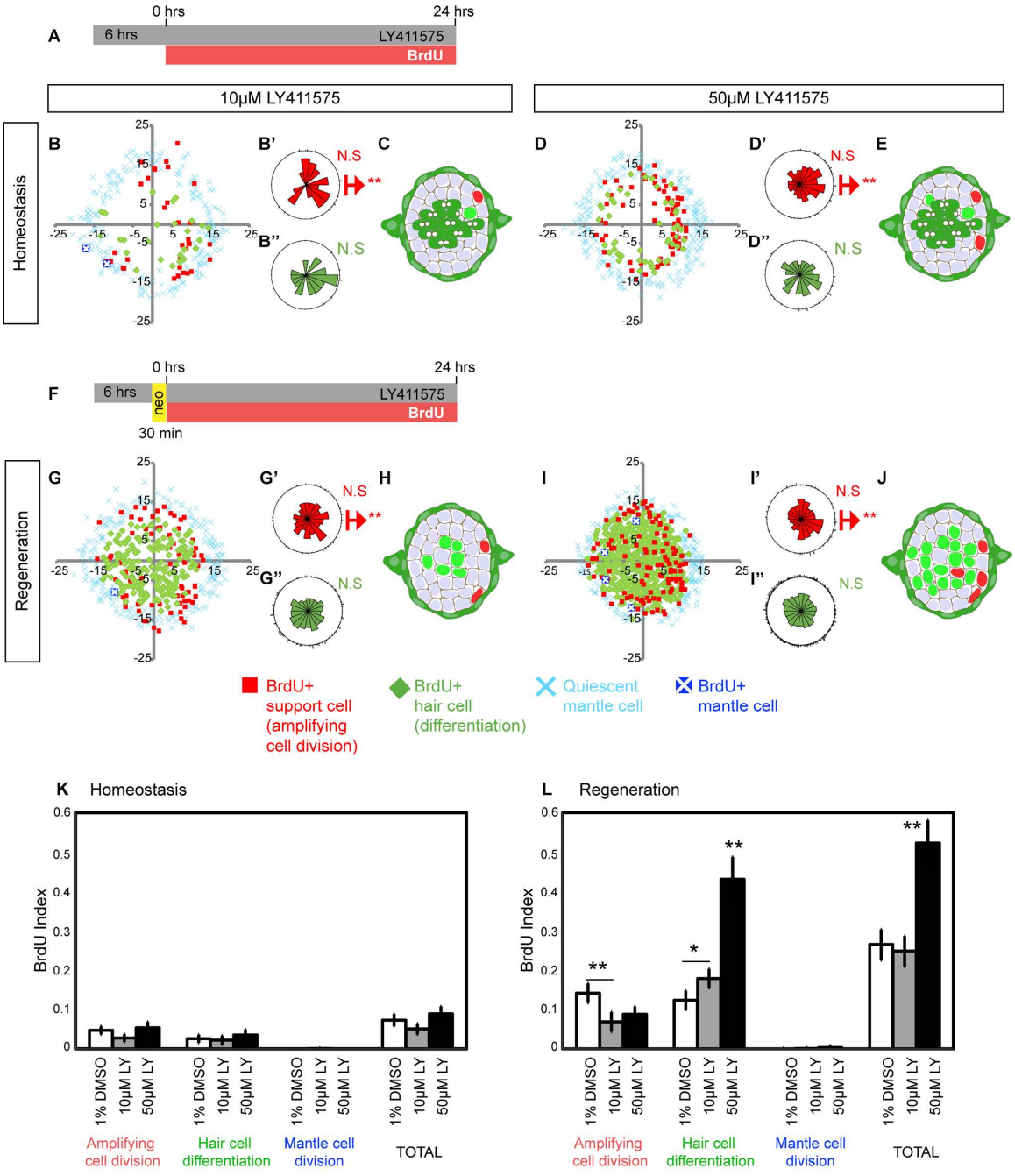
A
0 hrs
24 hrs
6 hrs
LY411575
BrdU
10μM LY411575
50μM LY411575
Homeostasis
B
B'
B''
C
D
D'
D''
E
N.S
**
F
neo
30 min
Regeneration
G
G'
G''
H
I
I'
I''
J
BrdU+ support cell (amplifying cell division)
BrdU+ hair cell (differentiation)
Quiescent mantle cell
BrdU+ mantle cell
K Homeostasis
L Regeneration
BrdU Index
1% DMSO
10μM LY
50μM LY
Amplifying cell division
Hair cell differentiation
Mantle cell division
TOTAL
*

Figure 3.5. Notch signaling inhibits proliferation via Wnt inhibition and via a Wnt-independent mechanism during homeostasis and regeneration.
(A) Heat-shock protocol to experimentally induce *hs:nicd* or *hs:dkk2* expression in regenerating NMs. Larva required 1hr-heat-shock pulses at least 12hrs before hair cell ablation in order to activate expression of the tagged reporter (c-Myc-tag or RFP respectively, not shown).
(B-E) BrdU plots for primI-derived regenerating NMs in sibling, Wnt activated (using the GSK3β inhibitor 1-Azakenpaullone, AZK) and Notch activated *Tg(hsp70l:Gal4); Tg(UAS:myc-Notch1a-intra)* transgenic larvae, referred to as (*hs:nicd*). All larvae carry the *sqet4* transgene.
(B) In DMSO-treated, heat-shocked (*hs*) siblings amplifying cell divisions occur in the D-V poles and differentiating divisions in the center.
(C) AZK (3μM) increases support cell proliferation in the D-V poles.
(D) Notch activation in *hs:nicd* larvae disrupts the proliferative compartments and reduces total proliferation.
(E) Activation of Wnt in *hs:nicd* larvae using AZK restores the clustering of support cell amplification and proliferation rates.
(F-I) BrdU plots for primI-derived regenerating NMs in sibling or Wnt-inhibited *Tg(hsp70l:Gal4); Tg(UAS:dkk2-RFP);sqet4*, referred to as (*hs:dkk2*) transgenic larvae.
(G) Wnt inhibition in *hs:dkk2* larva depletes amplifying cell divisions and reduces differentiating divisions in the center.
(H) Notch inhibition disrupts polar compartments but maintains amplifying divisions and increases differentiating divisions in the center.
(I) Combined Notch and Wnt inhibition (*hs:dkk2* + LY) depletes amplifying divisions in the poles but leaves differentiating divisions unaffected.
(J-K) BrdU indexes of amplifying, differentiating and total divisions after individual and combinatorial manipulations of the Wnt and Notch pathways. Error bar = 95% CI.
See also Figures 3.S5.

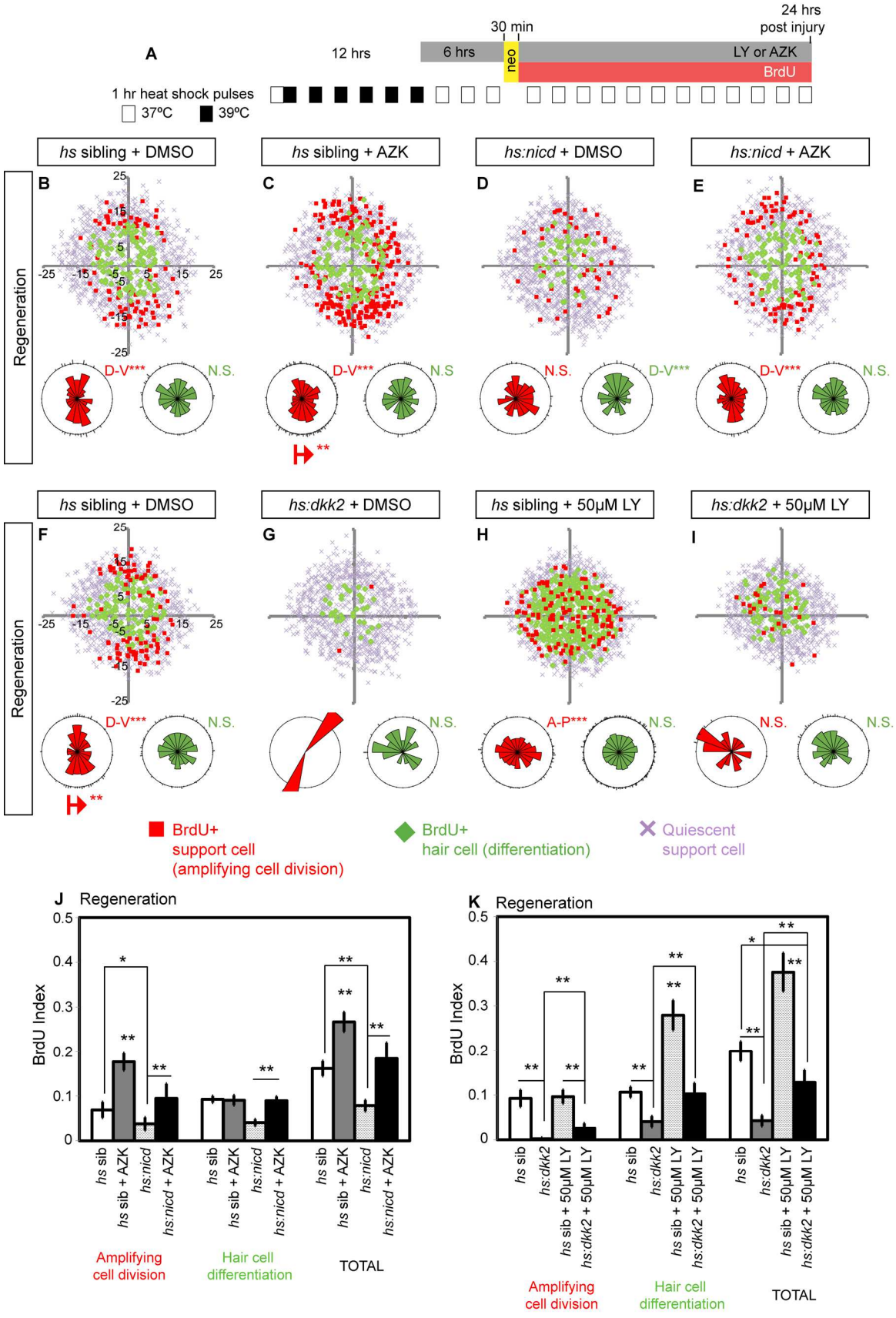
A
12 hrs
6 hrs
30 min
neo
24 hrs
post injury
LY or AZK
BrdU
1 hr heat shock pulses
37ºC
39ºC
hs sibling + DMSO
hs sibling + AZK
hs:nicd + DMSO
hs:nicd + AZK
Regeneration
B
C
D
E
D-V***
N.S.
**
hs sibling + DMSO
hs:dkk2 + DMSO
hs sibling + 50μM LY
hs:dkk2 + 50μM LY
F
G
H
I
A-P***
BrdU+
support cell
(amplifying cell division)
BrdU+
hair cell (differentiation)
Quiescent
support cell
J Regeneration
K Regeneration
BrdU Index
hs sib
hs sib + AZK
hs:nicd
hs:nicd + AZK
hs:dkk2
hs sib + 50μM LY
hs:dkk2 + 50μM LY
Amplifying
cell division
Hair cell
differentiation
TOTAL

Figure 3.S5. Notch signaling inhibits proliferation via Wnt inhibition and via a (A) Heat shock protocol to experimentally induce *hs:nicd* or *hs:dkk2* expression in neuromasts during homeostasis.
(B-E) BrdU plots for siblings and primI-derived *Tg(hsp70l:Gal4); Tg(UAS:myc-Notch1a-intra),* (*hs:nicd*) transgenic larvae and siblings carrying the *sqet4* hair cell marker.
(F-I) BrdU plots for siblings and primI-derived *Tg(hsp70l:Gal4); Tg(UAS:dkk2-RFP),* (*hs:dkk2*) transgenic larvae.
(J,K) Proliferation dynamics of different lineages in homeostatic (I) and regenerating neuromasts (J). Error bar = 95% CI.
Wnt-independent mechanism in homeostatic neuromasts. Related to Figure 3.5.

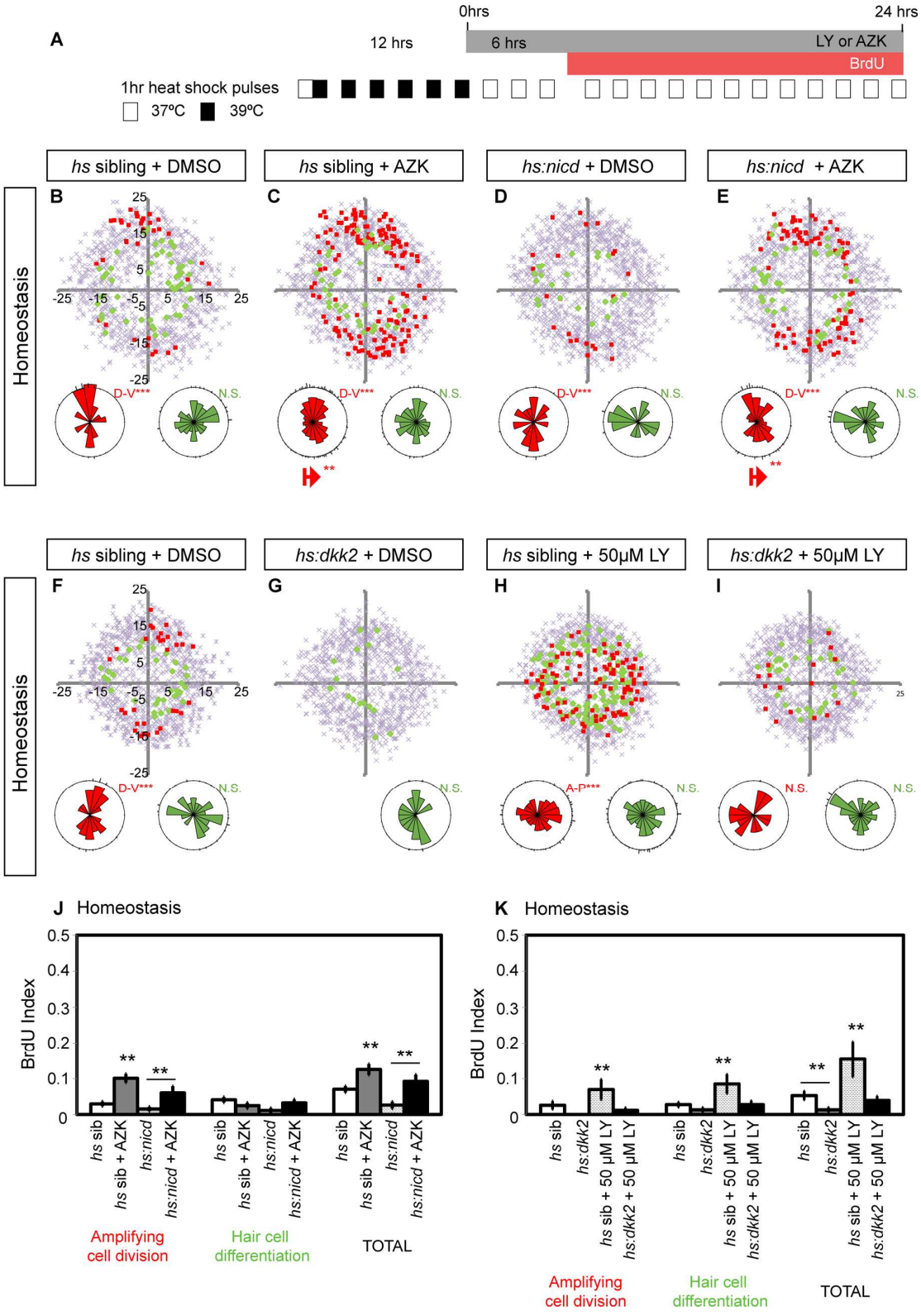
A
0hrs
24 hrs
12 hrs
6 hrs
LY or AZK
BrdU
1hr heat shock pulses
37ºC
39ºC
hs sibling + DMSO
hs sibling + AZK
hs:nicd + DMSO
hs:nicd + AZK
Homeostasis
B
C
D
E
D-V***
N.S.
**
hs sibling + DMSO
hs:dkk2 + DMSO
hs sibling + 50μM LY
hs:dkk2 + 50μM LY
F
G
H
I
A-P***
J Homeostasis
K Homeostasis
BrdU Index
hs sib
hs sib + AZK
hs:nicd
hs:nicd + AZK
hs:dkk2
hs sib + 50 μM LY
hs:dkk2 + 50 μM LY
Amplifying cell division
Hair cell differentiation
TOTAL

Figure 3.6. Wnt controls proliferation in the poles but does not affect hair cell differentiation.
Heat-shock and drug treatment protocol to induce *hs:nicd* and *hs:dkk2* during homeostasis.
(A) Notch pathway genes are active during homeostasis, whereas Wnt targets are absent, with the exception of *wnt2* (A8).
(B) Notch inhibition causes activation of the Wnt reporter *Tg(6xTcf/LefBS-miniP:d2EGFP)* (B7) and Wnt targets *wnt2* (B8) and *wnt10a* (B9).
(C) AZK-induced Wnt activation has no effect on hair cell differentiation markers, such as *atoh1a* (C4), Notch pathway genes (C1-2), or *dkk2* (C6).
(D) LY and AZK combined phenocopy the effects of LY alone.
(E) *hs:dkk2* does not affect the expression of Notch pathway genes
(F) LY-induced upregulation of Wnt target genes is reversed by *hs:dkk2* induction.
(G) Increased Notch signaling in *hs:nicd* larvae enhances Notch reporter expression. Only 20% of neuromast cells express *nicd* (data not shown).
(H) *hs:nicd* inhibits the AZK-induced activation of *wnt10a* (H9) and the Wnt reporter (H7).
(I-Q) BrdU plots for primI-derived homeostatic and regenerating *sqet4+* NMs. Larvae were treated with DMSO, AZK, 50µM LY or AZK+LY according to Figures 3A and 3F.
(I, N) In homeostatic and regenerating NMs amplifying cell divisions are clustered in the poles. During regeneration, centrally located support cells divide and differentiate.
(J, O) AZK enhances support cell amplification in the polar compartments without affecting hair cell differentiation.
(K, P) LY enhances hair cell differentiation and disrupts the polar compartments.
(L, Q) Combined Wnt activation and Notch inhibition disrupts the polar compartments and randomizes amplification and differentiation.
(M, R) BrdU indexes of amplifying, differentiating and total divisions after single and combinatorial manipulations of the Wnt and Notch pathways. Error bar = 95% CI.
See also Figure 3.S6.

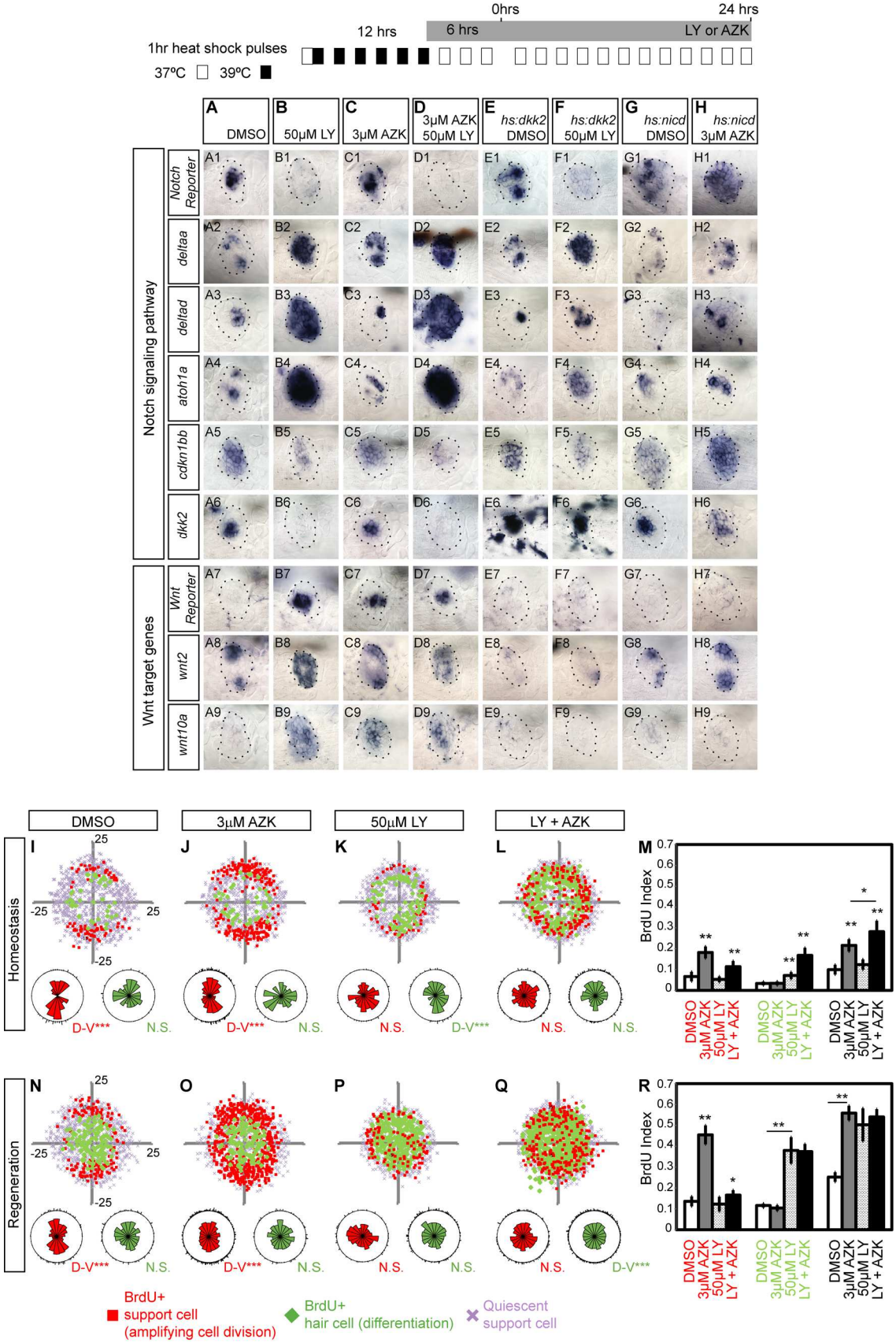
0hrs
24 hrs
12 hrs
6 hrs
LY or AZK
1hr heat shock pulses
37ºC
39ºC
A DMSO
B 50μM LY
C 3μM AZK
D 3μM AZK 50μM LY
E hs:dkk2 DMSO
F hs:dkk2 50μM LY
G hs:nicd DMSO
H hs:nicd 3μM AZK
Notch signaling pathway
Notch Reporter
deltaa
deltad
atoh1a
cdkn1bb
dkk2
Wnt target genes
Wnt Reporter
wnt2
wnt10a
DMSO
3μM AZK
50μM LY
LY + AZK
Homeostasis
Regeneration
D-V***
N.S.
BrdU Index
BrdU+ support cell (amplifying cell division)
BrdU+ hair cell (differentiation)
Quiescent support cell

Figure 3.S6. 72hrs treatments with AZK modestly increase the number of hair cells. Related to Figure 3.6.
(A) Pulse-chase experiment of AZK-treated proliferating cells that were labeled for 24 hrs and raised until 72hrs to determine if Wnt signaling induces hair cell differentiation. (B) AZK induces an increase in total hair and support cell numbers at 72hrs post injury. The neuromast cell numbers at 24hrs post hair cell death has increased mostly due to the formation of new support cells during the unlabeled period.
(C) BrdU indexes for hair cell differentiation divisions remain the same in larvae fixed at 24hrs or 72hrs after hair cell death indicating that the slight increase in hair cell numbers (in B) is proportional to the increase of support cell numbers and not because Wnt affects differentiation. Error bar = 95% CI.

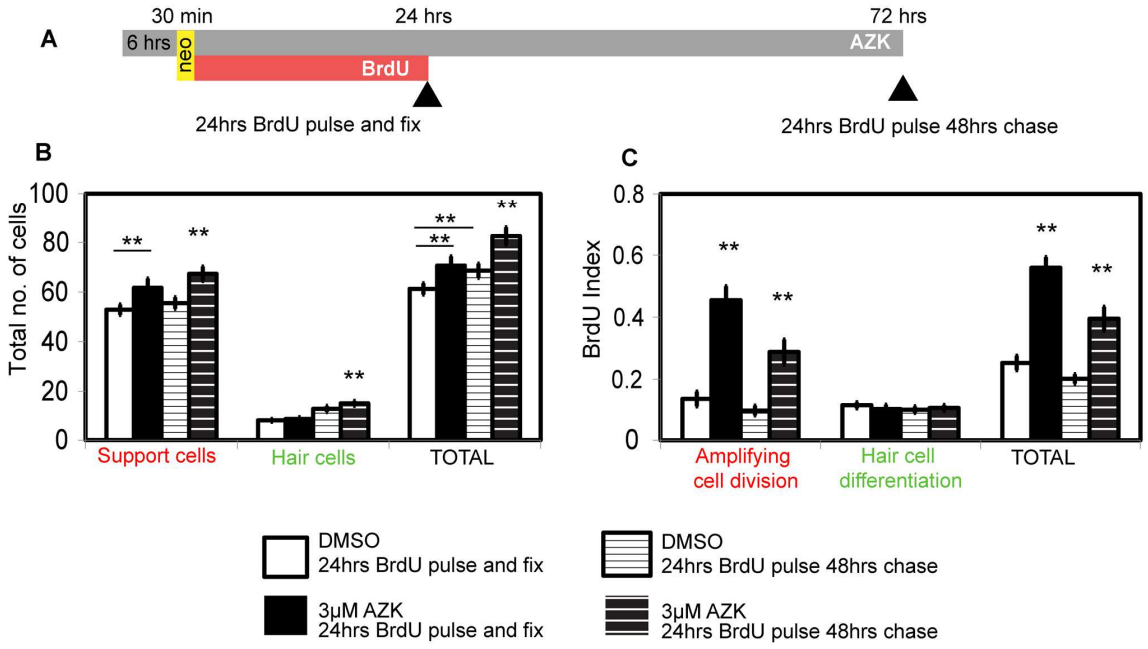
A
30 min
24 hrs
72 hrs
6 hrs
neo
BrdU
AZK
24hrs BrdU pulse and fix
24hrs BrdU pulse 48hrs chase
B
Total no. of cells
100
80
60
40
20
0
Support cells
Hair cells
TOTAL
C
BrdU Index
0.8
0.6
0.4
0.2
0
Amplifying cell division
Hair cell differentiation
TOTAL
DMSO 24hrs BrdU pulse and fix
3μM AZK 24hrs BrdU pulse and fix
DMSO 24hrs BrdU pulse 48hrs chase
3μM AZK 24hrs BrdU pulse 48hrs chase

Figure 3.7. Mantle cells are quiescent stem cells.
(A) Protocol that transforms most support cells into hair cells, followed by neo treatment to test the mantle cell response.
(B-G) BrdU incorporation in primI-derived *sqet20* NMs at different time points. Scale bar = 10μm.
(H) *sqet20*+ mantle cells are reduced 10hrs after the second neo treatment but recover by 24hrs.
(I) Mantle cell BrdU index (No. of BrdU+, *sqet20*+ cells / total No. of *sqet20*+ cells). The proliferation of mantle cells significantly increases between 10-36hrs after the second neo treatment.
(J) In *Tg(cldnb:mKO2-zCdt1) cldnb* drives the Cdt1-tagged *mKO2* fluorescent protein in NMs. The Cdt1 ubiquitination domain forces degradation of mKO2 once DNA replication begins.
(K) The quiescent state of mantle cells was analyzed 24hrs after the second neo treatment.
(L-L') mKO2-zCdt1 expression is strong in mantle cells (O).
(M,M') Treating embryos twice with neo does not affect the quiescent state of mantle cells.
(N-O) Depletion of support cells by LY in *sqet20;sqet4* larvae causes some mantle cells to lose mKO2-zCdt1 expression suggesting that they re-entered the cell cycle. Error bar = 95% CI.
See also Figure 3.S7.

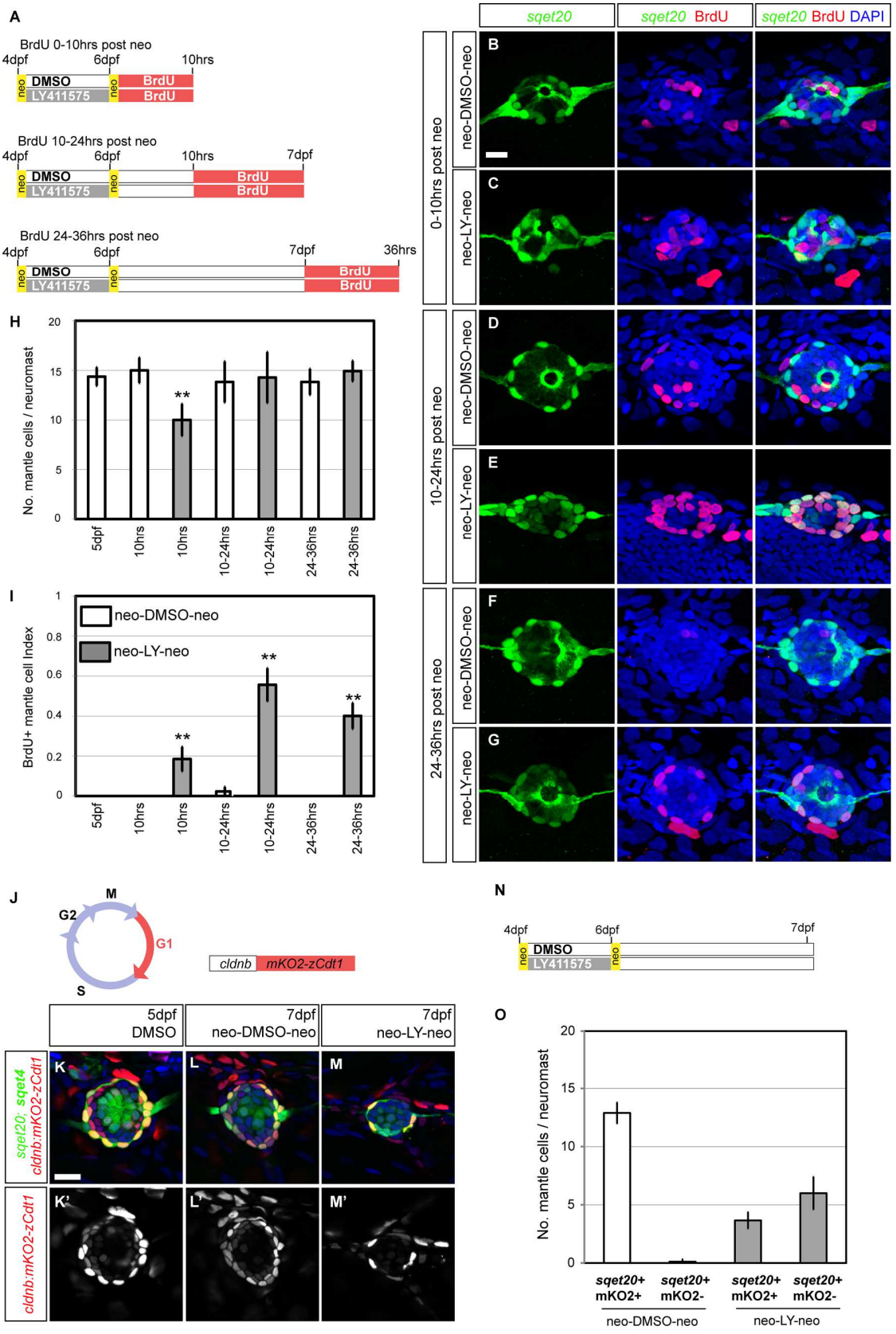
A
BrdU 0-10hrs post neo
4dpf
6dpf
10hrs
DMSO
LY411575
neo
BrdU
BrdU 10-24hrs post neo
7dpf
BrdU 24-36hrs post neo
36hrs
sqet20
sqet20 BrdU
sqet20 BrdU DAPI
0-10hrs post neo
10-24hrs post neo
24-36hrs post neo
neo-DMSO-neo
neo-LY-neo
B
C
D
E
F
G
H
No. mantle cells / neuromast
5dpf
10hrs
10-24hrs
24-36hrs
**
I
BrdU+ mantle cell Index
J
M
G2
G1
S
cldnb
mKO2-zCdt1
5dpf DMSO
7dpf neo-DMSO-neo
7dpf neo-LY-neo
sqet20: sqet4
cldnb:mKO2-zCdt1
K
L
M
K'
L'
M'
N
O
sqet20+ mKO2+
sqet20+ mKO2-

Figure 3.S7. Related to Figure 3.7
(A) Neuromasts are damaged after a second round of neomycin and LY treatment and recover between 10-24hrs after neo. (B-D) BrdU incorporation in *sqet4* larvae demonstrates that 24hrs of LY treatment during regeneration causes the overproduction of hair cells and loss of support cells. Error bar = 95% CI. Scale bars = 10 μm.

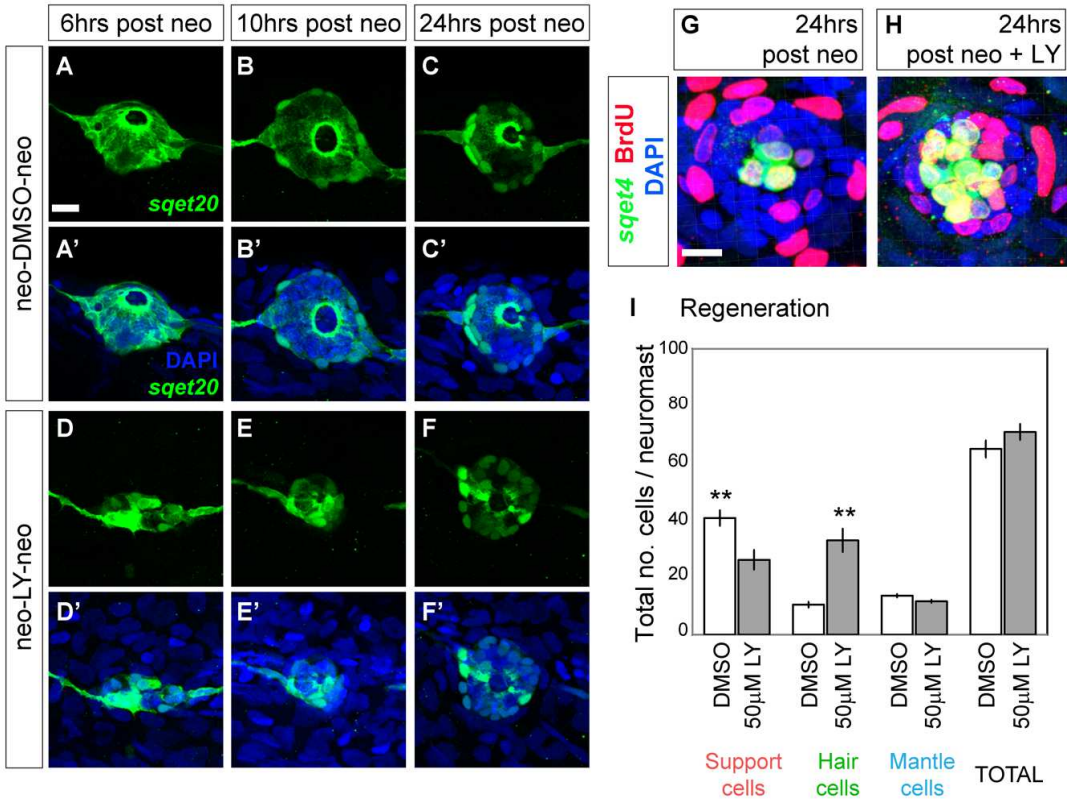
6hrs post neo
10hrs post neo
24hrs post neo
neo-DMSO-neo
neo-LY-neo
A
B
C
A'
B'
C'
D
E
F
D'
E'
F'
sqet20
DAPI
sqet20
G 24hrs post neo
H 24hrs post neo + LY
sqet4 BrdU DAPI
I Regeneration
Total no. cells / neuromast
100
80
60
40
20
0
**
**
DMSO
50μM LY
Support cells
Hair cells
Mantle cells
TOTAL

Figure 3.8. Model of the molecular control of cell behaviors during regeneration. Notch signaling controls tissue homeostasis in the NM by restricting proliferation and differentiation through Wnt-dependent and -independent mechanisms. During regeneration Notch is transiently downregulated activating Wnt and proliferation in the center and D-V poles.
(A) Support cell amplification (red nuclei) occurs in the D-V compartments (red cytoplasm) next to peripheral, green mantle cells. Amplifying cells express *wnt2* and *deltaa*. Hair cell differentiation occurs in the central, Notch+ domain (yellow). Notch signaling is likely oscillating to allow hair cell differentiation.
(B) Wnt/Notch signaling interactions. In the center (outlined in yellow), Notch inhibits differentiation by inhibiting *atoh1a* and *delta* ligands. Notch inhibits proliferation possibly via *cdkn1bb* and also by inhibiting Wnt signaling through the activation of *dkk2*. Wnt signaling activates proliferation of hair cell progenitors in the center and non-cell autonomously of support cell progenitors in the poles. The mechanisms by which Wnt initiates proliferation in the poles and the roles of *wnt10a* and *wnt2* have yet to be discovered. Red lines show inhibition, blue arrows indicate activation and dashed arrows show indirect, non-cell-autonomous activation of proliferation.

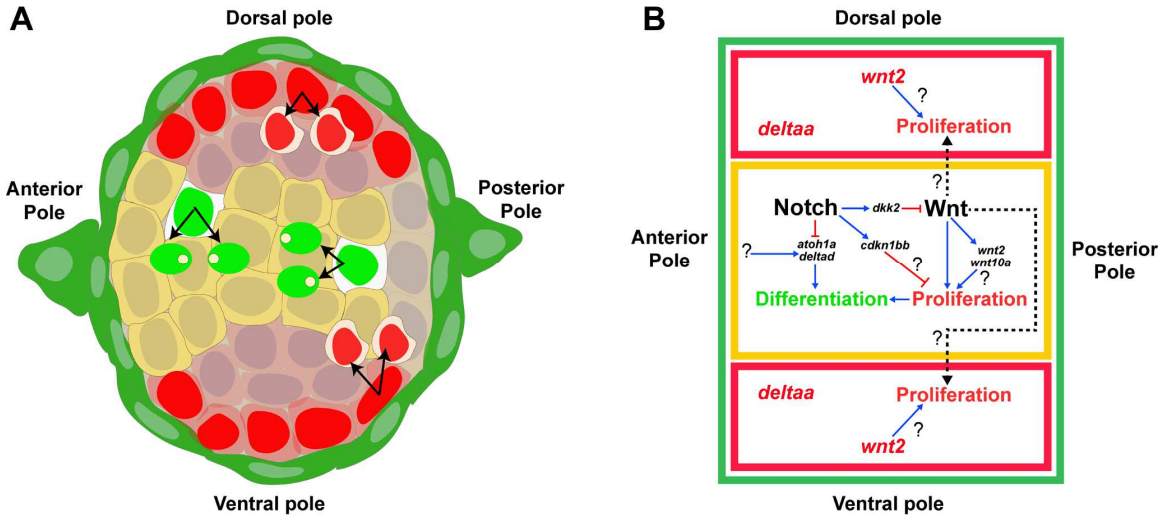
A
Dorsal pole
Anterior Pole
Posterior Pole
Ventral pole
B
Dorsal pole
wnt2
?
deltaa
Proliferation
?
Notch
dkk2
Wnt
atoh1a
deltad
cdkn1bb
wnt2
wnt10a
?
?
?
?
Differentiation
Proliferation
?
deltaa
Proliferation
wnt2
?
Anterior Pole
Posterior Pole
Ventral pole

Movie legends

Movie S1. 72hrs time lapse of a homeostatic neuromast of a cuadruple transgenic larvae *Tg(sqet20;sqet4;cldnb:lynGFP;cldnb:H2A-mCherry)* starting at 5dpf. The movie is composed of single, shifting focal planes to track dividing support cells and their daughter cells. Time is in hours and minutes. 20 frames/minute.
(A) Shows a differentiating cell division at 19hrs 29min (Figures 1I, 1J, CD3).
(B) Shows two amplifying cell divisions at 3hrs 58min (Figure 1I, 1J, CD1, CD2). Support cell progeny maintain their relative position to mantle cells and an undifferentiated state during the time-lapse experiment.

Movie S2. Time-lapse of the first 26hrs of a 70hr regenerating neuromast starting at 5dpf. (A) 4D movie of only the mCherry+ nuclei and (B) the same movie showing all channels of a single focal plane shifting over time to illustrate all mitotic events and their daughter cells. Time is in hours and minutes.
The movie in B shows the first seven cell divisions of the regenerating neuromast shown in Figures 1K and 1L. Metaphases are highlighted to illustrate the tracing and lineage analysis shown in Figure 1K and 1L. 10 frames/minute.
(C) Full tracking of cell division CD1in a single focal plane (Figures 1L and S1I). This support cell divides in the dorsal pole, attached to a mantle cell at 3hrs 14min. The most posterior daughter cell subsequently divides at 20hrs 46min. to form a pair of hair cells. 10 frames/minute.

Movie S3. Support cells do not move much during the course of regeneration**.** 4D movie generated for the cell movement analysis shown in Figures 1O and 1P of every cell that divided during the first 24hrs after hair cell death. Time in hours and minutes. 10 frames/minute.
To be able to measure cell movements we stabilized the neuromast center point to eliminate larval movement and drift. (A) shows dividing support cells color-coded depending on the cell fate of their daughter cells. Red dots denote amplifying cell divisions, green dots show differentiating cell divisions, and blue dots show a single mantle cell division. (B) shows the same movie with cells color-coded according to which lineage/cell division they belong to (Figure 1O).

CHAPTER 4

DISCUSSION AND FUTURE DIRECTIONS

The number of hair cells and support cells is actively maintained during zebrafish lifespan, through constant self-reneawal and regeneration (Cruz et al., 2015). In the present study, we describe a mechanism that controls tissue homeostasis in the zebrafish lateral line neuromasts through two spatially distinct progenitor populations and localized interactions between the Notch and Wnt signaling pathways. In the neuromast, the most central group of cells is responsive to Notch signaling, and from this support cell pool, hair cells seem to differentiate upon Notch signaling downregulation. There are also two clusters of support cell progenitors located in the dorso-ventral poles of the neuromast, attached to mantle cells, which respond to Wnt-dependent signals from the central compartment to generate more inner support cells. In central cells, Notch inhibits differentiation by inhibiting hair cell progenitor markers like *atoh1a* and *deltad* and inhibits proliferation by inhibiting Wnt signaling through *dkk2* (Figure 3.8). This proposed mechanism depends on two important components: a pool of competent progenitor cells and a set of signaling molecules.

Different pools of support cells maintain tissue homeostasis in the zebrafish lateral line neuromasts

Mantle cells as an independent cell population

Previous studies have only hypothesized the role of mantle cells as hair cell progenitors. These studies have shown conflicting observations of the amount and role of proliferation within different areas of the neuromast, suggesting that the outermost cell population proliferates at a different rate after hair cell death and even claim these progenitors migrate towards the center of the neuromast to differentiate (Ghysen and Dambly-Chaudière, 2007; Ma et al., 2008; Steiner et al., 2014; Williams and Holder, 2000). The conflict of these results comes from the lack of a consensus of the actual definition of a mantle cell and the neuromast boundaries. To define the role of mantle cells in tissue homeostasis, we used live imaging and spatial analysis of proliferating cells to manually track every support and mantle cell during homeostasis and regeneration. This provides a potent and unbiased approach to distinguish lineages and cell behaviors within a progenitor pool (Brown and Greco, 2014). For our analysis, we defined mantle cells as the outermost circle of cells that expresses cytoplasmic GFP from the *sqet20* transgene with higher intensity (Parinov et al., 2004). According to our results, this population is distinct to the support cells because of its inherent quiescence (Figure 3.1M, 3.S1A, 3.S2A, 3.S4K, 3.S4L, and 3.7I). Other reports have also shown *sqet20*+ cell quiescence, even when the neuromast is severely damaged, using copper sulfate (Hernández et al., 2007). By inhibiting Notch signaling during regeneration, we show that the

reduction of support cells due to excess differentiation does not trigger mantle cell proliferation (Figure 3.4L). Still, mantle cells are not post-mitotic differentiated cells, and the loss of mantle cells, support cells, and hair cells (neo-LY-neo; Figures 3.7 and 3.S7) induces mantle cell proliferation that effectively recover the normal amount of mantle cells within 24 hrs. While mantle cell proliferation still occurs after 24 hrs, it is still unknown whether these proliferation events will contribute to hair cell formation or support cell replenishment. As a different possibility, mantle cells might be actively maintained latent neuromast precursor that will only proliferate and differentiate to replace neuromasts lost after fin ablation, as shown in zebrafish or the axolotl (Dufourcq et al., 2006; Jones and Corwin, 1993), or to generate more neuromasts in the adult fish through the process of budding (Wada et al., 2010). In fact, *sqet20* is also a marker for intereneuromast cells, which are latent neuromast precursors (Lush and Piotrowski, 2014). Another possibility is the constant flow from mantle cells to support cells without the necessity of proliferation. This occurs during neuromast development where the outermost cells of the recently deposited neuromasts acquire *sqet20* expression and seem to be specified this early to become mantle cells (Figure 2.6H). In addition, although most mantle cells and interneuromast cells do not express *sox2,* some mantle cells do (Hernández et al., 2007), which might represent an intermediate step, but does not show the direction of differentiation, either towards a mantle cell or to a support cell fate. To test these possibilities, we are currently working in tools to conditionally label the mantle cells and track them for longer periods of time.

The support cells are multipotent progenitors that self-renew and differentiate into hair cells

To compare, support cell amplification and differentiation occur at the same rate and are always balanced in homeostasis and regeneration (Figures 3.1M, 3.S2A, 3.4K and 3.4I). Therefore, the amount of support cell proliferation is sufficient to sustain the loss of progenitors due to differentiation, without contribution from the mantle cells. The radial analysis combined with statistical analysis of the angular position demonstrated that the support cells progenitors proliferate in the periphery of the neuromast, attached to the mantle cells, and clustered in the dorso-ventral poles (Figure 3.2 and 3.S2). The support cells that act as hair cells progenitors show no spatial clustering and undergo differentiation anywhere in the neuromast, but close to its geometrical center and close to hair cells (in homeostasis). The nature of these compartments is highly conserved since hair cell death only increases proliferation within the polar compartments. After hair cell death, we also see proliferation in the normally quiescent posterior compartment; therefore, the anterior support cells are the most quiescent. These results have recently been confirmed in the adult zebrafish neuromast by using label retention assays from a photoconvertible nuclear label (Cruz et al., 2015). Through a drastically different approach, this group has been able to detect higher label retention in the anterior compartment, less retention in the posterior compartment, and no retention in the central and dorso-ventral compartments. In this manuscript we present a description of the cell fate that distinguish each compartment and present a mechanism of support

cell and hair cell maintenance.

Heterogeneities within the neuromasts mantle and support cells guide cell fate decision

In our study, we have statistically demonstrated the lack of active migration of cells within the neuromast and the existence of multiple populations of support cells depending on their proliferative behavior. According to this, there must be multiple signaling heterogeneities that guide cell behavior from quiescence to proliferation and from self-renewal to differentiation. Our results are amazingly similar to the ones obtained using newly developed intravital imaging of the hair follicle niche and the intestinal crypt in mice. In the intestinal crypt, the spatial organization defines the fate of the intestinal stem cells, and the cells located in the center of the circular crypt are prone to transit amplify themselves and populate the crypt through passive cell rearrangement and space competition. Quiescent stem cells, on the outermost cell row (+4), can either contribute to the transit amplifying pool or undergo differentiation (Ritsma et al., 2014). In the case of the hair follicle, heterogeneities in the niche are so powerful that when the complete pool of stem cells is ablated, epithelial cells that repopulate the injured follicle can acquire hair follicle “stemness” depending on their position (Rompolas et al., 2013). These observations are compelling evidence that stem cells compete for a spatial position relative to signals that allows self-renewal. We think that the neuromast support cells although equivalent in their potency to differentiate or self-renew, are competing for a

position that defines its fate. Accordingly, our spatial analysis predicts the existence of signals that maintain quiescence in the mantle cells, signals that maintain quiescence in the anterior-posterior compartments of support cells, signals that restrict proliferation and inhibit differentiation in the poles, and signals that restrict proliferation but promote differentiation, close to the center of the neuromast. The source of these signals and the cellular environment where the signals are active would be considered as a stem cell niche.

A compartment for hair cell differentiation?

The lack of clustering of hair cell progenitors and the fact that differentiation occurs close to the center of the neuromast suggest the existence of a centralizing signal that induces differentiation in the neighboring support cells. This result contrasts with a previous report that claimed the expression of *notch3* provides Notch-free compartments (dorso-ventral) were hair cell differentiation occurs (Wibowo et al., 2010). The authors proposed this mechanism only based in the observation that, during hair cell development, new hair cells are stereotypically added to the dorsal or ventral side of previously formed hair cells (Lopez-Schier & Hudspeth, 2006). By analyzing the total displacement of dividing cells during regeneration, we discarded this possibility since cells that amplify or differentiate do not move more than a single cell diameter within the first 24 hrs after hair cell death, and the origin of hair cell progenitors is close to the center of the neuromast but not statistically clustered. This might be a crucial difference between hair cell development and the process

of regeneration.

Notch signaling

The centralizing signal is most likely to be associated or interacting with Notch signaling. In spite of the number of ligands and Notch receptors expressed in the lateral line, and their diverse expression patterns, Notch reporter activity is consistently expressed in the central region of the neuromast, with more Notch active cells in the anterior pole (Figure 3.2K-3.2L). Through Notch gain and loss of function, we have demonstrated that Notch inhibits support cell differentiation in the mature neuromast, and that transient downregulation of Notch signaling is required for hair cell regeneration. This confirms our previous gene expression analysis that registered such changes in Notch signaling (Jiang et al., 2014). This mechanism is not only exclusive to the neuromast since in adult neurogenesis, Notch downregulation is necessary for progenitor re-entrance to the cell cycle and further differentiation (Alunni et al., 2013). Importantly, Notch is a repressive signal that inhibits differentiation and proliferation; therefore, the actual signals that drive *atoh1a* or *deltad* expression and subsequent differentiation are yet to be discovered.

The mechanisms that activate Notch in central support cells are also a matter of debate. The expression pattern of the Notch reporter clearly shows Notch is not active in hair cells, but hair cells are directly interacting with Notch responsive support cells. Similar to what has been described in the avian or mammalian inner ear development, Notch ligands like *Delta, Jagged,* or *Serrate*

in hair cells could be trans-activating Notch signaling in neighboring support cells (Brooker et al., 2006; Chrysostomou et al., 2012). However, the *delta* genes are expressed in single cells and their pattern resembles the one of hair cell progenitors. To compare, *jagged2b* is expressed in central cells that resemble the hair cells (Figure 3.3A), and it is a good candidate as the main activator of Notch signaling in central cells.

The expression patterns of different Notch receptors and lignands suggest, first, that hair cell progenitors have different Notch-Delta interactions than mature hair cells, and finally, that changes in the expression of Notch ligands might reflect different steps in the differentiation process. Since Notch downregulation is required for hair cell regeneration, the expression of Notch ligands in newly formed hair cells might also be the negative-feedback mechanism through which the neuromast controls organ size (Ma et al., 2008). Conditional silencing and other functional analysis are required to address the role of the Notch ligands in each step of the regenerative process.

Wnt signaling

Wnt is not a differentiation signal in the mature zebrafish neuromast. Our results show that central cells are also Wnt responsive cells which transiently activate Wnt target genes during regeneration, and overexpress Wnt target genes under sustained Notch inhibition (Figure 3.3). However, Wnt hyper-activation through the GSK3β inhibitor 1-Azekenpaullone (AZK) does not induce differentiation or the expression of differentiation markers (Figures 3.6C, 3.6J,

3.6O). This can be explained by the epistatic effect of Notch over Wnt signaling. Manipulations in Notch signaling have an effect on Notch and Wnt target genes, while manipulations of Wnt signaling do not affect Notch target genes (Figures 3.6B and 3.6C).

Wnt is not important for support cell fate either. This was easily addressed by inhibiting Notch signaling and activating Wnt signaling at the same time. The results show every proliferating cell will differentiate into hair cells (Figures 3.6L, 3.6Q, and 3.6R). Hence, Wnt is a proliferation signal and the fate of the proliferating cells is defined by the presence of Notch signaling and hair cell differentiation markers.

A Wnt-Notch negative feedback loop control tissue homeostasis in the neuromast

Although not required for cell fate decision, Wnt is necessary and sufficient to induce proliferation in the polar compartments (Figures 3.5G, 3.5K, 3.6J, 3.6O, 3.6M, and 3.6R). Our results of Wnt gain and loss of function are consistent with previous reports that have shown increase in proliferation using AZK or other GSK3β inhibitor (Lithium Chloride, LiCl), and that *dkk2* disrupts neuromast growth (Head et al., 2013; Jacques et al., 2014; Wada et al., 2013). We have also demonstrated that *dkk2* is a Notch target gene, and propose a feedback loop mechanism on which hair cell death induces Notch downregulation and subsequent *dkk2* downregulation, which triggers transient proliferation in the polar compartments until Notch signaling is restored by new

hair cells. Accordingly, Notch downregulation induces overproliferation and differentiation which are rescued by activating *dkk2* (Figures 3.5I and 3.5K), and Notch activation reduces the overproliferation phenotype caused by AZK (Figures 3.5I and 3.5J). A previous report suggested that *dkk2* is expressed in hair cells and that hair cell production of *dkk2* was sufficient to restrict neuromast growth in the regenerating neuromast (Wada et al., 2013). This previous model fails to integrate the important role of Notch signaling. We have demonstrated that *dkk2* is expressed in the central cells that are in contact to hair cells and are Notch responsive (Figure 3.3B). The human *DKK2* gene has also been predicted to be a notch target since it has two RBPJ-κ binding sites on its promoter (Katoh and Katoh, 2007). In addition, the Notch-Wnt feedback loop is not exclusive to the lateral line neuromasts. In the mammalian inner ear, Notch silencing induces Wnt activation (Li et al., 2014). Also, in the mice intestine, it has been recently shown that inhibition of Wnt signaling at the level of the receptors, using antibodies against the Wnt co-receptor Lrp6, rescues the overdifferentiation phenotype caused by Notch inhibition (Tian et al., 2015). Our results are the first functional demonstration to our knowledge of Notch signaling inhibiting Wnt signaling through the activation of a *dkk* secreted antagonists.

In spite of the consistent overall effects of Wnt signaling manipulations, it is still unclear how Wnt signaling drives proliferation. First, AZK does not drive proliferation in the central support cells. This is contradictory to the fact that AZK or LY specifically induce Wnt target gene expression in central cells, and Wnt signaling is never active in the dorso-ventral poles, as seen by the expression of

the Wnt reporter and *wnt10a* (Figures 3.3D-3.3I, 3.3J-3.3O row10, 3.6A-3.6H row 7). One possibility would be that Wnt activation in central cells induces an unknown proliferative signal that activates proliferation non-cell autonomously. Hair cell death, AZK and LY induce the expression of *wnt2* and *wnt10a* in a Wnt-dependent manner. We are currently working on testing the role of these signals in inducing proliferation. As another option, we might not be detecting other Wnt target genes that respond to Wnt signaling activation in the polar compartments. For example, *wnt2* is specifically expressed in the polar compartments and is upregulated after AZK or LY treatments (Figures 3.2G, 3.2H, 3.6A-3.6H row 8).

Notch signaling has dose-dependent effect over proliferation and Wnt signaling activation

We have described in the neuromast two main effects of the dose-dependent Notch activity: The activation of proliferation and the activation of Wnt signaling. To compare, most known target genes are responsive to low doses of the γ-secretase inhibitor LY411575 (LY). Changes in the levels of notch signaling have been previously proposed as the main mechanism controlling quiescence, proliferation, and differentiation in adult brain stem cells (Chapouton et al., 2010; Guentchev and McKay, 2006). Recently, it has been shown that the dose-dependent effect is related to the variable effect and strength of different Notch-Delta combinations (Okigawa et al., 2014). Our experiments suggest each Notch-ligand interaction might have a different sensitivity to LY, or that there is a negative stoichiometric correlation between the molarity of the LY inhibitor and

the transcriptional activity of the Notch intracellular domain. Both possibilities require extensive testing.

Hair cell death changes the proliferative state of the neuromast in a Notch-independent manner

In this manuscript, we have demonstrated that Notch signaling directly inhibits differentiation by inhibiting *atoh1a,* and restricts Wnt-dependent proliferation through *dkk2.* However, it is puzzling that even though Notch is upstream Wnt signaling and Notch inhibition activates Wnt target genes, it does not induce overproliferation in homeostatic neuromasts (Figure 3.4B, 3.4D, 3.4K, 3.S5H, 3.S5K, 3.6K, and 3.6M). In the same way, although low doses of LY already induce overexpression of *deltad* and *atoh1a,* we could not detect ectopic differentiation in homeostatic neuromasts. From these despair results, it is clear that our Wnt-Notch feedback loop still require of other unknown signals modulated by hair cell death that positively induce proliferation and differentiation in the center of the neuromast, and other signal that drives proliferation in the polar compartments.

Other differentiation signals

Since Notch inhibits Wnt signaling, it is possible Notch is also inhibiting other pro-differentiating signals through unknown mechanisms. In addition, other signals might respond to hair cell death, independent of Notch signaling. During neuromast formation, Wnt-induced FGF signaling interacts with Notch to specify

the central cell that expresses the ligands *atoh1a* and *deltad* (Figure 1.3.). This mechanism is necessary for neuromast deposition, and the specification of the first hair cell progenitor (Matsuda and Chitnis, 2010). In the mature neuromast, FGF signaling is altered early after hair cell death and its role during regeneration is currently unknown (Jiang et al., 2014).

Other possibilities may involve the activation of unknown hair cell precursor markers. In Chapter 2, we presented *sall1b* as one possible and plausible hair cell precursor marker that responds to hair cell death and might be involved in the active decision of hair cell formation (Figure 2.7.). These results highlight the importance of gene expression analysis to discover new molecules and pathways important for hair cell development and regeneration.

Other regulators of proliferation

cdkn1bb is the zebrafish orthologue of the tumor suppressor *p27/kip,* which is an important cell cycle inhibitor that promotes G0 quiescence in multiple tissues including the inner ear (Chen et al., 2003; Walters et al., 2014; Wander et al., 2011; White et al., 2006). Although there is an effect of LY over *cdkn1bb* expression, hair cell death is much more effective inhibiting the expression of this cell cycle inhibitor (Figure 3.3J-3.3O row 6; 3.6A-3.6H row 5). Wnt signaling is also not affecting *cdkn1bb*. The expression pattern of *cdkn1bb* resembles the one of *notch3* or even the Notch reporter. Hence, *cdkn1bb* might be inhibiting proliferation and differentiation in central cells independent of Notch signaling, and hair cell death-mediated *cdkn1bb* downregulation might enhance the

proliferative state of the neuromast. This event might also promote cell proliferation independent of Wnt signaling. For example, while Wnt inhibition affects differentiation (Figures 3.5G, 3.5K), hair cell differentiation is exclusively rescued when Wnt and Notch signaling are simultaneously inhibited (Figures 3.5I, 3.5K).

Since proliferation in the polar compartments is possibly driven by non-cell autonomous mechanisms, and *cdkn1bb* might not be active in the polar compartments, our model also requires a proliferating signal, possibly secreted, that activates proliferation in the poles. In zebrafish retina regeneration, it has been shown that injury triggers multiple proliferation signals such as FGF, HB-EGF, *stat3,* and β-catenin, all of which seem to interact and synergize to induce compensatory proliferation (Wan et al., 2014).

Polar compartments

The reasons why support cells exclusively self-renew in the dorso-ventral poles of the neuromast are puzzling. According to the proposed mechanism, Notch is required and sufficient to maintain the polar compartments. Indeed, *deltaa* (Figure 3.2) is specifically expressed in these compartments, which suggests that the cells from these compartments might be isolated from the Notch expressing cells to the poles through lateral inhibition. This raises the possibility that the polar cells are differentially specified through development and actively maintained during homeostasis. Hair cell death induces transient changes in the expression patterns of these genes. Still, it is currently unknown

whether the number of *wnt2* or *deltaa* expressing cells matches the number of proliferating cells and the exact role of these ligands.

Steiner et al. (2014) found from a gene expression profiling in mantle cells, that *tspan1, fat1b,* and *robo3*, and even the *sqet20* enhancer show specific expressionin the mantle cells, and some level of anterior-posterior differences in gene expression (Steiner et al., 2014; Wibowo et al., 2011). *sqet20* and *robo3* are enriched in the most anterior and posterior mantle cells, *tspan1* is in the most anterior mantle cells, and *fat1b* is in the most posterior. Although correlational to the pattern of quiescence we uncovered, we hypothesize that *tspan1 and fat1b* might play a role in the maintenance of the most quiescent support cell compartments. Importantly, the protocadherin Fat together with Dachsous, play an important role in stablishing epithelial planar cell polarity, both in *Drosophila* and in vertebrates, polarizes growth, and promote quiescence through the activation of the Hippo pathway (Bosveld et al., 2012; Zhao et al., 2011). *tspan1* plays an important role in the polarization of integrins (Yáñez-Mó et al., 2001), which might be important for polarization of other membrane-bound signals. Still, functional analyses of these hypotheses are needed. It is also possible that some unknown signals are expressed in the most polar mantle cells to drive support cell self-renewal.

Planar cell polarity is also involved, through unknown mechanisms, in the establishment of the proliferative compartments. In the mature neuromast, Notch is required to restrict the number of regenerated hair cells (Ma et al., 2008) and to maintain hair cell mirror symmetry (Mirkovic et al., 2012). The fact that Notch

can regulate hair cell planar cell polarity and proliferation within the same organ confirm that Notch lies within signaling crossroads that control multiple events of Neuromast development and homeostasis. In the neuromast, the epithelium has a mirror-symmetric polarization along the anterior-posterior compartments, as seen by the polarization of the hair cell kinocilia (López-Schier and Hudspeth, 2006; López-Schier et al., 2004). Neuromasts derived from the second primordium have a dorso-ventral porlarization. We demonstrate that the proliferative compartments are mirror-symmetric and its axis is rotated 90º respect to the polarity of the epithelium (Figure 3.2 and Figure 3.S2).

We are currently developing transgenic tools to label and target this population. In addition, we are screening for more markers that show this biased gene expression pattern in order to elucidate the cell autonomous mechanisms that control self-renewing in the polar compartments.

Mantle cells

The maintenance of quiescence in mantle cells is still elusive and the evidence provided does not support a joint mechanism that control proliferation in support cells and mantle cells equally. Indeed, mantle cells might exit the cell cycle earlier than other neuromast cells, as evidenced by the quiescence marker *cldnb:mKO2-cdt1.* According to this, mantle cells are actively maintained in in G1-G0 phase of the cell cycle through mechanisms still unknown (Figure 3.7K and 3.7O). New evidence suggests mantle cells quiescence might be achieved through more complex mechanisms. In a gene expression analysis for mantle

cells, Steiner et al (2014) isolated multiple trans-membrane receptors expressed exclusively in mantle cells: *fat1a*, *fat1b*, *fgfr1a*, *fndc7*, *robo3,* and *tspan1* (Steiner et al., 2014). The enrichment for such diverse receptors might imply different signaling pathways guiding the mantle cell quiescence phenotype; possibly without signaling cross-talk with the WNT-Notch pathways.

Conclusion

We propose a two-signal mechanism that control tissue homeostasis and regeneration in the zebrafish lateral line neuromasts through a proliferative signal, Wnt signaling, that is negatively regulated by Notch signaling through *dkk2.* This mechanism, although effective in proposing a way to restrict proliferation and neuromas growth, lacks of a link that completes the feedback loop to orderly activate Notch signaling and restore quiescence after full regeneration has been accomplished. To close this gap, it is crucial to address, first the signaling role of hair cells. These cells are the main outcome of regeneration and their numbers are strictly controlled during this process; therefore, signals coming from the hair cells might close the negative feedback loop that restricts neuromast growth in a Notch-dependent manner (Ma et al., 2008). In addition, it is necessary to address the existence of unknown proliferative signals that possibly interact with Wnt, are inhibited in homeostatic neuromasts, and respond to hair cell death.

This complex scenario predicts the existence of a regenerative potential in the support cells that are responsive to hair cell death, first to proliferate and then

to self-renew or differentiate. This regenerative potential depends on the ability of support cells to activate a determined transcriptional program that allows them to respond to Wnt, Notch ligands and possibly other signaling molecules. This potential might be fueled by a nuclear transcriptional landscape which might be the main difference between mammals and other vertebrates that can regenerate support cells. Indeed, the stem cell-like properties of the zebrafish support cells differ drastically from the ones of the mature mammalian inner ear support cells, which seem to have traded off their proliferative capacity for a transcriptional program that sustains a highly specialized epithelium (Warchol, 2011). Indeed, Notch signaling is no longer active in the mature mammalian inner ear sensory epithelium (Maass et al., 2015), and these cells are no longer responsive to mitogenic treatments such as Wnt activators. Therapies focused on nuclear reprograming of inner ear support cells might be able to restore their ability to respond to proliferating and differentiating signals, and ultimately induce regeneration.

References

Alunni, A., Krecsmarik, M., Bosco, A., Galant, S., Pan, L., Moens, C.B., and Bally-Cuif, L. (2013). Notch3 signaling gates cell cycle entry and limits neural stem cell amplification in the adult pallium. Development *140*, 3335–3347.

Bosveld, F., Bonnet, I., Guirao, B., Tlili, S., Wang, Z., Petitalot, A., Marchand, R., Bardet, P.-L., Marcq, P., Graner, F., et al. (2012). Mechanical control of morphogenesis by Fat/Dachsous/Four-jointed planar cell polarity pathway. Science *336*, 724–727.

Brooker, R., Hozumi, K., and Lewis, J. (2006). Notch ligands with contrasting functions: Jagged1 and Delta1 in the mouse inner ear. Development *133*, 1277–1286.

Brown, S., and Greco, V. (2014). Stem Cells in the Wild: Understanding the World of Stem Cells through Intravital Imaging. Cell Stem Cell *15*, 683–686.

Chapouton, P., Skupien, P., Hesl, B., Coolen, M., Moore, J.C., Madelaine, R., Kremmer, E., Faus-Kessler, T., Blader, P., Lawson, N.D., et al. (2010). Notch activity levels control the balance between quiescence and recruitment of adult neural stem cells. J. Neurosci. *30*, 7961–7974.

Chen, P., Zindy, F., Abdala, C., Liu, F., Li, X., Roussel, M.F., and Segil, N. (2003). Progressive hearing loss in mice lacking the cyclin-dependent kinase inhibitor Ink4d. Nat. Cell Biol. *5*, 422–426.

Chrysostomou, E., Gale, J.E., and Daudet, N. (2012). Delta-like 1 and lateral inhibition during hair cell formation in the chicken inner ear: evidence against cis-inhibition. Development *139*, 3764–3774.

Cruz, I.A., Kappedal, R., Mackenzie, S.M., Hailey, D.W., Hoffman, T.L., Schilling, T.F., and Raible, D.W. (2015). Robust regeneration of adult zebrafish lateral line hair cells reflects continued precursor pool maintenance. Dev. Biol.

Dufourcq, P., Roussigné, M., Blader, P., Rosa, F., Peyrieras, N., and Vriz, S. (2006). Mechano-sensory organ regeneration in adults: the zebrafish lateral line as a model. Mol. Cell. Neurosci. *33*, 180–187.

Ghysen, A., and Dambly-Chaudière, C. (2007). The lateral line microcosmos. Genes Dev. *21*, 2118–2130.

Guentchev, M., and McKay, R.D.G. (2006). Notch controls proliferation and differentiation of stem cells in a dose-dependent manner. Eur. J. Neurosci. *23*, 2289–2296.

Head, J.R., Gacioch, L., Pennisi, M., and Meyers, J.R. (2013). Activation of canonical Wnt/β-catenin signaling stimulates proliferation in neuromasts in the zebrafish posterior lateral line. Dev. Dyn. *242*, 832–846.

Hernández, P.P., Olivari, F.A., Sarrazin, A.F., Sandoval, P.C., and Allende, M.L. (2007). Regeneration in Zebrafish Lateral Line Neuromasts: Expression of the Neural Progenitor Cell Marker Sox2 and Proliferation-Dependent and -Independent Mechanisms of Hair Cell Renewal. Dev. Neurobiol. *67*, 637–654.

Jacques, B.E., Montgomery, W.H., Uribe, P.M., Yatteau, A., Asuncion, J.D., Resendiz, G., Matsui, J.I., and Dabdoub, A. (2014). The role of Wnt/β-catenin signaling in proliferation and regeneration of the developing basilar papilla and lateral line. Dev. Neurobiol. *74*, 438–456.

Jiang, L., Romero-Carvajal, A., Haug, J.S., Seidel, C.W., and Piotrowski, T. (2014). Gene-expression analysis of hair cell regeneration in the zebrafish lateral line. Proc. Natl. Acad. Sci. E1383–E1392.

Jones, J.E., and Corwin, J.T. (1993). Replacement of lateral line sensory organs during tail regeneration in salamanders: identification of progenitor cells and analysis of leukocyte activity. J. Neurosci. *13*, 1022–1034.

Katoh, M., and Katoh, M. (2007). WNT antagonist, DKK2, is a Notch signaling target in intestinal stem cells: Augmentation of a negative regulation system for canonical WNT signaling pathway by the Notch-DKK2 signaling loop in primates. Int. J. Mol. Med. *19*, 197–201.

Li, W., Wu, J., Yang, J., Sun, S., Chai, R., Chen, Z.-Y., and Li, H. (2014). Notch inhibition induces mitotically generated hair cells in mammalian cochleae via activating the Wnt pathway. Proc. Natl. Acad. Sci. *112*, 201415901.

López-Schier, H., and Hudspeth, A.J. (2006). A two-step mechanism underlies the planar polarization of regenerating sensory hair cells. Proc. Natl. Acad. Sci. U. S. A. *103*, 18615–18620.

López-Schier, H., Starr, C.J., Kappler, J.A., Kollmar, R., and Hudspeth, A.J. (2004). Directional cell migration establishes the axes of planar polarity in the posterior lateral-line organ of the zebrafish. Dev. Cell *7*, 401–412.

Lush, M.E., and Piotrowski, T. (2014). ErbB expressing Schwann cells control lateral line progenitor cells via non-cell-autonomous regulation of Wnt/β-catenin. Elife *3*, e01832.

Ma, E.Y., Rubel, E.W., and Raible, D.W. (2008). Notch signaling regulates the extent of hair cell regeneration in the zebrafish lateral line. J. Neurosci. *28*, 2261–2273.

Maass, J.C., Gu, R., Basch, M.L., Waldhaus, J., Lopez, E.M., Xia, A., Oghalai, J.S., Heller, S., and Groves, A.K. (2015). Changes in the regulation of the Notch signaling pathway are temporally correlated with regenerative failure in the mouse cochlea. Front. Cell. Neurosci. *9*.

Matsuda, M., and Chitnis, A.B. (2010). Atoh1a expression must be restricted by Notch signaling for effective morphogenesis of the posterior lateral line primordium in zebrafish. Development *137*, 3477–3487.

Mirkovic, I., Pylawka, S., and Hudspeth, A.J. (2012). Rearrangements between differentiating hair cells coordinate planar polarity and the establishment of mirror symmetry in lateral-line neuromasts. Biol. Open *1*, 498–505.

Okigawa, S., Mizoguchi, T., Okano, M., Tanaka, H., Isoda, M., Jiang, Y.-J., Suster, M., Higashijima, S.-I., Kawakami, K., and Itoh, M. (2014). Different combinations of Notch ligands and receptors regulate V2 interneuron progenitor proliferation and V2a/V2b cell fate determination. Dev. Biol. *391*, 196–206.

Parinov, S., Kondrichin, I., Korzh, V., and Emelyanov, A. (2004). Tol2 transposon-mediated enhancer trap to identify developmentally regulated zebrafish genes in vivo. Dev. Dyn. *231*, 449–459.

Ritsma, L., Ellenbroek, S.I.J., Zomer, A., Snippert, H.J., de Sauvage, F.J., Simons, B.D., Clevers, H., and van Rheenen, J. (2014). Intestinal crypt homeostasis revealed at single-stem-cell level by in vivo live imaging. Nature *507*, 362–365.

Rompolas, P., Mesa, K.R., and Greco, V. (2013). Spatial organization within a niche as a determinant of stem-cell fate. Nature *502*, 513–518.

Steiner, A.B., Kim, T., Cabot, V., and Hudspeth, A.J. (2014). Dynamic gene expression by putative hair-cell progenitors during regeneration in the zebrafish lateral line. Proc. Natl. Acad. Sci. U. S. A. *111*, E1393–E1401.

Tian, H., Biehs, B., Chiu, C., Siebel, C.W., Wu, Y., Costa, M., de Sauvage, F.J., and Klein, O.D. (2015). Opposing Activities of Notch and Wnt Signaling Regulate Intestinal Stem Cells and Gut Homeostasis. Cell Rep. *11*, 33–42.

Wada, H., Ghysen, A., Satou, C., Higashijima, S.-I., Kawakami, K., Hamaguchi, S., and Sakaizumi, M. (2010). Dermal morphogenesis controls lateral line patterning during postembryonic development of teleost fish. Dev. Biol. *340*, 583–594.

Wada, H., Ghysen, A., Asakawa, K., Abe, G., Ishitani, T., and Kawakami, K. (2013). Wnt/Dkk negative feedback regulates sensory organ size in zebrafish. Curr. Biol. *23*, 1559–1565.

Walters, B.J., Liu, Z., Crabtree, M., Coak, E., Cox, B.C., and Zuo, J. (2014). Auditory hair cell-specific deletion of p27Kip1 in postnatal mice promotes cell-autonomous generation of new hair cells and normal hearing. J. Neurosci. *34*, 15751–15763.

Wan, J., Zhao, X.-F., Vojtek, A., and Goldman, D. (2014). Retinal injury, growth factors, and cytokines converge on β-catenin and pStat3 signaling to stimulate retina regeneration. Cell Rep. *9*, 285–297.

Wander, S.A., Zhao, D., and Slingerland, J.M. (2011). p27: a barometer of signaling deregulation and potential predictor of response to targeted therapies. Clin. Cancer Res. *17*, 12–18.

Warchol, M.E. (2011). Sensory regeneration in the vertebrate inner ear: differences at the levels of cells and species. Hear. Res. *273*, 72–79.

White, P.M., Doetzlhofer, A., Lee, Y.S., Groves, A.K., and Segil, N. (2006). Mammalian cochlear supporting cells can divide and trans-differentiate into hair cells. Nature *441*, 984–987.

Wibowo, I., Pinto-Teixeira, F., Satou, C., Higashijima, S., and López-Schier, H. (2011). Compartmentalized Notch signaling sustains epithelial mirror symmetry. Development *138*, 1143–1152.

Williams, J.., and Holder, N. (2000). Cell turnover in neuromasts of zebrafish larvae. Hear. Res. *143*, 171–181.

Yáñez-Mó, M., Tejedor, R., Rousselle, P., and Sánchez -Madrid, F. (2001). Tetraspanins in intercellular adhesion of polarized epithelial cells: spatial and functional relationship to integrins and cadherins. J. Cell Sci. *114*, 577–587.

Zhao, B., Tumaneng, K., and Guan, K.-L. (2011). The Hippo pathway in organ size control, tissue regeneration and stem cell self-renewal. Nat. Cell Biol. *13*, 877–883.